ADVANCED FUNCTIONAL MATERIALS
www.afm-journal.de

Circularly Polarized Organic Ultralong Room-Temperature Phosphorescence: Generation, Enhancement, and Application

Jiao Liu, Xinyu Zhou, Xinzhou Tang, Yuqi Tang, Junjie Wu, Zhenpeng Song, Haoyi Jiang, Yun Ma, Bingxiang Li, Yanqing Lu,* and Quan Li**

Circularly polarized luminescent (CPL) materials have garnered tremendous attention owing to their expanded optical properties beyond emission wavelength and intensity. Among these, the emerging circularly polarized organic ultralong room-temperature phosphorescence (CP-OURTP) materialsdemonstrating elegant and distinct features are of significant importance for their extended emission lifetime, which represent a novel frontier in research with promising scientific and technological applications across diverse fields. This review systematically outlines the traditional strategies to achieve CP-OURTP including organic crystals, copolymerization, host–guest doping, a combination of the copolymerization and host–guest doping, spinning and twisting technology, and supramolecular polymer assembly. Importantly, the recent significant progress of CP-OURTP in the chiral soft materials, such as liquid crystals (LCs) involving lyotropic LCs (cellulose nanocrystals, CNCs) and chiral thermotropic LCs (cholesteric LCs and chiral LC elastomers), is showcased. Finally, the practical applications of CP-OURTP materials are summarized, and the review concludes with the perspectives on the current challenges and future opportunities for CP-OURTP materials. This review aims to inspire the further innovations in the fabrication of advanced CP-OURTP materials and enrich their promising applications.

1. Introduction

Chirality is omnipresent in living matter, which is of paramount significance in multidisciplinary fields ranging from chemistry to biology, physics, material sciences, and medicine.[1–10] As one of the most fascinating occurrences, chirality is a ubiquitous geometric characteristic across various length scales from the galaxies to the conformation of molecules.[11–15] Identified in the separation of tartaric acid crystals by Louis Pasteur in nineteenth century,[16] chirality refers to an object or a chiral point group whose mirror image cannot be superimposed on their mirror images by any translation or rotation, a concept understood through the absence of mirror symmetry.[17–24] The fabrication of chiral nanomaterials has garnered considerable attention in areas of life sciences, sensors, and catalysis, owing to their outstanding optical activities.[25] The widely used techniques for testing chirality are optical methods, such as circular dichroism spectroscopy that is applied to measure different absorption toward left-handed circularly polarized light (LCP) and right-handed circularly polarized light (RCP).[26–32] Circularly polarized luminescence (CPL) spectroscopy is performed to measure the different emission of LCP and RCP.[13,33–40]

Chiral functional materials featuring distinct CPL characteristics have attracted significant interest in advanced applications in 3D displays, optical storage devices, information and data

J. Liu, X. Zhou, X. Tang, J. Wu, Z. Song, H. Jiang, B. Li
College of Electronic and Optical Engineering & College of Flexible Electronics (Future Technology)
Nanjing University of Posts and Telecommunications &
National Laboratory of Solid State Microstructures
Nanjing University
Nanjing 210023, China
E-mail: bxli@njupt.edu.cn

Y. Tang, Q. Li
Institute of Advanced Materials & School of Chemistry and Chemical Engineering
Southeast University
Nanjing 211189, China
E-mail: quanli3273@gmail.com

Y. Ma
State Key Laboratory for Organic Electronics and Information Displays & Jiangsu Key Laboratory for Biosensors
Institute of Advanced Materials (IAM)
Nanjing University of Posts and Telecommunications
Nanjing 210023, China

Y. Lu
National Laboratory of Solid State Microstructures & Collaborative Innovation Center of Advanced Microstructures & College of Engineering and Applied Sciences
Nanjing University
Nanjing 210093, China
E-mail: yqlu@nju.edu.cn

The ORCID identification number(s) for the author(s) of this article can be found under https://doi.org/10.1002/adfm.202414086

DOI: 10.1002/adfm.202414086

storage, organic light-emitting diodes (OLEDs), and biological imaging.[41–51] CPL refers to the phenomenon that chiral luminescent systems emit LCP and RCP with different intensities under the excitation of light source, reflecting the chirality of an object in an excited state.[52,53] In particular, CPL exhibits left- or right-handed characteristics that can provide an additional dimension of information with regard to regular light. The CPL characteristic of a molecule can be assessed by the luminescent dissymmetry factor (g_{lum}), described by the equation: $g_{lum} = 2 \times (I_L - I_R)/(I_L + I_R)$, in which I_L and I_R refer to the intensity of LCP and RCP, respectively.[36,50,54–61] g_{lum} values are in the range between −2 and +2, where the positive signal indicts larger intensity of LCP than that of RCP and vice versa. $g_{lum} = \pm 2$ indicates a total L- or R-CPL emission, while $g_{lum} = 0$ signifies the unpolarized luminescence.[53] Traditionally, the effective approaches for achieving CPL-active materials include chiral organic small molecules,[62] aggregation-induced-emission - active aggregates,[34] supramolecular assembly,[63–65] liquid crystal (LC) templates,[11,66–68] CPL-active polymers,[69,70] LC metal-organic frameworks,[71] inorganic nanomaterials,[5] and photon upconversion systems.[72–77] With advancement in CPL materials, the applications of CPL-active materials are emerging as a burgeoning field in optoelectronic devices, and multiplexing confidentiality for encoding and encrypting multilevel data.[45,52,78–88]

When an electron absorbs energy and transitions from the ground state (S_0) to the excited singlet state (S_1), fluorescence occurs if the electron returns directly to S_0 from S_1, and this transition between S_0 and S_1 is spin-allowed. Phosphorescence is a distinct photophysical phenomenon, where the intersystem crossing (ISC) from S_1 to T_n is required. This ISC process is spin-forbidden and is typically promoted by the mixing of singlet and triplet states with different molecular orbital configurations.[89] Unlike fluorescent materials, phosphorescent materials have the characteristics of large Stokes shift and prolonged afterglow emission, with lifetime often up to microseconds or seconds.[89] Thermally activated delayed fluorescent (TADF) materials, on the other hand, can be achieved by minimizing energy gap between the singlet and triplet levels.[90] Accordingly, materials can utilize both singlet and triplet excitons for light emission via reverse intersystem crossing (RISC) process from T_1 to S_1, resulting in delayed emission. After all, the singlet excitons generated decay rapidly, yielding fluorescence. Two triplet excitons can combine to form a singlet exciton via triplet–triplet annihilation, enabling delayed fluorescence, while the direct radiative decay of triplet excitons leads to phosphorescence.[91] Recently, considerable endeavors have been dedicated to the investigations of room temperature phosphorescence (RTP) materials due to their ultralong-lived excited states,[92,93] enabling the long lasting emission from seconds to several hours after stoppage of the excitation.[94–101] RTP materials exhibit the distinct attributes, including large Stokes shifts,[102,103] prolonged emission,[104] and advantageous processability,[105] which offer unprecedented advantages in various fields such as biological imaging, OLEDs, and security protection.[91,106–117] RTP occurs upon the excitation of triplet states through the efficient ISC and the afterglow can persist for a while at room temperature once the excitation source is switched off. In order to attain efficient RTP, two prerequisites are essential: 1) the triplet excitons should be effectively populated to accelerate the ISC between singlet and triplet excited states. 2) The nonradiative transitions are suppressed while the radiative transitions are enhanced from the excited T_1 to the S_0.[118–121] The well-known RTP has been considered as a typical feature of inorganic and organometallic traditional metal-based complexes, but is plagued by the intrinsic limitations of poor processability, instability, high cost, limited resources, and potential toxicity that hinder its practical applicability.[122–124] Therefore, organic RTP materials have emerged as extensively utilized alternatives in phosphorescent materials, offering advantages such as environmental friendliness and ease of modification. Proverbially, organic RTP materials, enabled by crystallization aggregation,[101,114,125–128] embedding of organic phosphors into polymer matrix[129,130] or host–guest doping,[131–134] have received extensive attention as a cutting-edge research field.[135] Specifically, RTP polymers not only exhibit the outstanding characteristics such as excellent flexibility, low cost, good processability, and high thermal stability,[136–140] but also provide rigid matrices to inhibit nonradiative decay process, resulting in phosphorescent emission.[140]

Researchers from multidisciplinary fields have dedicated their efforts to exploring RTP materials featuring chiral architectures for a wide range of applications. The integration of chirality with organic RTP has established numerous sophisticated functional materials with circularly polarized phosphorescence (CPP) performance,[141,142] which can be applied in information storage, 3D optical displays, and anti-counterfeiting devices.[34,142–145] Developing the cutting-edge fields of ultra-dissymmetric CPP materials requires the judicious design of molecular structures,[146] which are essential to satisfy the requirements of practical applications. Typically, there are two main approaches for fabricating CPP materials. One approach involves utilizing building blocks that exhibit both RTP characteristics and chirality, while the other approach requires co-assembling achiral RTP emitters with chiral materials. Due to significant advancement in CPP materials, there is a necessary for a comprehensive review article that is expected to invigorate and facilitate the further progress in this specialized research field.

While there have been numerous excellent reviews concentrating on the molecular design, self-assembly, and applications of CPL-active materials,[5,135,147–151] to the best of our knowledge, there has never been such a review that systematically embraces the flourishing topic of circularly polarized organic ultralong room-temperature phosphorescence (CP-OURTP, lifetimes over 0.1 s)[152–155] materials, and particularly the recent progress in chiral soft materials have been unraveled. We believe that it is of paramount need for an easy-to-access introduction of CP-OURTP materials. In this review, we provide a state-of-the-art account on the recent advancement in the persistent CP-OURTP materials emphasizing on the design approaches, fundamental principles, and potential technological applications. As shown in **Figure 1**, we mainly concentrate on traditional strategies for enhancing CP-OURTP, such as through organic crystal aggregation, copolymerization, host–guest doping, the combination of copolymerization and host–guest doping, spinning and twisting technology, and supramolecular systems based on the well-established understanding of RTP mechanisms, and the extensive investigations of the luminescent system design, performance enhancement, and potential applications. In addition, the more sophisticated CP-OURTP systems with high g_{lum} in

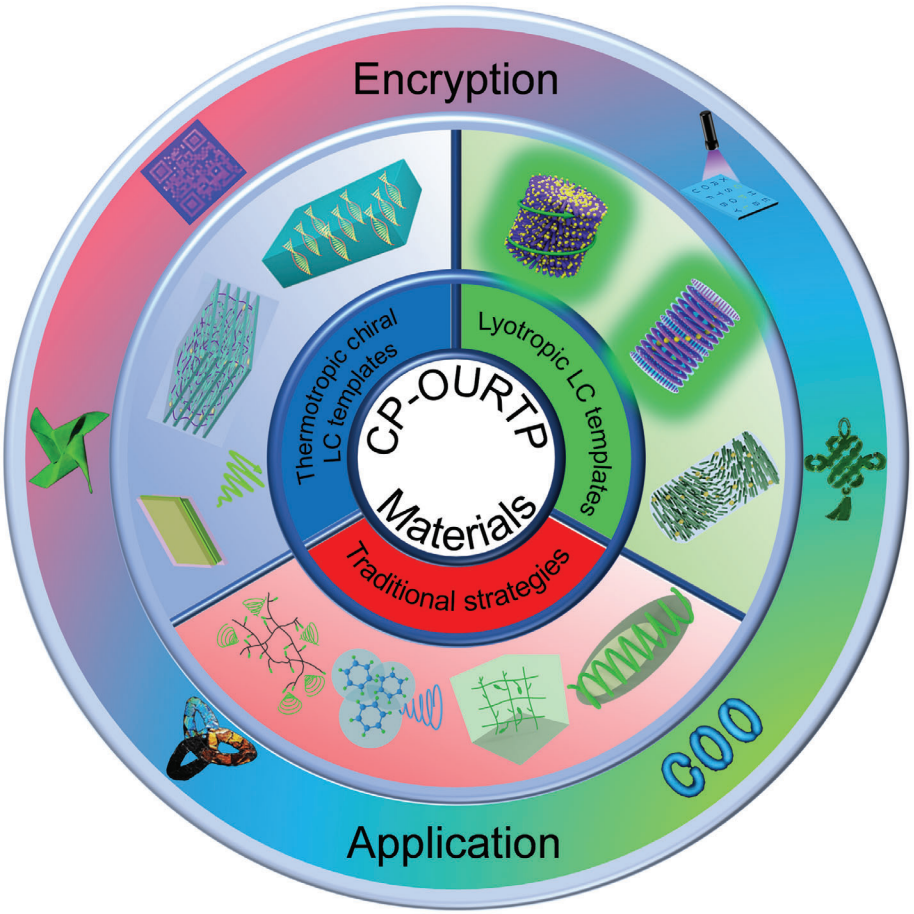

Figure 1. Schematic of circularly polarized organic ultralong room-temperature phosphorescence (CP-OURTP) materials fabricated by traditional strategies and new strategies based on thermotropic chiral liquid crystal (LC) templates and lyotropic LC templates and their applications.

chiral soft matter systems, including lyotropic cellulose nanocrystals (CNCs) and thermotropic chiral nematic LCs (i.e., cholesteric LCs and chiral LC elastomers) are discussed. Chiral soft materials, such as cholesteric LCs, can selectively reflect circularly polarized light due to photonic bandgaps (PBGs), enabling cholesteirc LCs (CLCs) to reflect light of the same handedness as the helix of helicoidal superstructure, while transmitting the opposite handedness. Consequently, CLCs are regarded as an exceptional medium for constructing CPL-active materials with g_{lum} values that are two orders of magnitude greater than those achieved with traditional methods. We next highlight the practical applications of CP-OURTP materials, which hold great potential for further development of the next-generation advanced CP-OURTP materials in encryption display technologies. Finally, this review concludes with a perspective on their applications, the current challenges, and further opportunities for the high-performance CP-OURTP materials endowed with exceptional photophysical features. It is anticipated that this review will aid in the construction and advancement of the novel CP-OURTP materials.

2. Traditional Strategies for Generating CP-OURTP

Organic RTP has experienced rapid growth due to its extended emission lifetimes and diverse excited-state characteristics, that holds great potential in the fields such as information anti-counterfeiting, displays, and bioimaging. The majority of excellent persistent luminescent materials are confined to inorganic phosphors. However, metal-based luminescent materials frequently encounter challenges such as high preparation conditions, which obstruct their development in practical applications. Some endeavors have been made to overcome these limitations by seeking for new substitutable materials. Various approaches for RTP materials including crystal aggregation, supramolecular self-assembly, and host–guest have been proposed to enhance the efficiency of the ISC and stabilize triplet excitons at room temperature, resulting in high-quality organic RTP materials. Despite significant progress have been made in designing and synthesizing organic RTP materials with prolonged lifetimes, high luminescent efficiencies and quantum yields, emission color tunability, and stimuli-responsive emission properties, there have been rare investigation of organic RTP materials that exhibit CPP characteristics. As such, the ongoing development of organic RTP materials that possess both long lifetimes and CPP characteristics remains a significant challenge. Nonetheless, CP-OURTP materials have emerged as one of the promising candidates in contemporary research for expanding the horizons of optical signal dimensionality.

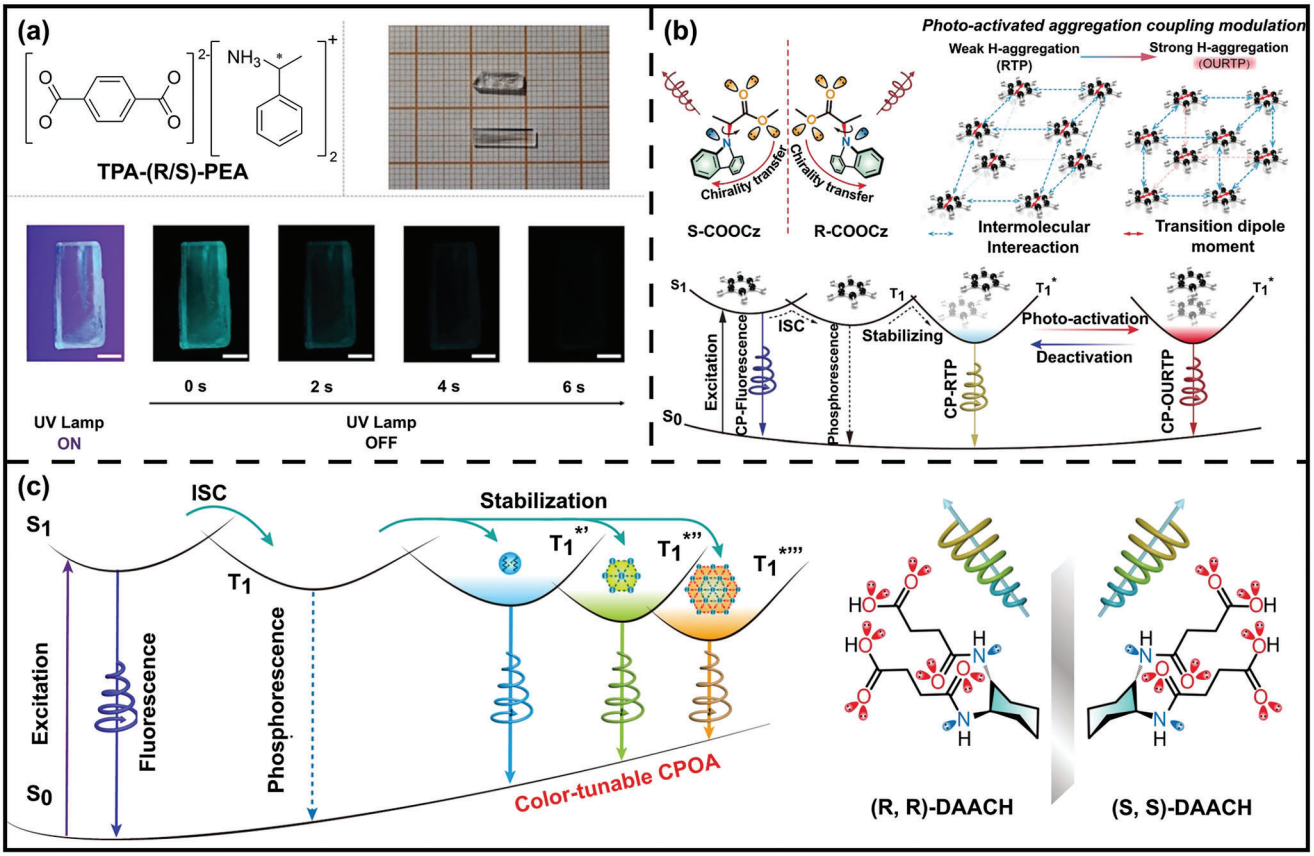

Figure 2. a) Long-lasting luminescence emitted by terephtalic (*R*/*S*)-phenylethyamine (TPA-(*R*/*S*)-PEA). Reproduced with permission.[79] Copyright 2018, John Wiley and Sons. b) Constructing photo-activable CP-OURTP molecules. Reproduced with permission.[156] Copyright 2020, John Wiley and Sons. c) Schematic diagram for generating color-tunable circularly polarized organic afterglow (CPOA) and molecular design for CPOA with tunable colors. Reproduced with permission.[166] Copyright 2022, Springer Nature.

2.1. CP-OURTP Based on Organic Crystals

Long-lived phosphorescence can be achieved in the chiral organic ionic crystal system. Duan, Liu, and co-workers[156] achieved CP-OURTP in chiral organic crystals by designing and incubating terephtalic (*R*/*S*)-phenylethyamine (TPA-(*R*/*S*)-PEA) (**Figure 2a**). In such system, the luminescence was produced through the intermolecular charge-transfer excitons. The remarkable long-persistent phosphorescence occurred due to the planar terephthalic acid (TPA)molecules adopting a twisted conformation, which was fixed by the crystallization process, thereby generating the restricted chiral environment. Upon the irradiation of ultraviolet (UV) light, the crystals showed the sapphire emission. However, the emission color gradually turned to greenish and persisted for several seconds after ceasing the irradiation of UV. As a result, the long persistent phosphorescence was realized through the rigid structures of TPA-(*R*/*S*)-PEA crystals by efficiently reducing the non-radiative decay of triplet excitons. Chen, Huang, and co-workers[79] developed a stimuli-responsive single-component CP-OURTP molecular system in a solid state by covalently bonding an achiral phosphor to the chiral ester chain (Figure 2b). The flexible chiral ester enabled the chirality transfer to the carbazole, which functioned as both the chiral unit and the conformation regulator, resulting in the efficient control of the molecular arrangement and successful aggregation coupling upon external stimulus. It should be noted that the existence of heteroatoms in the carbazole luminous phosphor, can logically stabilize the triplet excitons through the ISC and inhibit the non-radiative decay by H-aggregation.[138] Simultaneously, the molecule's regulation was predominantly influenced by the conformation control of the chiral ester chain during the photo-irradiation treatment for robust aggregations, leading to the stimuli-responsive CP-OURTP with g_{lum} of 2.2×10^{-3}, and a lifetime over 0.6 s. These findings provide an efficient roadmap for fabricating the advanced functional CP-OURTP materials with potential applications in organic optoelectronic and lifetime-resolved device applications.

Multicolor CPL materials with remarkable stimuli-responsive attributes, exhibit great potential as emissive media for stereoscopic displays and optical marker recognition.[157,158] Multicolor CPL emissions can be achieved within multicomponent material systems through the diverse design strategies, such as supramolecular assembly, excited state modulation by chemical additives, and structural color change enabled by solvation effects, etc.[65,70,159–162] However, the afterglow emission colors of circularly polarized organic afterglow (CPOA) materials have been limited to fixed colors under ambient conditions, mostly in yellow or yellowish green. Thus, developing CPOA materials

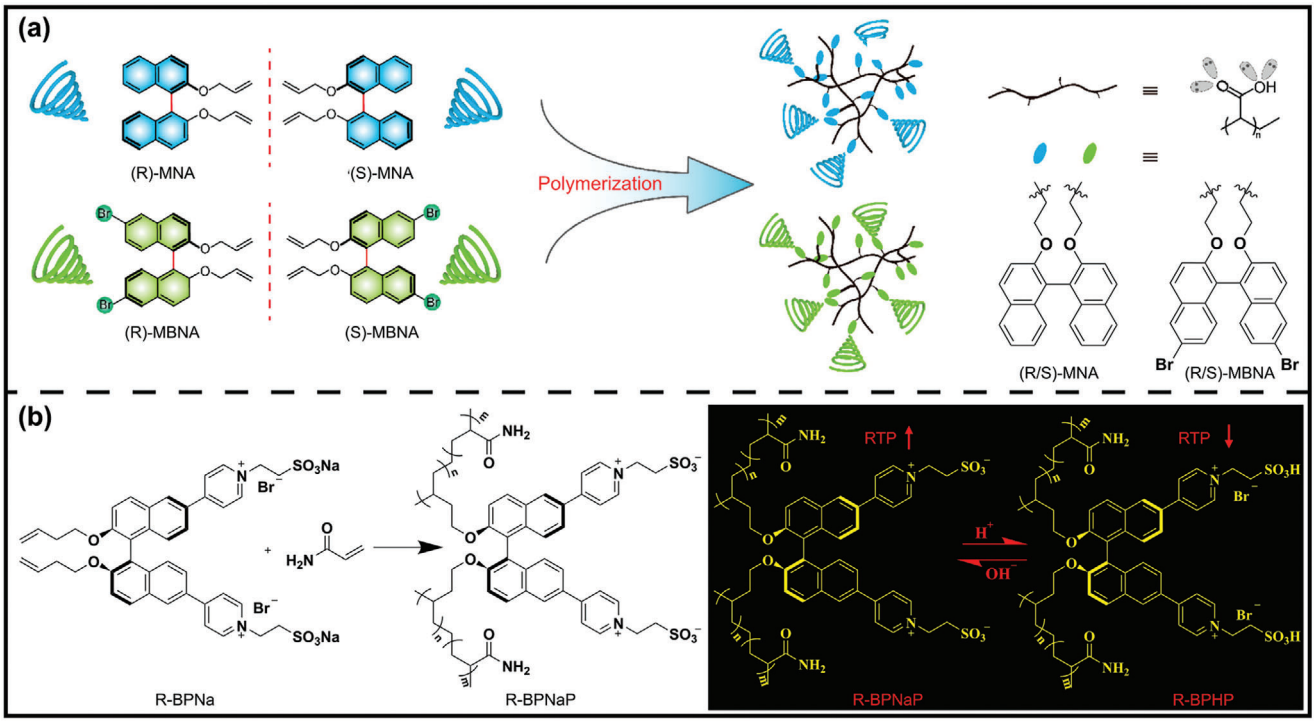

Figure 3. a) Design strategy of circularly polarized phosphorescence (CPP) copolymers. Reproduced with permission.[167] Copyright 2021, American Chemical Society. b) Preparation of the amorphous polymer *R*-BPNaP. Reproduced with permission.[169] Copyright 2021, Elsevier.

with tunable multicolor emission remains a daunting challenge owing to the complex chirality transfer between RTP and the chiral units for producing CPL, together with the inefficient manipulation of the multicolor emission of RTP, particularly within a single molecule. CPOA materials, possessing both excellent CPL characteristics and ultralong-lived triplet excited state of RTP, have garnered considerable attention due to their remarkable photophysical properties and their potential for numerous remarkable applications.[163–165] Chen, Zheng, Huang, and co-workers[166] achieved the multicolor-tunable CPOA by introducing a chiral center into single-component non-conjugated organic cluster through chiral clustering (Figure 2c). Concretely, the single-component chiral cluster crystal demonstrated the clusterization-triggered emission via through-space conjugation, enabling the color-tunable afterglow due to the existence of different cluster sizes in the luminescent centers. In addition, the non-conjugated chiral cluster was made of a pair of the enantiomer, consisting of chiral trans-1,2-diaminocyclohexane and two succinic acid groups (*R*, *R*)-DAACH and (*S*, *S*)-DAACH. In such system, one-step amidation reaction occurred between trans-(1*R*, 2*R*)/(1*S*, 2*S*)-diaminocyclohexane and succinic anhydride. The non-conjugate clusters demonstrated the emission properties dependent on the sizes of the clusters, that is, color-tunable organic afterglow emission can be tailored by varying the cluster sizes. As a result, emission colors from blue to yellowish green can be observed with a lifetime of 587 ms and g_{lum} over 2.3×10^{-3} under the irradiation of different UV wavelengths. The on-demand multicolor CPOA with color-tuning features provides significant insights into the further development of CP-OURTP materials.

2.2. CP-OURTP Based on Copolymerization

Numerous CP-OURTP materials have been developed by restricting the chiral molecule motions in the crystalline state. However, the limited flexibility of crystalline materials has prompted to the investigation of superior strategies for obtaining CP-OURTP materials. Polymer-based RTP materials have emerged as promising solutions to address this challenge due to their benefits including excellent stretchability, processability, and reproducibility. Therefore, there is a strong demand to enhance polymer-based CP-OURTP materials for practical applications in displays, data encryption, biological imaging, etc. Zhao, Huang, An, and co-workers[167] introduced a convenient and versatile method for achieving CP-OURTP materials from amorphous copolymers, by incorporating the axially chiral chromophores into the rigid polymer chains through radical cross-linked polymerization. The obtained copolymers of (*R*/*S*)-PBNA exhibited a g_{lum} value of 9.4×10^{-3}, and a high efficiency of 30.6% (**Figure 3**a). The polymer matrix polyacrylic acid (PAA) could not only enhance the ISC to promote the formation of triplet excitons owing to its abundant carboxylic groups, but also was able to stabilize the molecular motions and reduce the nonradiative decay. It is worth noting that the axially chiral binaphthol derivatives[168] were covalently bonded to the polymer chains to achieve CP-OURTP. These findings not only establish the formidable platform for fabricating the novel amorphous polymers with CP-OURTP attributes but also broaden the range of RTP materials. Additionally, Ma and co-workers[169] achieved a pristine amorphous polymer, *R*/*S*-BPNaP, by combining the attributes of both CPL and RTP through radical copolymerization

of two components containing the binaphthyl derivatives and acrylamide (Figure 3b). The presence of the S═O double bond in SO^{3-} facilitated the spin–orbit coupling, enhancing the ISC process; the existence of hydrogen bond networks between ion cross-linking networks and polyacrylamide polymer chains could restrict molecular motions, thus diminishing the non-radiative deactivation. Moreover, the intermolecular heavy atom effect induced by bromine (Br) from hydrogen bromide (HBr), served to enhance the intensity of RTP. Thus, a controllable responsive switching RTP with g_{lum} of 0.84×10^{-3} was achieved, which offered a versatile approach to designing CP-OURTP materials.

2.3. CP-OURTP Based on Host–Guest Doping

Encapsulating a chiral emitter into a solid matrix is an efficient approach to achieve CPP. Organic RTP materials have currently been developed by employing diverse strategies, including leveraging heavy atom effects, hydrogen, or halogen bonding, etc. While significant progress in organic RTP materials with CPL has promoted the widespread applications of luminescent materials in technology. The versatile approach to attach axial chiral phosphors to polyacrylamide chains for achieving CP-OURTP emission in an amorphous state as mentioned above, has limitations in the responsiveness and sensitivity to various stimuli. To overcome these disadvantages, Ma, Tian, and co-workers[170] have modified the rigidification of polymer network to accurately control the photoresponsive behaviors by uniformly distributing chiral polyacetylenes into the polymethyl methacrylate (PMMA) matrix through the copolymerization of phosphor BrNpA and chiral phNA (**Figure 4a**). The resulting helical system played the crucial role for the transmission of circularly polarized light and demonstrated distinctive optical properties with g_{lum} up to 0.019, respectively. Meanwhile, UV irradiation triggered the dynamic chiro-optical functionality due to the oxygen consumption of the films, enabling the precise and remote control of CP-OURTP with remarkable advantages, such as wireless operation, fatigue resistance, and contactless manipulation. In contrast to the single-component systems, the approach of host–guest doping offers a viable approach to fabricating CP-OURTP materials with tunable emission. The distinctive materials with dynamic attributes can be employed in anti-counterfeiting applications, especially those involving photo programmability. Vacha and co-worker[171] realized CP-OURTP with long-enduring emission characteristics in chiral binaphthyl structures by incorporating enantiomers of *N*, *N*′-dimethyl-1,1′-binaphthyldiamine (DMBDA) binaphthyl into a *β*-estradiol-based amorphous hydroxylated steroid matrix (Figure 4b). In this blend system, the yellow persistent RTP can be detected with a quantum yield of 2.3%, a g_{lum} of 2.3×10^{-3}, and a lifetime of 0.67 s.

He and co-workers[172] developed an efficient strategy to achieve strong CP-OURTP from a separable bidibenzo[*b*, *d*]furan scaffold (*R*)-1, which was accomplished through kinetic resolution reaction. As a result, incorporating the bidibenzo[*b*, *d*] furan scaffold (*R*)-1 into a rigid polyvinyl alcohol (PVA) matrix[173] resulted in a significant g_{lum} value of 0.12 and an extended lifetime of 0.56 s (Figure 4c). Specifically, PVA was selected as a versatile host predominantly due to its abundance of hydroxyl groups, which were able to constrain inter-/intramolecular motions through hydrogen bonding, and confine the phosphors within a rigid polymer matrix, thus decreasing nonradiative pathways and improving the g_{lum} in the axial chirality of bidibenzo[*b*, *d*] furan. This study provides important impetus toward the design and fabrication of CP-OURTP materials for achieving the enhanced circularly polarized emission in small organic molecules. Xing and co-workers[174] introduced a host–guest strategy with both fluorescence and phosphorescence features dependent on the excitation wavelengths of the host, enabling an efficient UV-light detection (Figure 4d). The direct bonding of naphthalimides to chiral segments triggered the supramolecular chirality, which facilitated the chirality transfer and amplification. Interestingly, when the excitation wavelengths were lower than 320 nm, incorporating tetracyanobenzene as the host matrix resulted in red CP-OURTP with g_{lum} ranging from 1.0×10^{-3} to 5.0×10^{-3} due to the ISC between tetracyanobenzene and chiral compound. Excitation wavelengths above 320 nm led to the predominant blue fluorescence with deactivated CP-OURTP. This excitation wavelength-dependent CP-OURTP material exhibited a discernible red-blue change together with the activation and deactivation of RTP, allowing for an intelligent regulation of the activation/deactivation of CPP state and UV light detection. This study introduces a robust method for achieving dynamic color-tunable and UV light-detectable CP-OURTP material, which opens up new opportunities to broaden the applicability of CP-OURTP materials for various applications. Li, Xie, and co-workers[175] employed a chiral perturbation method by incorporating chiral binaphthol with a phenoselenazine derivative in polystyrene (PS) film to produce CPP, which displays a g_{lum} value and RTP lifetime up to 9.32×10^{-3} and 40.0 ms, respectively. The PS film's high sensitivity to oxygen and temperature allows for the tunable emission colors, transitioning from green to off-white and blue under different conditions. The emission pattern can be adjusted by altering afterglow time with different hosts or changing UV irradiation time to obtain deep blue circularly polarized fluorescence (CPF) and green CPP, respectively. Moreover, the CPP property can be applied for decoding encrypted information using right- and left-handed polarizers.

CP-OURTP materials with tunable emission colors are highly desirable in optoelectronic applications. Although the host–guest doping is a versatile and universal choice for constructing CP-OURTP materials with rich phosphorescence properties, the resulting doped materials encounter limitations in accommodating a variety of guests with different luminescent properties. Huang, Tao, and co-workers[176] have developed a doped CP-OURTP system with different afterglow colors of green, yellow, and red, respectively, which was achieved by integrating chiral amides into phenanthrene, phosphors-naphthalene, and pyrene monomers with *R* and *S* configurations as guests, and polyvinyl pyrrolidone/PVP[177] as the host (**Figure 5**). The phosphorescence in CP-OURTP system primarily originated from three guests, with the phosphorescence lifetime from 341 to 1017 ms (Figure 5c), and g_{lum} ranging from 0.001 to 0.0021. As the excitation wavelengths shifted from 300 to 365 nm, the persistent afterglow emitted changed from green to yellow, and ultimately to red. Additionally, the persistent luminescence shifted from red to green under 365 nm UV irradiation due to different phosphorescence lifetime of these guests, which enabled the time-dependent phosphorescent emission. This study offers a valuable

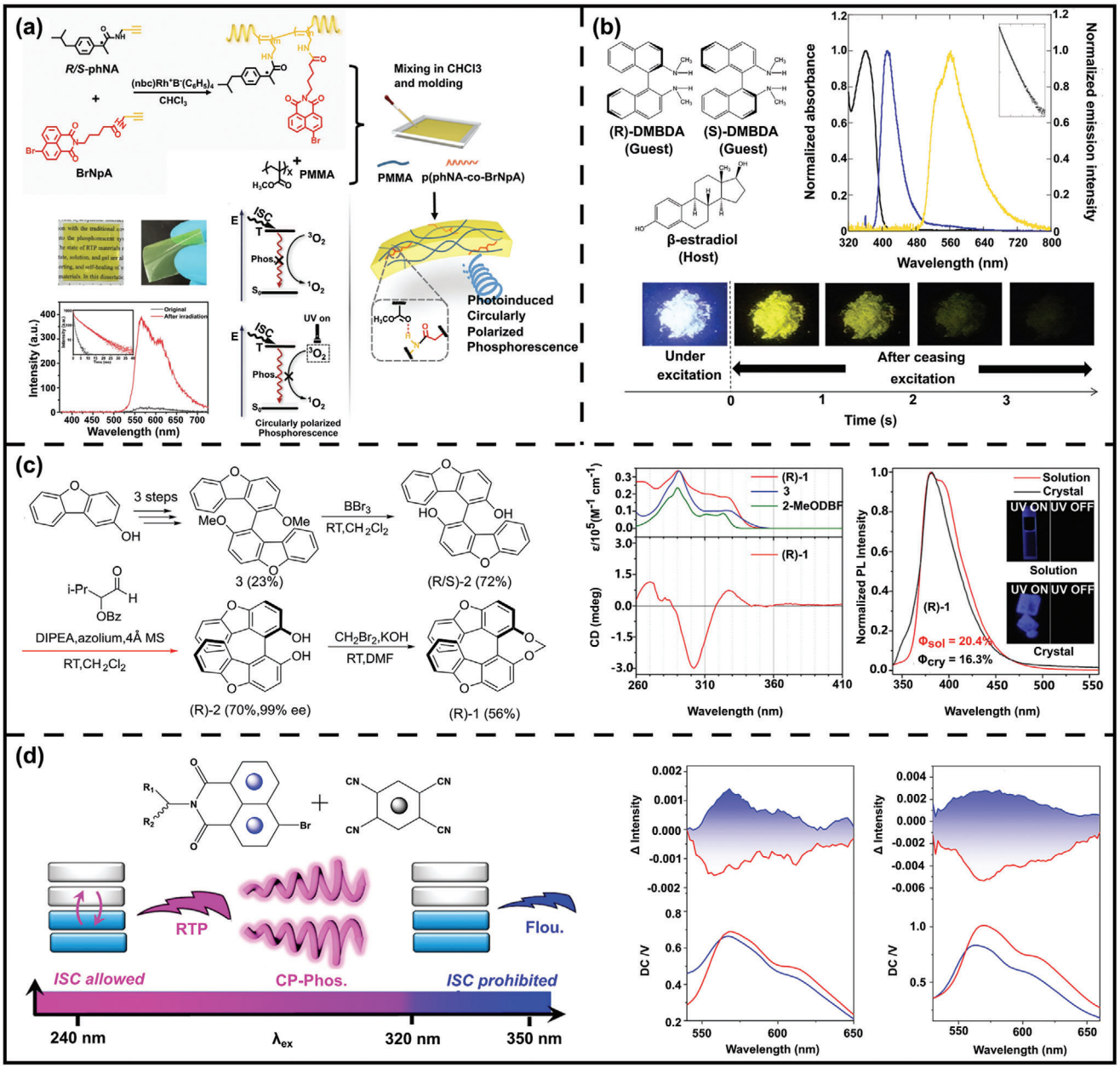

Figure 4. a) Formation of the helical films. Reproduced with permission.[170] Copyright 2022, Springer Nature. b) Structures of host *β*-estradiol and guests of (*R*)-DMBDA, (*S*)-DMBDA, and spectroscopic properties of (*R*)-DMBDA-doped *β*-estradiol film. Reproduced with permission.[171] Copyright 2016, American Chemical Society. c) Synthesis of bidibenzo[*b*, *d*]furan scaffold (*R*)-1 and photoluminescence (PL) of (*R*)-1 in organic solvent and crystal at room temperature. Reproduced with permission.[172] Copyright 2022, John Wiley and Sons. d) Ultraviolet (UV) light detectable UV light-detectable CP-OURTP in chiral naphthalimide self-assembly. Reproduced with permission.[174] Copyright 2021, American Chemical Society.

platform for fabricating novel CP-OURTP materials with color-tunable phosphorescence.

Utilizing solid-state host–guest complexation holds significant promise for fabricating phosphorescent materials. The development of chiral hosts doped with diverse achiral guests across a wide range of guest types would undoubtedly broaden the chiroptical applications. Hao, Xing, and co-workers[178] reported the complexation of steroid-aromatic compounds in the solid phase, which enabled the effective CPP (**Figure 6**). Steroids have been regarded as one of the excellent candidates for entrapping aromatic molecules with diverse functionalities.[179–182] Progesterone (Pg) exhibited a strong affinity to diverse aromatic compounds in the solid state, which acted as a host to hold small aromatic guests, like pyrene (Py), tetraphenylethylene, and other luminophores in the solid state (Figure 6a,b). Pg cocrystallized via CH–π interactions, creating a stable chiral microenvironment for encapsulating the aromatic luminophores within its cavities. The handedness of CPL can be tailorable by small molecular

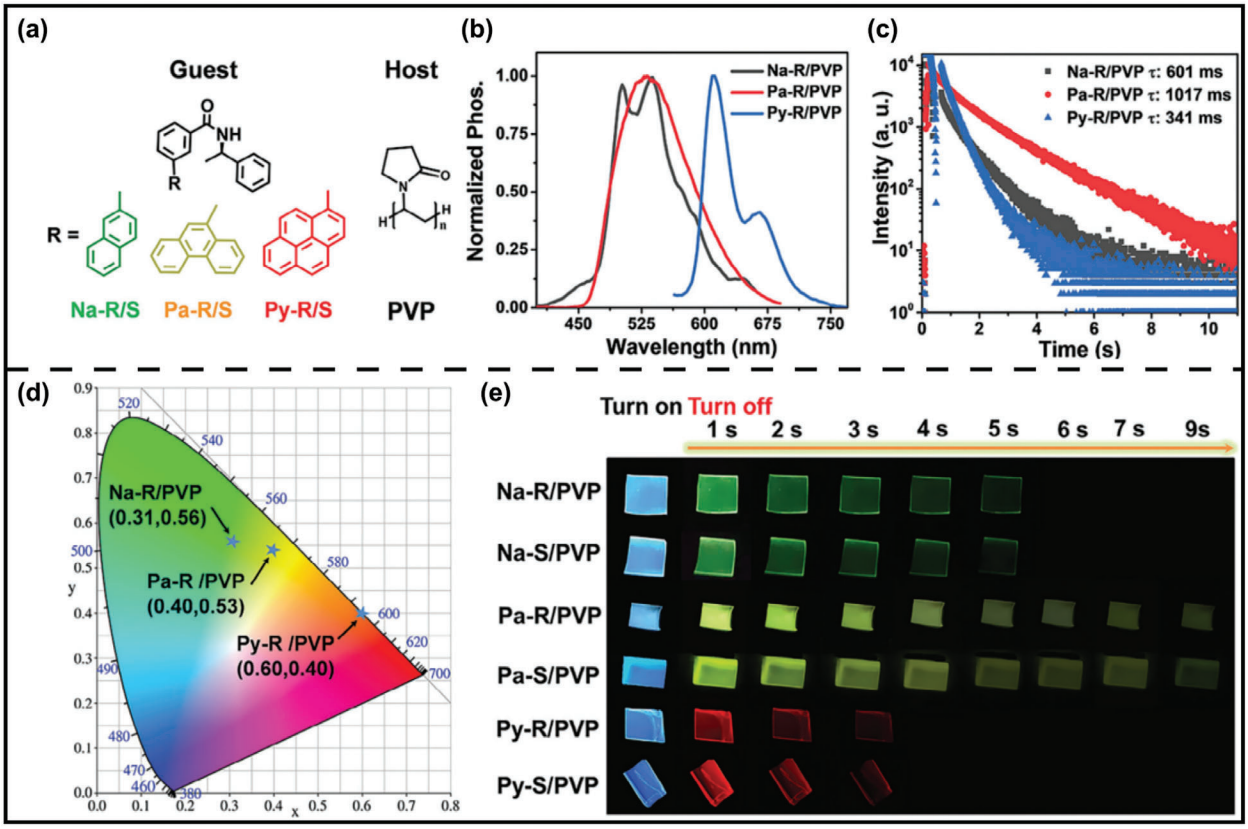

Figure 5. a) Molecular structures of the materials made of the host (PVA) and guest (Na-R/PVP, Pa-R/PVP, and Py-R/PVP). b) PL spectra, c) phosphorescence decay curves, d) CIE coordinates, and e) Luminescence photographs of all materials. Reproduced with permission.[176] Copyright 2023, John Wiley and Sons.

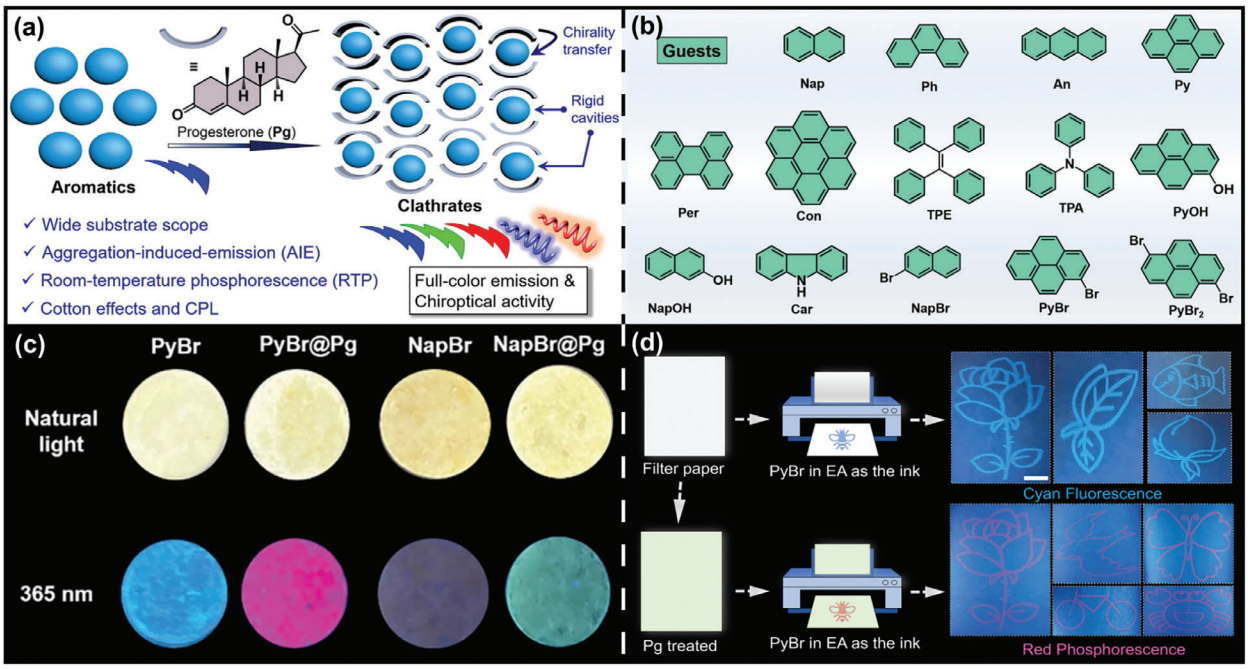

Figure 6. a) Host–guest complexation between progesterone (Pg) and aromatics enables the full-color emission and chiroptical activity. b) Chemical structures of various guests. c) Photographs of the samples under natural light and the irradiation of 365 nm UV. d) Multiple color demonstration based on pyrene bromide (PyBr) in ethanol (EA) as the ink. Reproduced with permission.[178] Copyright 2022, American Chemical Society.

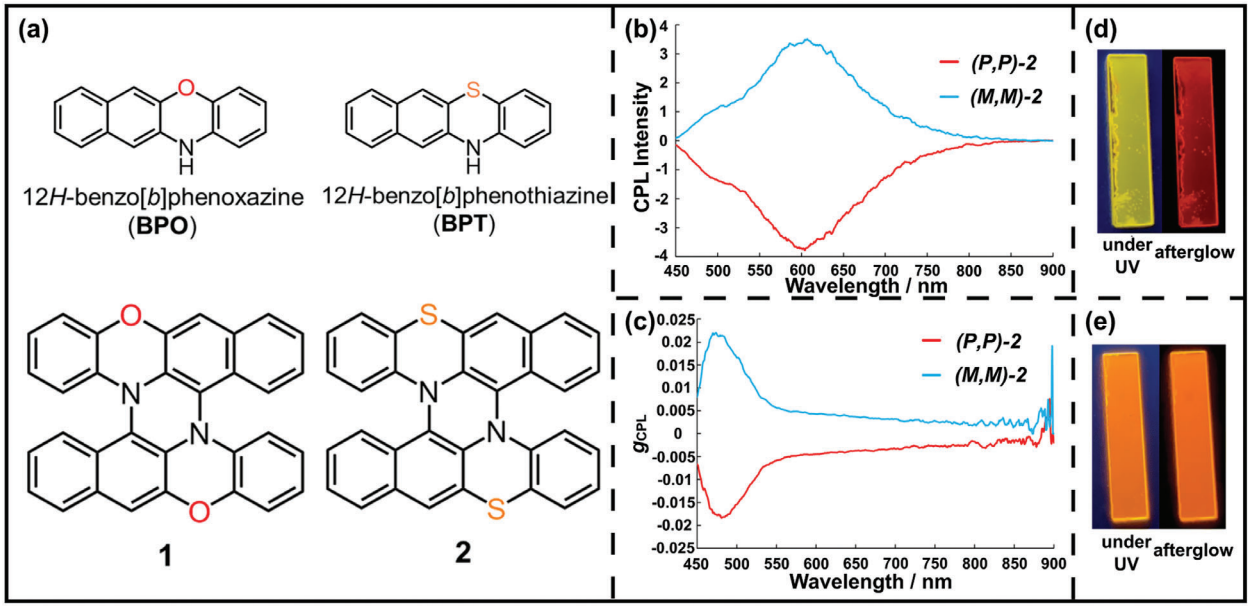

Figure 7. a) Structures of double heterohelicenes 1, 2 and their monomers. b) CPL spectra and c) g_{CPL} of 2 doped in β-estradiol. d,e) Photographs of 1 and 2 doped in β-estradiol upon the excitation of 365 nm UV and after turning it off. Reproduced with permission.[185] Copyright 2023, Royal Society of Chemistry.

guests, depending on their geometry. The intrinsic chirality of Pg enabled the chirality transfer to aromatic moieties, resulting in the full-color luminescence and the realization of circularly polarized room temperature phosphorescence (CPRTP). The interaction between Pg and pyrene bromide (PyBr) in host–guest complexation facilitated the selective presentation on various substrates (Figure 6d). This work demonstrates the utility of the steroid complexation as phosphorescent materials, which shows great potential a promising candidate for developing CPRTP materials.

Heterohelicenes have recently garnered considerable interest as promising materials with outstanding electronic and optical properties due to their chirality, including distinctive chiroptical features.[183,184] Recently, Hideki Fujiwara et al.[185] put forward a novel method to achieve a double *N, S*-hetero[5]helicene (compound 2) consisting of two benzo[*b*]phenothiazines (BPT), which demonstrated CP-OURTP properties (**Figure** 7a). Compared with the *N,O*-analogue consisting of two benzo[*b*]phenoxazines, compound 2 exhibited stronger phosphorescence with an extended lifetime of 0.16 s in a frozen solution at temperatures near that of liquid nitrogen when doped into a β-estradiol matrix. The films of (*P, P*)- and (*M, M*)-2 in β-estradiol showed mirror images (Figure 7b,c), and different afterglows after switching off UV light (Figure 7d,e). The weak fluorescence shoulder bands were observed at 500 nm with g_{CPL} of 1.7×10^{-2} and the CPL at 600 nm was from CPP with g_{CPL} of 5×10^{-3}. Compound 2 is a distinct representative of organic helicenes that exhibits CP-OURTP without aggregation.

CP-OURTP materials represent a burgeoning research frontier with promising prospects across diverse fields due to their extended triplet states and extended emission properties. Subi J. George et al.[146] designed a bischromophoric molecule which was made of enantiomeric diaminocyclohexane (DAC) chiral core, modified with pyromellitic diimide (PmDI) phosphor to realize the solution-processable, ambient CP-OURTP emission. The solution-processable polymer films, composed of (*RR*)/(*SS*)-BrPmDI and (*RR*)/(*SS*)-Br2PmDI within PMMA matrix, exhibited the mirror-image CPP emissions (**Figure** 8a–c) with high phosphorescence quantum yields ranging from 10% to 18% and significant g_{lum} values from 1.3×10^{-3} to 4.0×10^{-3}. To be specific, the existence of carbonyl groups and heavy atoms was capable of promoting the ISC to realize the phosphorescence in the monomeric states. This strategy provides a valuable design map for constructing CP-OURTP materials.

2.4. CP-OURTP Based on Copolymerization and Host–Guest Doping System

Despite significant progress in developing circularly polarized organic afterglow (CPOA) materials, creating a blue CPOA system with non-radiative transitions, high triplet energy levels, and strong chirality remains a considerable challenge. One potential method to improve CPOA emission is through chiral crystal engineering. However, this method relies on ordered molecular packing, leading to the loss of triplet excitons due to triplet–triplet annihilation and causing a shift of the emission spectrum toward longer wavelengths. In contrast, CPOA emission can undergo a blue shift when a single molecule is effectively confined within a polymer matrix, resulting in the stabilization of triplet excitons for an ultralong lifetime. Based on this principle, a strategy was proposed based on self-confinement of isolated chiral chromophores within a rigid polymer matrix to reduce non-radiative transitions and enhance blue CPOA polymers. These CPOA polymers were synthesized via radical copolymerization with fluorescent materials acting as guests, enabling CPOA emissions with

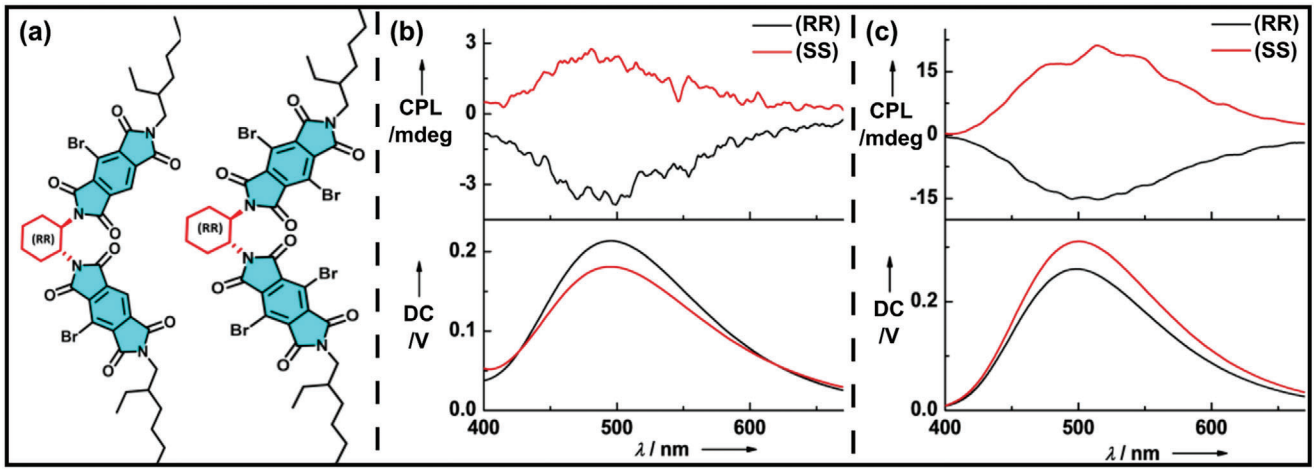

Figure 8. a) Molecular structures of (*RR*)-BrPmDI and (*RR*)-Br2PmDI. b,c) CPL and direct current (DC) spectra of (*RR*/*SS*)-BrPmDI and (*RR*/*SS*)-Br2PmDI. Reproduced with permission.[146] Copyright 2022, John Wiley and Sons.

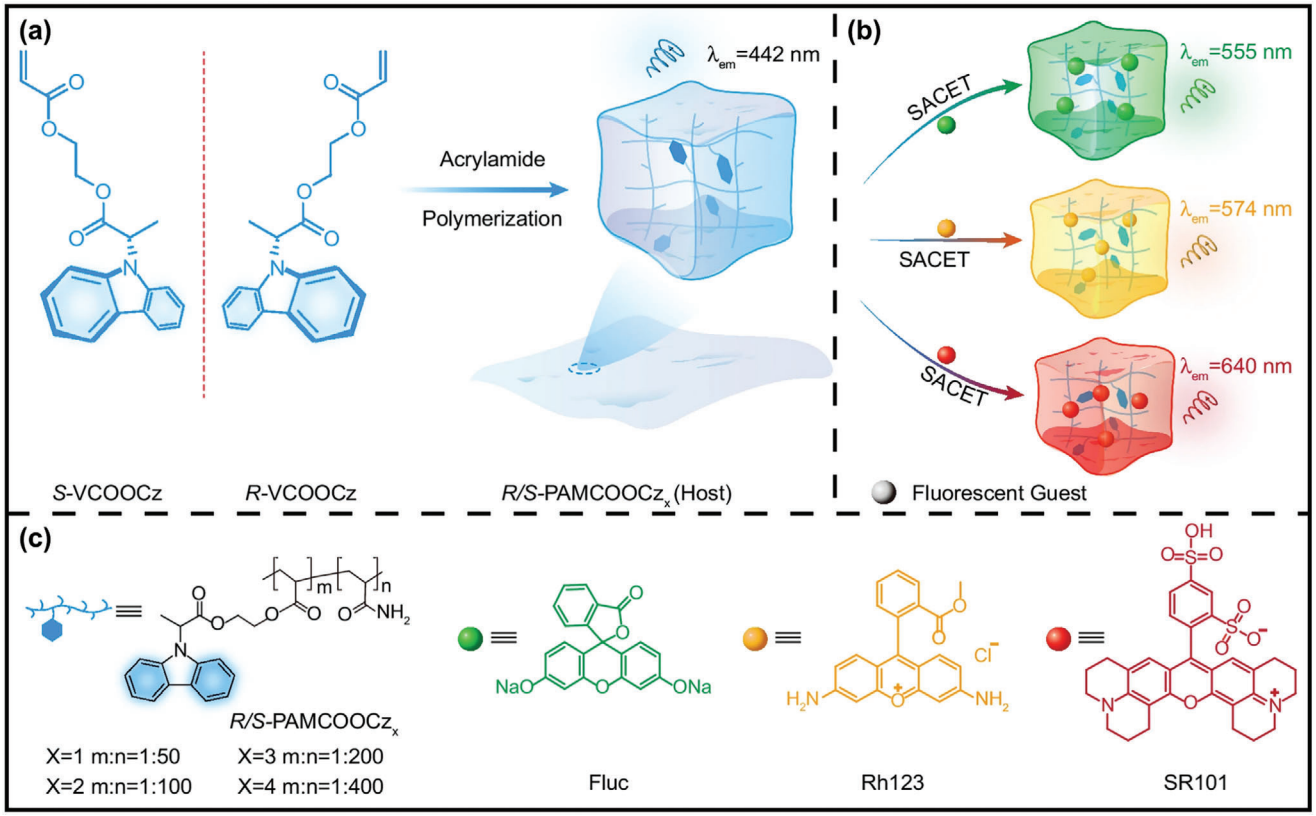

Figure 9. a) Schematic diagram of blue circularly polarized organic afterglow (CPOA) polymers for full-color afterglow emission. b) Full-color CPOA polymers obtained by synergistic afterglow and chirality energy transfer (SACET). c) Molecular structures of *R*/*S*-PAMCOOCZ$_x$ (X = 1–4), Fluc, Rh123, and SR101. Reproduced with permission.[186] Copyright 2024, Springer Nature.

green, red, and even white. Developing a blue CPOA system with non-radiative transitions, high triplet energy levels, and strong chirality poses a significant challenge. Huang, Chen, Tao, and co-workers[186] have proposed a straightforward approach to realize the blue CPOA through self-confining chiral chromophores into the rigid polymer matrix to enhance blue CPOA polymers (**Figure 9**). Interestingly, by leveraging the synergistic afterglow and chirality energy transfer (SACET), CPOA polymers with tunable color ability were successfully obtained through incorporating colorful fluorescent guests with green, red, and even white CPOA emission (Figure 9b). Chiral polymers *R*/*S*-PAMCOOCzX (X = 1–4) were produced via radical copolymerization, employing

the self-engineered chiral monomer of *R*/*S*-VCOOCz and acrylamide with molar ratio of 1:50, 1:100, 1:200, and 1:400, respectively (Figure 9c). The existence of strong hydrogen bonds provided a stabilized molecular state of chiral chromophores, resulting in the CPOA polymer with blue emission, and a g_{lum} value of $\approx 10^{-2}$. This study establishes a foundation for the streamlined design of blue CPOA materials, confirms the viable approach of SACET to fabricate the full-color CPL materials, and expands their potential applications in various fields.

2.5. CP-OURTP Based on Spinning and Twisting Technology

CP-OURTP fibers can be produced by wet spinning technique, followed by mechanical twisting in a dry state with the assistance of PVA and quinoline derivatives. In this strategy, the quinoline derivatives act as organic phosphors guests within the PVA aqueous solution. This solution is extruded into a specialized coagulation bath, where the phase separation takes place via a double diffusion process governed by the concentration gradient. After the solvent is removed by heating, fibers embedded with quinoline derivatives and exhibiting RTP properties are obtained. These dry fibers are then twisted to form helical structures with different helical directions. The phosphorescence behavior of the organic phosphors is facilitated by the hydrogen bonding interaction between quinoline molecules and PVA polymer chains. The helical structure of twisted fibers forms a chiral medium that enables CP-OURTP through selective reflection and transmission. Producing CP-OURTP materials with more versatility, simplicity, and practicality remains challenging. Cheng, Zhang, and coworkers[187] prepared the novel CP-OURTP material using a combination of wet spinning and twisting technique, which yielded the continuous fabrication of RTP fibers with twist helical chirality, and the multiple characteristics of flexibility, handedness, phosphorescence, knittability in a single system (**Figure 10**a). To be specific, PVA was chosen for incorporating three quinoline derivatives with amino, hydroxy, and carboxy groups, respectively. By leveraging the hydrogen bonding interactions between each other, coupled with the rigid environment provided by PVA, the Q-NH_2@PVA (Figure 10b) fiber exhibited the remarkable phosphorescent properties with a lifetime of 1.08 s and a quantum yield of 24.6%, along with the enhanced tensile strength. The mechanism for producing CPRTP fibers was shown in **Figure 11**c. Remarkably, the CP-OURTP was obtained by imparting left- or right-handed helical structure through basic twisting, facilitating the mass generation of chiral Q-NH_2@PVA fiber with a g_{lum} value of 10^{-2}. The helical microstructures led to the conversion of PVA-based fibers into CPRTP fibers, thereby creating new possibilities for the fabrication of CP-OURTP materials, that can be applied in cutting-edge anti-counterfeiting technology.

2.6. CP-OURTP Based on Supramolecular Polymer Assembly

In the existing approaches for CPP materials, the method of the crystallization of chiral phosphors faces many disadvantages, such as the limited flexibility, stretchability, poor processability. Meanwhile incorporating phosphors into amorphous polymer matrixes yields unsatisfied chiroptical signals due to the lack of chirality communication. In addition, the majority of advanced RTP materials have been restricted to the solid-state applications due to the quenching effect of dissolved oxygen on triplet excited states and free molecular motion in liquid states. Therefore, extensive endeavors have been dedicated to the omnipotent CPL materials through supramolecular assembly. The supramolecular polymers with various functionalities including reversibility and responsiveness have been rapidly developed.[188,189] Supramolecular polymers composed of disordered and intertwined coils demonstrate the flexible and elastomeric mechanical characteristics, processability, recyclability, and self-healing abilities due to their reversible transitions between monomeric and polymeric states. In addition, supramolecular polymers play an important role in soft materials due to their tunable, dynamic, and responsive characteristics. Ma et al.[190] developed the soluble helical supramolecular polymers with CP-OURTP properties by host–guest doping. The transformation from predominant fluorescence to nearly exclusive RTP emission was accomplished through assembly. Accordingly, the terminal groups of a two-branched chiral monomer (AHBP) were encapsulated within the cavity of CB[8],[191] as illustrated in Figure 11, leading to the formation of a head-to-tail helical supramolecular polymers (SPs). These SPs exhibit the sustained RTP due to the charge-transfer triplet state within the CB[8] cavity. In this helical supramolecular polymerization, CPRTP with a g_{lum} of 2.2×10^{-3} was obtained in water. This approach for realizing CPRTP based on helical supramolecular polymers paves the novel way for the streamlined design of the intelligent functional materials.

Kim et al.[192] had developed a novel chiral self-assembly approach to achieve CP-OURTP by incorporating chiral chains into purely organic phosphors for obtaining the bright CP-OURTP (**Figure 12**). The CP-OURTP molecules were constructed from an aromatic carbonyl framework, leveraging the heavy atom effect of bromine (Br) to enhance the spin–orbit couplings (SOCs) and facilitate the ISC, consequently enabling the bright CP-OURTP.[193–199] The chiral chains were deliberately designed to possess robust hydrogen bonding, van der Waals interactions, and a chiral center to guide the chirality of the self-assembled supramolecular nanostructures. The obtained densely packed supramolecular nanostructures restricted the molecular motions, reducing the non-radiative decay and enhancing the emission of CP-OURTP. These small purely organic phosphors can self-assemble into the supramolecular nanostructures via helical assembly, depending on the left-handed or right-handed chirality of the side chain (Figure 12a,b). LGluP and DGluP self-assembled to nanofibers (NFs), which subsequently transformed into *M*-helix (left-handed) and *P*-helix (right-handed) helical nanofibers, respectively. These helical NFs emitted blue circularly polarized fluorescence (CPF) from a singlet state at 410 nm (Figure 12c). The self-assembly process resulted in the formation of nanobundle with green CP-OURTP from a triplet state at 500 nm (Figure 12d). The self-organized supramolecular structures exhibited CP-OURTP with a g_{lum} value of appropriately 10^{-3}, a lifetime of 180 ms and the quantum yield of 4.1%. The proposed molecular design for CP-OURTP will open up a novel path for the fabrication of cutting-edge luminescent materials.

Various strategies have been developed to construct the intriguing CP-OURTP materials involving chiral aggregates

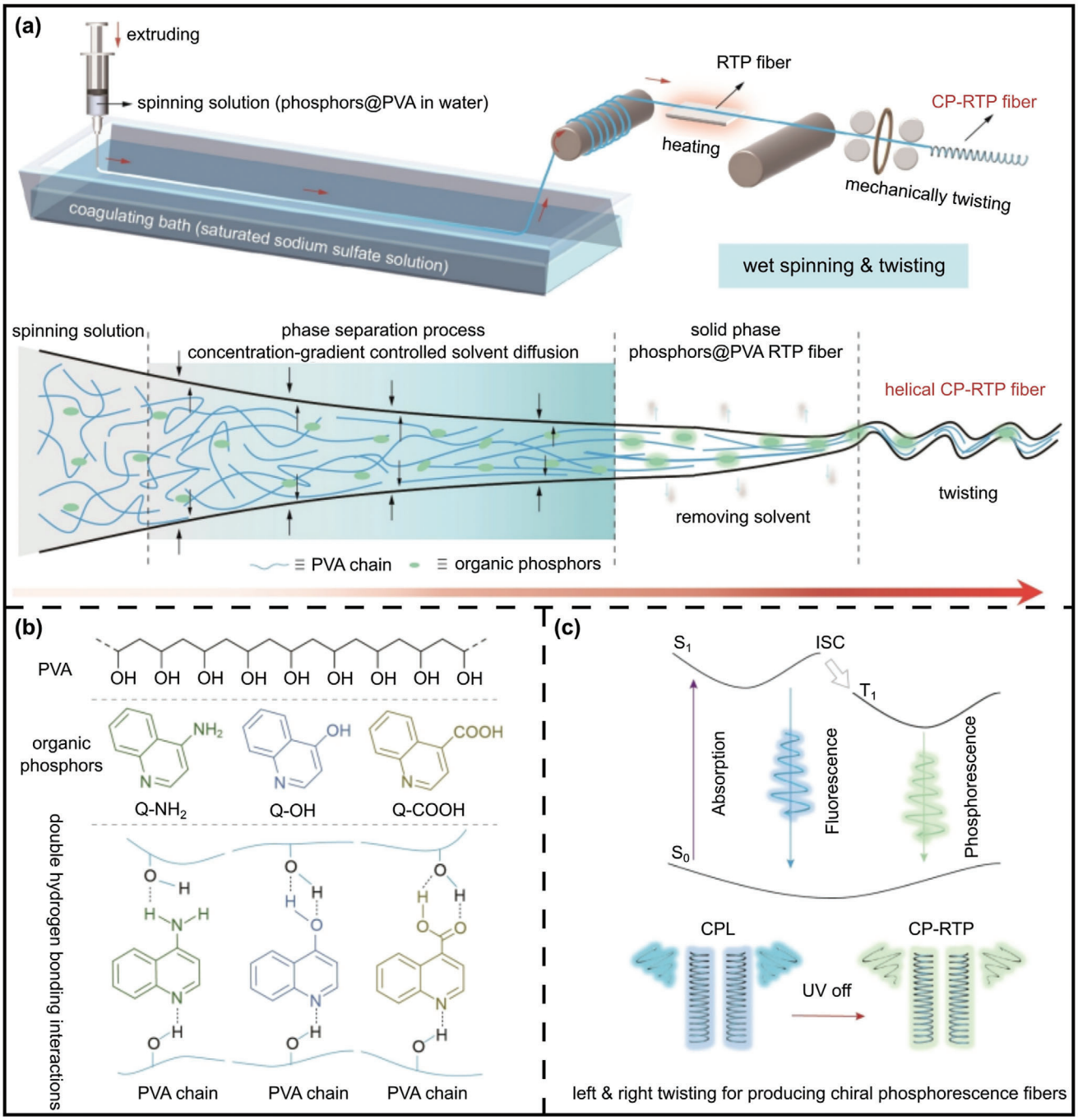

Figure 10. a) Schematic illustration of CPRTP fibers by wet spinning and twisting technique. b) Chemical structures of PVA and three quinoline derivatives, and the double hydrogen bonding interactions. c) Underlying mechanism of CPRTP fibers. Reproduced with permission.[187] Copyright 2024, John Wiley and Sons.

through supramolecular self-assembly methods[188] owing to the ineffective intra-/intermolecular $\pi-\pi^*$ electronic coupling, which is urgently needed for generating strong chiral signals. For RTP polymers, the luminous and persistent emission typically arise from isolated chromophores. It is highly desirable to design molecules exhibiting the decent CP-OURTP behaviors at the monomeric level and possessing the remarkable advantages such as versatile tunability, cost-effectiveness, and excellent biocompatibility. Tremendous endeavors have been dedicated to achieving dynamic control over the amplification or inversion of CPL.[200–202] Particularly, the precise photo-induced control of CPL can be achieved through the incorporation of photoactive chromophores.[203,204] However, accurately quantifying chiroptical signals through the molecular chiral packing remains

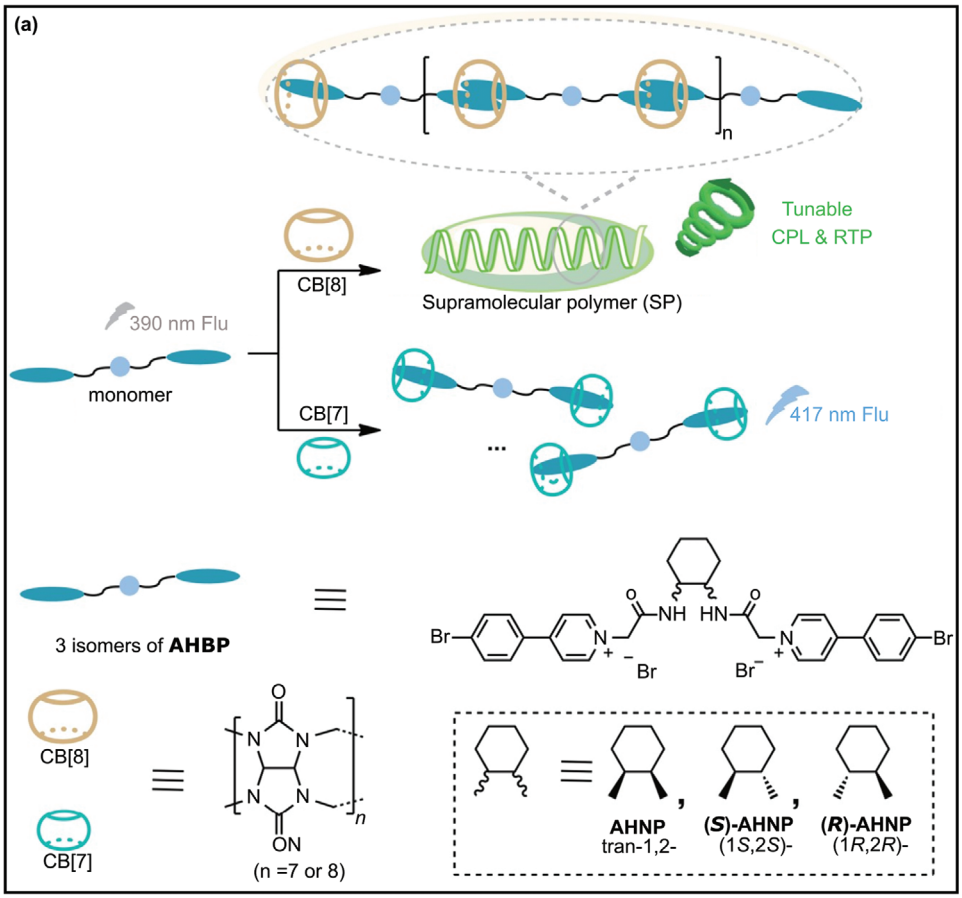

Figure 11. Design of the complexation of by using the monomer with CB[8] or CB[7] to generate the supramolecular polymers (SPs) to produce CPL and RTP. Reproduced with permission.[190] Copyright 2021, Springer Nature.

challenging. Zhu and co-workers[205] reported an efficient and flexible strategy for rationally manipulating the CP-OURTP of solid-state materials composed of closely packed molecules, by utilizing microphase separation through the assembly of a chiral block copolymer (cBCP) polystyrene-b-poly(L-lactide) (PS-b-PLLA) with a nonchiral luminophore based on hexathiobenzene (M-1) (**Figure** 13a). cBCP stands as a typical macromolecular system with ordered nanofeatures in solid state, enabling the self-assembly by two segments with polarity and rigidity differences. The CP-OURTP signal of the supramolecular assembly increased in the initial state as the proportion of luminophore to cBCP was added, until reaching a critical threshold. As expected, further increasing the proportion of luminophore resulted in a decrease of CP-OURTP signal, which was ascribed to the stretched helical pitch of M-1@PLLA (poly(L-lactide)) domain. It should be noted that the helical pitch of the molecular aggregation system retracted as the CP-OURTP signal recovered, driven by the photoexcitation-triggered molecular aggregation of M-1. More specifically, a chiral skeleton composed of PS-b-PLLA, was co-assembled with M-1 by hydrogen bonding (Figure 13a). M-1 was able to tailor the pitch of the helical nanostructures within M-1@PLLA domains (Figure 13b), thereby influencing the CP-OURTP signal in M-1@PLLA domain as the ratio of M-1 to cBCP changed. The helical microphase-separation could be observed due to the steric $\pi-\pi$ stacking. The mechanism of photoexcitation-induced molecular aggregation can be explained by the molecular conformational change of C1—C2—S—C3 bond (Figure 13c). This photoexcitation-induced molecular aggregation is a valid approach for rationally manipulating the supramolecular chiropticity of solid-state materials.

3. Enhancing CP-OURTP in Chiral Soft Materials

Keeping pace with the fast growth and progress in science and technology, numerous soft materials have made critically important strides into mainstream applications in luminescent soft materials. Soft materials, like liquid crystals (LCs), as one of the self-assembled supramolecular architectures, represents an intermediate phase or state of matter demonstrated by mesogens. LCs maintain the unique properties between isotropic liquid state and crystalline solid state with both positional order and orientation order.[206] Generally, LCs are classified into two categories, that is, thermotropic and lyotropic LCs (LLCs), depending on the way of the mesophases are obtained whether by varying the temperature or changing the concentration of the solution.[207,208] Thermotropic LCs can exhibit different mesophases associated with the changing of the temperature within a certain range, which consist of mesogenic compounds that showcase a range

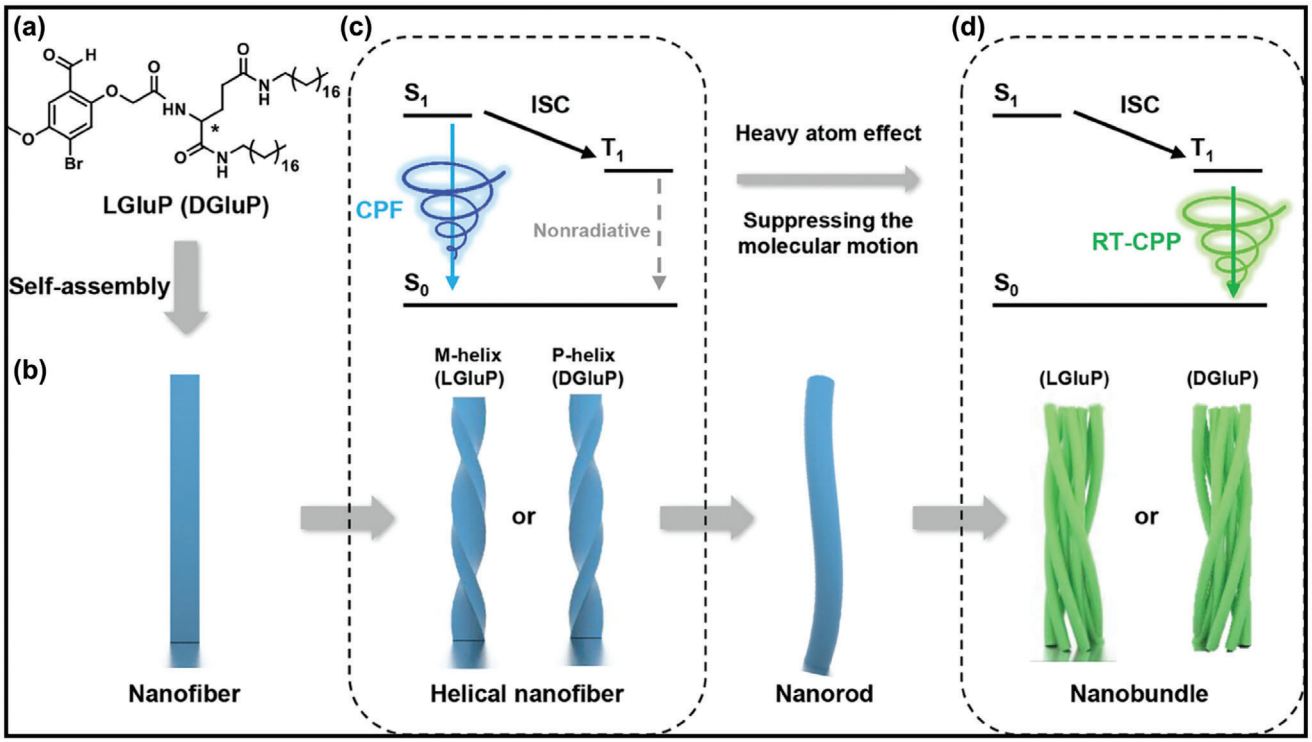

Figure 12. Schematic illustration of purely organic phosphors for self-assembled supramolecular helical nanostructures with CP-OURTP. a) Chemical structures of LGluP and DGluP. b) Self-assembly mechanisms from nanofiber to nanobundle. c) Excitation energy diagram of helical nanofiber and d) nanobundle. Reproduced with permission.[192] Copyright 2024, John Wiley and Sons.

of molecular geometries, including rod-like, disk-like, bowl-like, banana-shaped structures.[209–212] LLCs, which are of paramount importance in living matter as well as biological science, demonstrate a variety of mesophases including nematic, cholesteric, cubic, lamellar, and columnar phases. The formation of lyotropic LC depends on the concentration of anisotropic suspensions containing amphiphilic compounds dissolved in suitable solvents over a range of concentrations and temperature,[6,213–219] such as aqueous solutions of deoxyribonucleic acid (DNA), tobacco mosaic virus (TMV), carbon nanotubes, anisotropic nanorods, graphene derivatives, and cellulose nanocrystals (CNCs).[220–222] LCs, such as nematic, chiral nematic, smectic, blue phase, and cubic phases with intriguing optical properties, have been widely employed for fabricating functional materials.[46,206]

LCs are omnipresent in biological systems, where their chirality serves as an elegant and unique characteristic in specific plant tissues, as well as in the cuticles of various organisms such as arthropods, crabs, beetles, and many others.[223–225] Drawing inspiration from nature, scientists have recently dedicated substantial endeavors to developing chiral LC materials with self-assembled nanostructures and investigating their possible applications spanning from dynamic photonics to addressing energy and safety concerns.[217] The first LC phase was identified as a chiral nematic phase (cholesteric phase, CLCs),[226] which was observed in the cholesteryl benzoate by Reinitzer in 1888.[227,228] CLCs, functioning as responsive soft materials, can be obtained by doping the chiral compounds into the achiral nematic LCs.[229–232] One of the fascinating features of CLCs is the ability to selectively reflect circularly polarized light (photonic bandgaps, PBG) according to the Bragg's law.[233] This phenomenon allows CLCs to reflect light of the same handedness as the helix twist of helicoidal superstructure, but transmit the opposite handedness.[234–236] The self-organized periodic helical arrangements can also be observed in the cuticles of beetles and *pollia* fruit.[237] Nature systems such as cuttlefish, morpho butterfly wings, octopus, etc., are able to manipulate light due to their photonic helicoidal structural color.[238–240] Inspired by these living organisms, significant endeavors have been focused on the manipulation of light in CLCs.[234] The CLCs can reflect light within the visible spectrum. The wavelength λ of the reflected light can be characterized as

$$\lambda = np\cos\theta \tag{1}$$

Here, n denotes the average reflective index of the materials, while p represents the helical pitch of the CLCs. p is determined by the distance over which the director of CLCs rotates a complete 360°.[241] θ signifies the angle formed between the helix axis and the incident light.[242] The cholesteric helix can be viewed as a one-dimensional (1D) photonic crystal, with its bandgap determined by parameters such as p, n, and θ.

CPRTP can be achieved through organic crystal aggregation, where the conformation of the twisted molecules is fixed, thereby restricting chiral small molecule motion within the crystalline state. The restricted lattice structures allow for the observation of long-persistent phosphorescence, as the molecules form a highly ordered packing arrangement. The g_{lum} values in the range of 10^{-3} to 10^{-2} are attributed to the chiral structures of the twisted

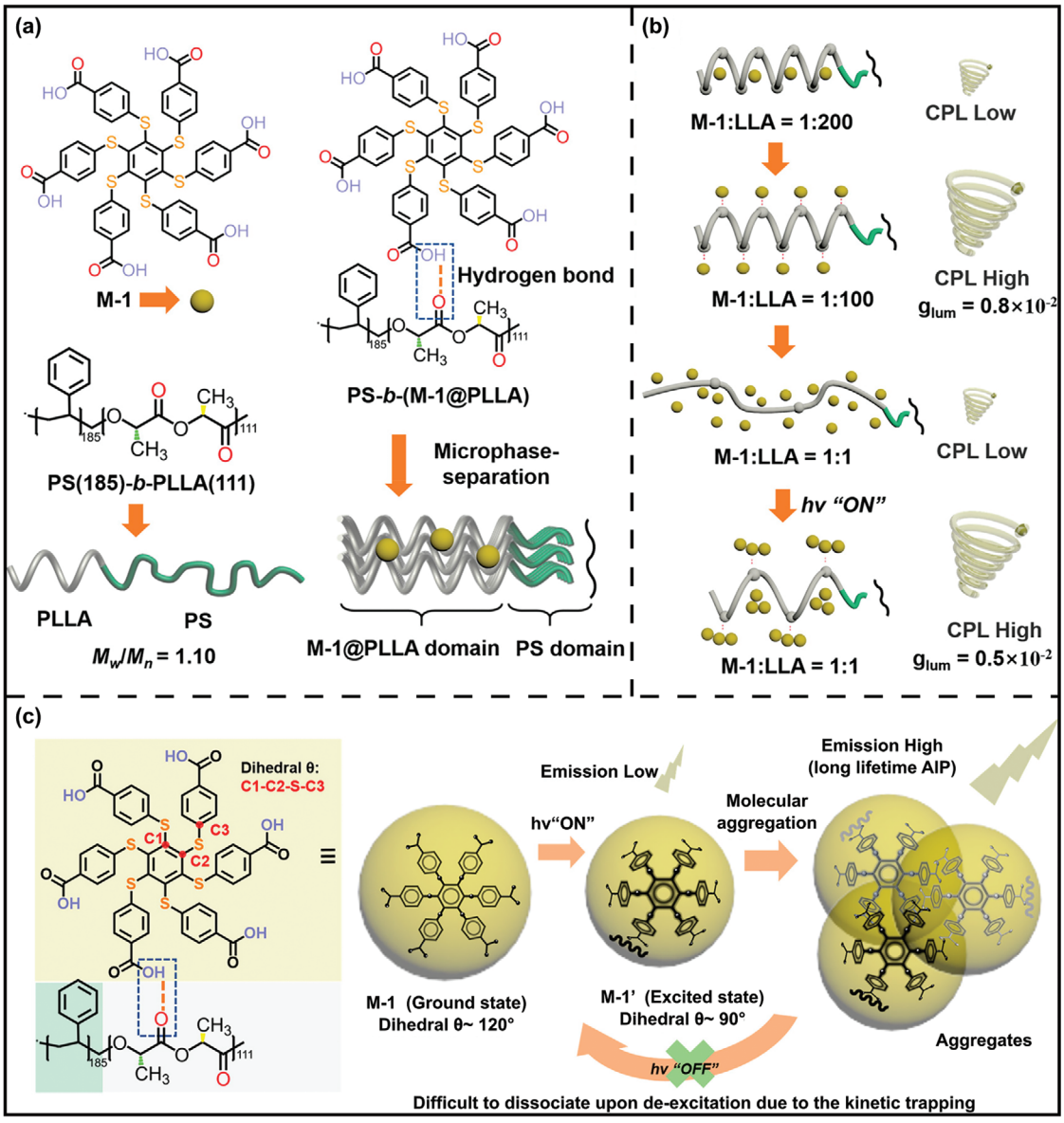

Figure 13. a) Chemical structures of hexathiobenzene (M-1) and polystyrene-b-poly(L-lactide) (PS-b-PLLA), supramolecular system of PS-b-(M-1@PLLA), and microphase-separation upon self-assembly. b) Method for CPL by controlling the ratio of M-1 to PS-b-PLLA. c) Conformational change of C1—C2—S—C3 bond in the hexathiobenzene-based skeleton due to molecular aggregation. Reproduced with permission.[205] Copyright 2022, American Chemical Society.

molecules caused by the strongly restricted chiral environment. Moreover, efficient CPRTP can be achieved through copolymerization of isolated chromophores with axial chirality within polymer chains under ambient conditions. Binaphthol derivatives with axial chirality, can be covalently bonded to polymer chains containing rich carboxylic groups. These groups can enhance the ISC process, boosting the generation of triplet excitons and effectively constraining the molecular motions of phosphors by forming a rigid polymer network. The incorporation of axial chiral chromophores into polymer chains enables the copolymers to exhibit CPRTP with a g_{lum} value of 10^{-3}. Additionally, the CPRTP can be produced through the interaction between chiral chromophores and a chiral environment, which restricts the motions of chiral small molecule within rigid host matrix. By purposely introducing chiral molecules into rigid polymer matrix, CPRTP with g_{lum} values on the order of 10^{-2} are achieved. The use of wet spinning and twisting technique allows for the continuous production of RTP fibers with twisting-induced helical chirality. The hydrogen bonding interactions and the rigid microenvironment provided by PVA chains, enable the distinct phosphorescent properties of fibers. The resulting fibers exhibit CPRTP with a g_{lum} of 10^{-2}, which are produced by introducing left- or right-hand helical structures through twisting. In supramolecular systems, the chirality of the side chain directs the chirality of the self-assembled supramolecular nanostructures, while the tightly packed supramolecular structures restrict molecular motions,

resulting in bright phosphorescence emission. These small organic phosphors self-assemble into supramolecular nanostructures via helical assembly based on the left-handed or right-handed chirality of side chains, forming large-scale chiral assembly by non-covalent interactions like hydrogen bonding and van der Waals interactions. Organic phosphors with a chiral side chain usually generate CPRTP with g_{lum} between 10^{-3} and 10^{-2}.

The g_{lum} values of reported long-lived CP-OURTP materials using traditional strategies including organic crystal aggregation, copolymerization, host–guest doping, the combination of copolymerization and host–guest doping, spinning and twisting technology, and supramolecular systems, fall within the range of 10^{-3} to 10^{-2}, which are significantly lower than the theoretical maximum of 2.0. These traditional strategies are obviously not effective for the high-performance optical multiplexing. Thus, developing a novel strategy for achieving persistent RTP with elevated g_{lum} values is highly desirable. The distinctions between traditional strategies and chiral soft matter systems, such as CLCs, lie in their ability to amplify chirality and significantly enhance g_{lum} values. CLCs are considered as an exceptional medium for CP-OURTP with ultrahigh g_{lum}. The unique characteristic of CLCs is their PBGs, which selectively reflect circularly polarized light with the same handedness as their helical superstructure while transmitting light with the opposite handedness. By adjusting the positional relationship between PBGs of CLCs and photoluminescent emission wavelengths, the g_{lum} values of CP-OURTP can be modulated from zero to their maximum values. Leveraging the inherent amplification effect of CLCs enables CP-OURTP materials to achieve g_{lum} values two orders of magnitude higher than those attained through traditional strategies.

3.1. CP-OURTP Based on Lyotropic Cellulose Nanocrystals

The latest development in CPRTP research involve the innovative synthetic approaches and emergence of the novel CPRTP materials.[43,243] Strategies for realizing CPRTP involve utilizing chiral phosphorescent organometallic complexes.[36,50,244] However, these methods typically exhibit low g_{lum} ranging between 10^{-3} and 10^{-1}, which often lack the precise control over chirality.[36,245] Smectic LCs composed of chiral organoplatinum complexes, which can generate CPRTP with g_{lum} of 4.0×10^{-2} due to the chirality amplification and LC-stabilized triplet excitons.[46] LLCs can be found in biological macromolecules such as proteins, nucleic acids, and carbohydrates.[217] LLCs are commonly used in templating, as their LC phases are compatible with many precursors, such as desoxyribonucleic acid (DNA) and cellulose nanocrystals (CNCs).[51,246–250] Particularly, chiral nematic CNCs are regarded as the most abundant biosourced materials produced by different organisms (trees, plants, and bacteria) in nature[251–255] that can form LLCs with excellent mechanical properties, optical properties, large specific surface area and electrochemical properties. They are also 1D nanostructures and rodlike lyotropic materials with outstanding characteristics such as recyclability, biocompatibility, wide availability, low cost, and low toxicity.[256] The precisely defined chirality and exceptional dispersion stability of CNCs enable their spontaneous arrangement into a left-handed CLC phase, which can be maintained when CNC suspensions are evaporated to form films.[246,257–260] The resulting helicoidal arrangement endows CNC films with iridescent structural colors and the pronounced circular polarization. Thanks to this inherent capability, CNC can split the incident light into two CPL components through selective reflection and transmission.[261] Due to the left-handed CLC with one-dimensional photonic properties, numerous cellulose nanocrystal-based superstructures have been investigated.[237]

The advancement of CNC-based nanomaterials offers new opportunities for fabricating novel CPL nanomaterials in the fields of biomedicine and nanoscience. CNC films, characterized by their cholesteric structures, are capable of controlling CPL. The integration of chromophores into chiral photonic crystals by using CNCs as a chiral bio-template to manufacture composites enables the precise regulation of spontaneous emission within PBGs, and thus resulting in the modulation of CPL. In this regard, Xu, Tang, and co-workers[262] demonstrated chiral nematic silica (CNS) films with on-demand chiroptical properties by evaporation-induced self-assembly (EISA),[260,263] followed by a calcination process at 550 °C for 6 h, resulting in nanoporous CNS films characterized by the defect photoluminescence with the controllable handedness and band wavelength (**Figure 14a**). When the phosphorescence band was modulated to overlap with the selective reflection band of CNS films, right-handed CPRTP (R-CPRTP) was generated, while left-handed CPRTP (L-CPRTP) occurred once the phosphorescence band was located near the selective reflection band of CNS films. Consequently, CP-OURTP with controllable handedness could be obtained with g_{lum} up to −0.130 (R-CPRTP) and 0.093 (L-CPRTP) and the afterglow lifetime of 1.082 and 1.04 s, respectively. By using the same EISA strategy, Liu, Zhang, and co-workers[164] synthesized hybrid photonic films with dual CPL and RTP through the co-assembly of CNCs, PVA, and carbon dots (CDs) (Figure 14b). CDs, as remarkable inorganic phosphors, exhibit outstanding characteristics, such as the tunable photoluminescence, excellent biocompatibility, high emission intensity, high chemical stability, and easy functionalization. These properties effectively address the drawbacks involving inherent toxicity by using heavy metals in their production,[264–266] making them highly desirable for biomedical applications. Fluorescence emission of quantum dots (QDs) embedded in LCs are able to produce CPL signals, which can be modulated either optically or electrically through changes in the helical arrangement of the LC matrix. In addition, CDs can be incorporated into CNC films to obtain CPL. By changing the ratio of CNC and PVA, the CP-OURTP with reversible handedness, tunable wavelengths, and an absolute g_{lum} value up to 0.27 was achieved. Specifically, the triplet excitons generated by CDs demonstrated distinct stability within the chiral photonic crystal surroundings, resulting in the adjustable right-handed CP-OURTP with an absolute value of g_{lum} up to 0.47. This provides a facile methodology for fabricating CP-OURTP materials that can be potentially used in optoelectronic.

Developing security materials that can hide needed information promote the development of the anti-counterfeiting technology. Circularly polarized long afterglow (CPLA) has garnered significant attention in security fields due to its distinct optical characteristics, such as prolonged afterglow and circular polarization, a combination of time-dependent and intensity-dependent characteristics. Zhuang et al.[267] successfully

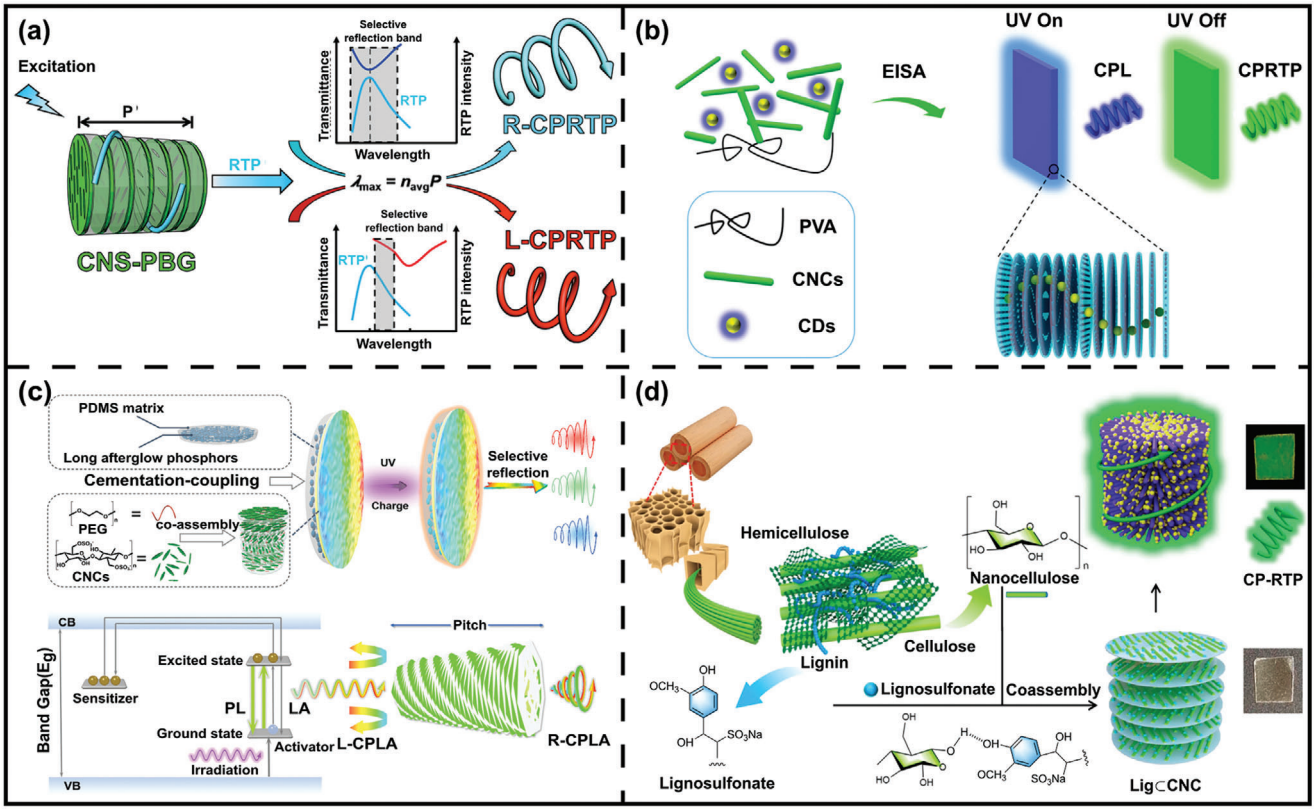

Figure 14. a) Left-handed chiral nematic nanoporous silica (CNS) films with the presence of defect phosphorescence. Reproduced with permission.[262] Copyright 2022, John Wiley and Sons. b) Schematic diagram of hybrid photonic films demonstrating dual CPL and CP-OURTP via evaporation-induced self-assembly (EISA) strategy. Reproduced with permission.[164] Copyright 2020, American Chemical Society. c) Fabrication and characterizations of circularly polarized long afterglow (CPLA) films. Reproduced with permission.[267] Copyright 2023, John Wiley and Sons. d) Schematic illustration for the preparation of the sustainable CP-OURTP material. Reproduced with permission.[268] Copyright 2024, Springer Nature.

fabricated a phosphor-CNCs-based bilayer-device with full-colored CPLA architectures, which consisted of the phosphorescence layer by embedding phosphors into a polymer (polydimethylsiloxane)(PDMS) and CNCs membrane (Figure 14c). This device exhibited the on-demand performance with a large g_{CPLA} of −0.67 and a long lifetime of 40 min which can be applied as a security label by taking the combinational advantages of circular polarization and persistent afterglow attributes. Remarkably, the complexity of information encryption was enhanced by the introduction of both time and intensity variations, presenting possibilities for advanced security technologies. Chen et al.[268] introduced biobased thin films exhibiting CPL with simultaneous RTP (Figure 14d). Phosphorescence-active lignosulfonate biomolecules were assembled with CNC in a chiral architecture. The lignosulfonate captured the chirality induced by CNCs within the films, resulting in the emission of CP-OURTP with a g_{lum} of 0.21 and a phosphorescence lifetime of 103 ms. Unlike traditional organic phosphorescent materials, this chiral system exhibited phosphorescence stability, showing no significant degradation in the extreme chemical environment. Additionally, the luminescent films, which exhibited resistance to water and humidity, were completely biodegradable under soil conditions. This resulting bio-based, environmentally friendly system for CP-OURTP is anticipated to provide a new avenue toward the advanced security technologies.

CNC films can serve as an outstanding chiral hosts or templates for integrating luminescent materials like CDs, silica, and dye, resulting in strong CPL. Nonetheless, there have been few reports on CNCs-based CP-OURTP, particularly lacking the control over handedness inversion and CPL wavelength. The majority of CP-OURTP materials reported thus far utilize the rigid environment to inhibit the non-radiative transitions for enhancing the phosphorescence, thereby constraining their stimulus-responsive capability. Recently, Ye, Meng, Duan, and coworkers[269] successfully fabricated the chiral luminescent films by incorporating the phosphors doped polymethyl methacrylate (PMMA) in CNCs, enabling the switchable handedness with an absolute g_{lum} value of 0.49 (**Figure 15**). Within these films, the phosphors functioned as guest emitters to produce both fluorescence and phosphorescence, the polymer matrix served as the host for RTP, and simultaneously the CNCs film behaved as a circularly polarized filter. The hybrid chiral luminescent films were fabricated by infiltrating CNCs films with polycyclic aromatic hydrocarbons (naphthalene, NP, and pyrene, PP) doped PMMA matrix, which were denoted as NP-CNC and PP-CNC, respectively (Figure 15a,b). Moreover, the dynamic modulation of CPRTP and CPF was realized under the irradiation of UV to reduce the triplet oxygen quenching. The tunable PBG of CNCs films permitted the modulation of the structural colors (Figure 15c,d), chirality, and wavelength of CPRTP and CPF

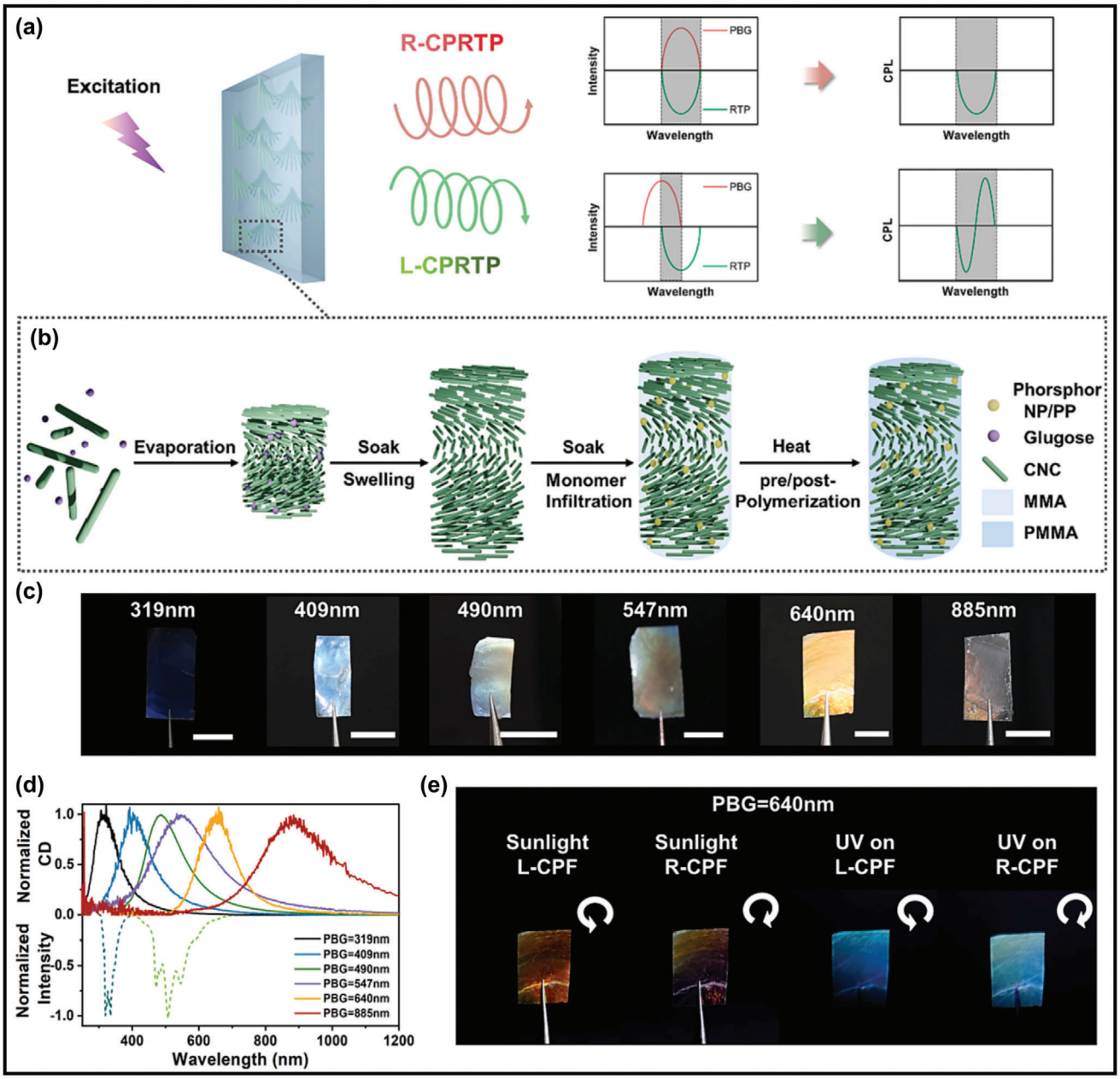

Figure 15. a) Schematic diagram for CPL/CP-OURTP and b) fabrication process of a hybrid film utilizing cellulose nanocrystals (CNCs). c) Photographs of naphthalene (NP)-CNC films. d) Circular dichroism and emission spectra of NP-CNC-films. e) Photographs of NP-CNC-640 under sunlight under left-handed circularly polarized filter (L-CPF) and right-handed circularly polarized filter (R-CPF), the irradiation of UV under L-CPF and R-CPF, respectively. Reproduced with permission.[269] Copyright 2024, Elsevier.

emission. By combining structural colors, fluorescence, phosphorescence, and CPRTP, a versatile security material was developed, capable of encoding diverse information under natural light, UV irradiation, and circularly polarized light. This CNC-based material shows promising applications in information storage, chiral polarizers, and advanced optics. Zhang and co-workers[270] fabricated full-color CPRTP materials by employing anionic cellulose derivatives and ionic achiral luminophores. The ionic achiral groups promoted the spontaneous formation of chiral helical structures through electrostatic repulsion. The anionic cellulose derivatives provided a chiral environment and confined the motion of achiral luminophores. The chirality was transferred to the luminophores driven by the interactions between anionic cellulose derivatives and the luminophores, and the non-radiative transition was suppressed. The resultant materials could be processed into large-scale films and flexible 3D objects with folding and curling characteristics. The phosphorescence of these materials depended on excitation, time, visible light, and they demonstrated multi-responsiveness to temperature, humidity, and pH. These findings provide valuable insights

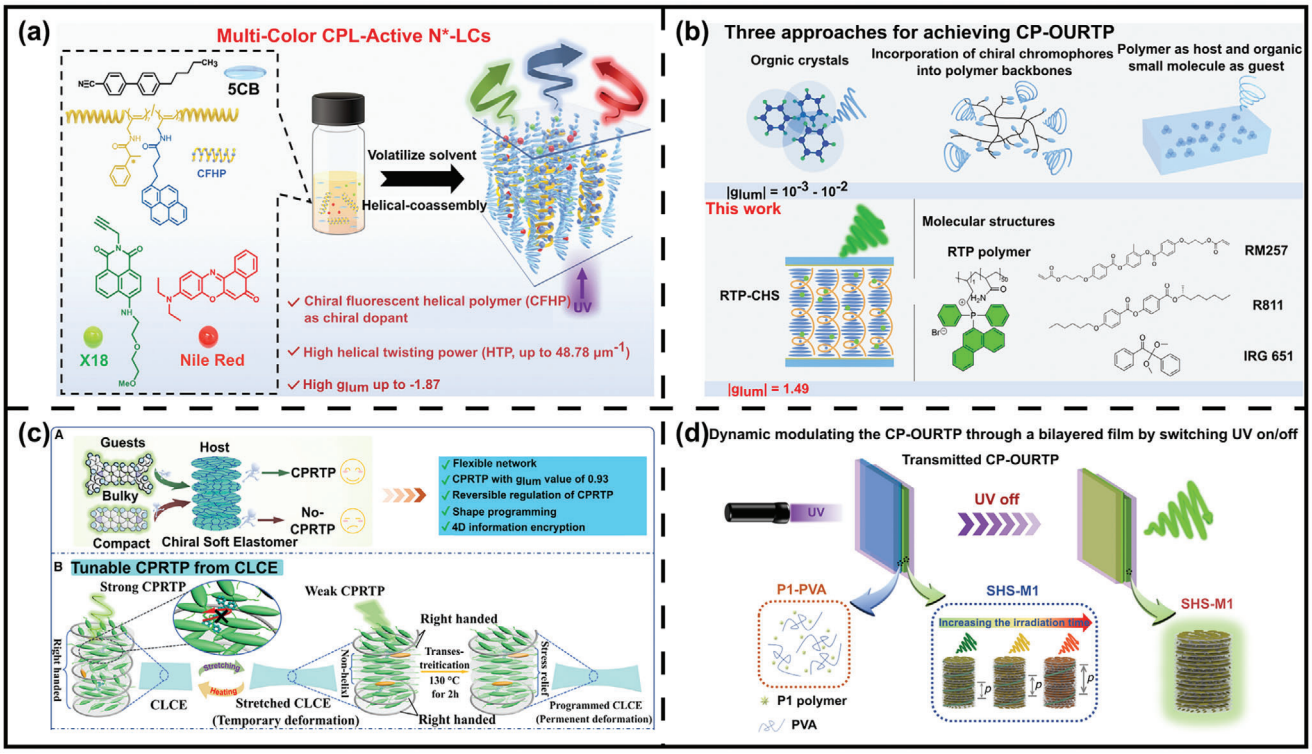

Figure 16. a) Schematic illustration of the multi-color CPL-active CLCs. Reproduced with permission.[273] Copyright 2023, John Wiley and Sons. b) Traditional approaches and new strategy to obtain CP-OURTP. Reproduced with permission.[274] Copyright 2023, John Wiley and Sons. c) Tunable CPRTP from chiral LC elastomer (CLCE). Reproduced with permission.[298] Copyright 2023, Elsevier. d) Dynamic modulation of CP-OURTP via a bilayered film. Reproduced with permission.[314] Copyright 2024, John Wiley and Sons.

for designing advanced optical materials for multilevel information management and chiral sensing. Chen and co-workers[271] developed a polymer-organic molecule with persistent photoluminescence by incorporating acridine flavin (AF) into a PVA matrix. This composite exhibited dual-persistent photoluminescent modes of both TADF and RTP, with long lifetime of hundreds of milliseconds. The rigid PVA network and intermolecular hydrogen-bonding between AF and PVA were crucial for the persistent photoluminescence of AF by confining its triplet excitons under excitation. On this basis, a circularly polarized persistent photoluminescence system was constructed by combining a suspension of AF, PVA, and bio-based CNCs. This organic molecule demonstrated long-lived TADF and RTP within PVA network, and the cholesteric structures of CNCs simultaneously endowed the dual-persistent photoluminescence with a circularly polarized effect.

3.2. CP-OURTP Based on Chiral Thermotropic LCs

Thermotropic LCs are recognized for exhibiting various mesophases as temperature changes within a specific range, consisting of mesogenic compounds with a range of molecular geometries, such as rod-like, bowl-like, and bent-shaped structures. Chiral thermotropic LCs contain a variety of mesophases, including cholesteric phases with helical arrangements, chiral smectic phases that exhibit the spontaneous polarization, double twist blue phases with cubic nanostructures, and twist grain boundary (TGB) phases exhibiting the frustrated helical superstructures.[19,272] LC emerges as an optimal medium for enhancing chirality, which is accessible for ultra-dissymmetric CP-OURTP. Deng et al.[273] developed the bilayered CPRTP device by incorporating 3,6-diphenylcarbazole (DPCz) into a PVA matrix for the RTP film layer, along with a chiral nematic LC layer doped with circularly polarized fluorescence polymer (CPFP) (**Figure 16a**). The resulting bilayered CPRTP device exhibited an afterglow with a lifetime over 18 s at room temperature. The reflection band of CLCs doped with 8 wt% CPFP effectively overlapped with the emission peak of RTP, leading to intense CPRTP with a contrast ratio up to +1.24/−1.57. This approach for the construction of emissive chiral nematic LCs establishes a foundation for future exploration of CPL-active chiral nematic LCs. However, the existing strategies suffer from the inherent limitations such as the inevitable phase separation, inferior flexibility, and the intricate process of selecting a rigid host for the doped composite systems. RTP polymers are outstanding candidates to address these challenges due to their advantageous attributes, including commendable processability, stretchability, and reproducibility. Therefore, it is highly desirable to find a controllable and predictable design approach for developing RTP polymer for practical applications. Polymer LCs offer the superior processability, thermal stability, and possess larger g_{lum} values compared to small molecular LCs, thus expanding their promising applications. Polymer CLCs can be obtained

by photoinduced polymerization, including LC monomers, photoinitiators and chiral dopants. Our group[274] has developed an efficient method for achieving CP-OURTP by employing RTP polymers and chiral helical superstructures (Figure 16b). The CP-OURTP material demonstrated a g_{lum} up to 1.49, surpassing previous records by over two orders of magnitude. This system exhibited exceptional stability after numerous cycles of photoirradiation and thermal treatment, making it suitable for applications in optical multiplexing. These findings are believed to establish a robust foundation for the advancement of CP-OURTP materials in photonic applications.

The remarkable intelligent and autonomous characteristics of living organisms have inspired significant advancement in the fabrication of smart materials capable of diverse motions when responding to external stimuli (heat, light, electric, or magnetic).[275–280] Inspired by human muscles, which exhibit various deformations and execute complicated biological functions in response to nerve signals, researchers have concentrated on the stimuli-responsive soft active materials of LC elastomers (LCEs) with multiple functionalities[281–284] such as polymer elasticity and mesogenic anisotropy. LCEs have the ability to perform reversible shape transformations,[284,285] including bending, walking, swimming, and twisting. LCEs with the capacity of reversible, large, and programmable deformation under external triggers[286] have been considered as the most promising active soft materials in the applications of autonomous robotic, soft robotics, adaptive optics devices, biomimetic devices, stimuli-responsive actuators, artificial muscles, and so forth.[279,287,288] Azobenzene and its derivatives have emerged as one of the most extensively investigated chromophores, due to their thermal stability, compatibility, and distinguished absorbance spectra of trans and cis conformers.[289–291]

By utilizing reactive mesogenic molecules, chiral LCEs (CLCEs) can be obtained within an elastomeric matrix, combining the remarkable optical characteristics of a chiral nematic phase with the viscoelasticity nature of rubber.[292–295] CLCEs represent soft and dynamic photonic components that couple the circularly polarized structural color from the cholesteric helix to the viscoelastic properties of rubbers. The physical characteristics and responsiveness of these materials to external stimuli are highly diverse, enabling a wide range of applications, such as photonic camouflage, soft robotics, biomedical sensors, and information protection and data security.[212,296,297] Despite the excellent achievements obtained in CLCEs, the CP-OURTP properties of CLCEs have been scarcely investigated. Guo et al.[298] have introduced a convenient and efficient method to achieve mechanical-tunable CP-OURTP by integrating phosphorescent tetra-N-phenylbenzidine (TPB) into CLCEs (Figure 16c). The phosphorescent lifetime and mechanical characteristics of CLCE films were influenced by the quantity of chain extender. The addition of bulky TPB addressed the limited rigidity of CLCEs, resulting in the robust CP-OURTP. Moreover, by stretching the CLCEs, the g_{lum} of the CP-OURTP can be tailored from 0.93 to nearly zero. Leveraging the reconfigurable nature of the CLCE network and the unique properties of CP-OURTP, a 4D encryption luminescent barcode was devised, demonstrating the considerable potential for information storage and encryption. Deng, Zhao, and co-workers[299] developed a versatile and effective approach to produce full-color CPRTP system with exceptionally high g_{lum} factors in a polymeric cholesteric superhelix network, using a combination of CLC polymers and chiral helical polymer (CHP). The chiral fluorescent helical polymers were served as chiral dopants in this system. Leveraging the strong helical twisting power of CHP, the resultant polymeric cholesteric superhelix network demonstrated excellent optical activity. Notably, by employing a straightforward double-layered structure composed of a cholesteric superhelix film and phosphorescent films, they achieved CPRTP emissions in blue, green, yellow, and red, with maximum $|g_{lum}|$ values of 1.43, 1.39, 1.09, and 0.84, respectively. This research provides valuable insights for designing polymeric cholesteric superhelix systems with significant CPRTP performance for advanced photonic devices. Cheng et al.[300] developed remarkable CPRTP materials by the photogenerated radical from chiral LC co-polymers. Three achiral co-polymers (P1/P2/P3) were co-assembled with the chiral inducer R/S-I. The resultant $(R/S\text{-}I)_m$-$(P1/P2/P3)_n$ exhibited rapid photochromic characteristics and strong RTP, facilitated by photothermal synergy. P2/P3 co-polymers formed a nematic LC phase upon self-assembly, while P1 was in an amorphous co-polymer. P1/P2 displayed bright phosphorescence in films at room temperature, which were attributed to radical anions. After UV exposure, the chiral co-assembled film showed stronger CPRTP emission with $|g_{lum}| = 7.89 \times 10^{-2}$ due to the formation of helical nanofibers. In addition, numerous endeavors have been dedicated to dynamically controlling the helicoidal superstructures of CLCs, including the modulation of the helical pitch, reflection colors, and handedness by light due to its remote, local, precise control, and temporal manipulation.[207,301–306] CLCs have demonstrated the ability to selectively reflect light in response to external stimuli including temperature, light, stress, and electric and magnetic fields, etc.[307–313] To achieve dynamic control of the g_{lum} for CP-OURTP, our group[314] introduced an efficient method for achieving chirality modulation driven through photoirradiation by employing a bilayered film, consisting of a light-driven molecular motor doped soft helical superstructures layer and RTP layer (Figure 16d). CLCs are stimuli-responsive soft superstructures, with their helical pitch tunable by different external stimuli such as electric field,[309,315–317] temperature,[241] and light.[207,235,301,318–322] Dynamic manipulation of the helical pitch of CLCs is a pivotal research area given the significance of their photonic applications in tunable color filters, sensors, and communications, etc.[320,323–326] The geometric changes of the molecular motors in the LC matrix induced a significant, reversible modulation of the CLC, resulting in the switchable chirality modulation of CPL. Traditional approaches for dynamic modulation of the chirality and supramolecular organizations in LCs are mainly based on molecular motors,[229,327] molecular switches,[328,329] and photoswitches.[314,321,323,330–332] Generally, the rotary motion of the molecular motors or chiral photoswitches can alter the self-organized helical structure of CLC, resulting in the handedness tunability. The obtained bilayered film exhibited CP-OURTP, featuring a lifetime of 805 ms and a tailored g_{lum} between 0.6 and 1.38 by photoirradiation. This novel approach provides valuable insights into the advancement of CP-OURTP materials aimed at manipulating the chirality in LC systems.

Guo et al.[333] engineered a CP-OURTP emission with an exceptionally high g_{lum} and outstanding visualization capability based on a bilayer photonic film, which was achieved by

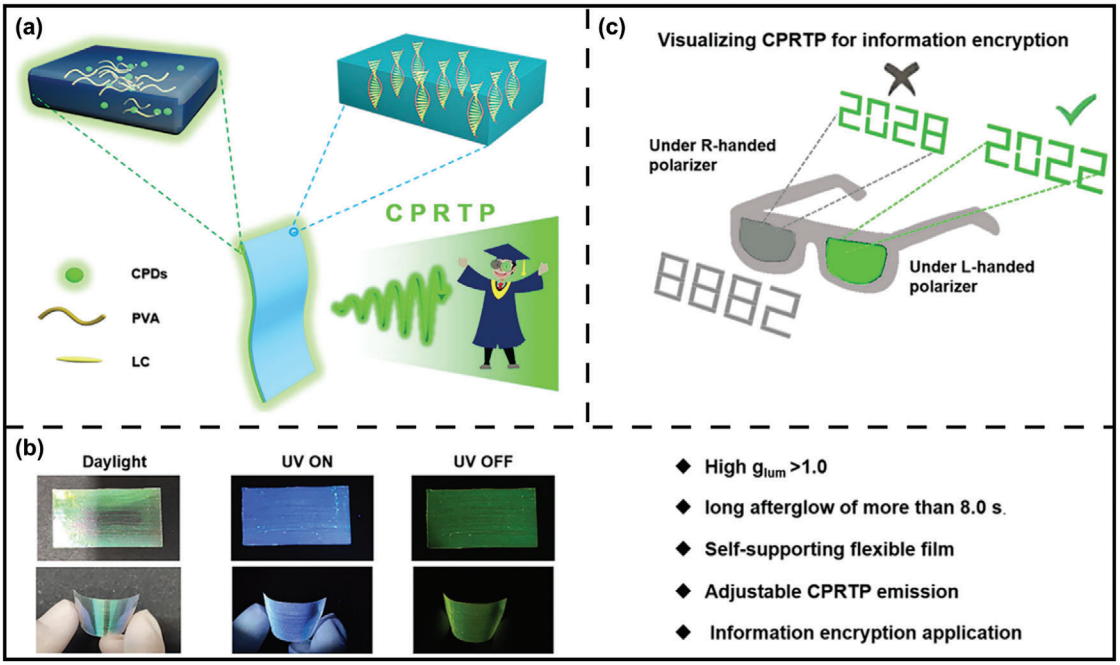

Figure 17. a) Schematic illustration of the bilayer photonic structure. b) Photographs of photonic films under daylight, UV on and UV off, respectively. c) Schematic illustration for the application of CP-OURTP. Reproduced with permission.[333] Copyright 2023, American Chemical Society.

incorporating N- and P-doped carbonized polymer dots (NP-CPDs) into PVA (**Figure 17**). More precisely, CLC polymer films were utilized as the selective reflective layer that converted the non-polarized emission of NP-CPDs into circularly polarized emission. The bilayer architecture of CPRTP system involved doping carbonized polymer dots (CPDs into a PVA matrix, and then embedded into the CLC polymer film, resulting in a high g_{lum} by tailoring the helical structure of the cholesteric polymer. CPDs not only possessed the polymer/carbon hybrid structure, but also maintained the outstanding optical activities, which allowed for the efficient self-trapping of the excited triplet states. PVA, serving as a polymer matrix, could significantly improve the stability of CPDs. Notably, the photonic film emitted the green afterglow for more than 8.0 s with a remarkable g_{lum} of 1.09. Additionally, composite photonic array films with encryption capabilities were produced by changing the LC phase states of the cholesteric polymer film and adjusting the dot coating position within the NP-CPDs/PVA layer. Furthermore, the unique graphical patterns featuring CP-OURTP characteristics were fabricated through changing the phase states of the cholesteric polymer films and the NP-CPD coating position, demonstrating potential for advanced information encryption.

Many efficient approaches have been developed to construct the high-performance CP-OURTP materials with long lifetime and high g_{lum} values, largely accelerating the advancement of CP-OURTP materials. Zhang, Yuan, and co-workers[66] introduced a straightforward and effective approach to design pure CP-OURTP materials with a high g_{lum} value based on CLCs, by incorporating a phosphorescent chromophore (dibenzofuran) into a chiral cholesterol mesogen through a flexible spacer (**Figure 18**). The resulting compound, Chol-C6-DF, could form CLCs with helical architectures that emitted yellow when excited by 380 nm UV light with a g_{lum} of −0.19, a lifetime of 567.7 ms, and the quantum yield of 3.2%. Figure 18a illustrated the CPRTP mechanism of Chol-C6-DF film. Interestingly, the chiral cholesterol also demonstrated the clustering-triggered emission characteristics. Multicolor-tunable CP-OURTP with different colors can be generated by changing the excitation wavelengths due to the existence of the dual phosphorescent chromophores. Nevertheless, because of the selective reflection of the CLC, left-handed CPL(L-CPL) was reflected, whereas right-handed CPL(R-CPL) was detected (Figure 18b). Upon excitation with 380 nm UV light, the Chol-C6-DF film exhibited an absolute g_{lum} value reaching up to 0.19 at 525 nm. While under the excitation of 255 or 460 nm light, the absolute values of g_{lum} measured 0.09 and 0.10 at 400 and 640 nm, respectively. These CP-OURTP materials showcase the considerable potential for advanced applications in anti-counterfeiting, and encryption technologies, and biological imaging.

Xie and co-workers[334] synthesized a series of (*R*/*S*)-B-n-CzO (where n = 4, 8, and 12) based on the binaphthol and the luminescent carbazole-dibenzofuran for CP-OURTP (**Figure 19**), which demonstrated the outstanding luminescent characteristics in both solution and the solid phase. Subsequently, the obtained compound was incorporated into a commercial LC monomer to produce CP-OURTP materials (P-(*R*/*S*)-B-*n*-CzO) through cross-linking the monomer by UV light (Figure 19a,c). Under the L-CPF filter, the RTP intensity of P-(*R*)-B-4-CzO LC polymer network surpassed that under the R-CPF filter, demonstrating CP-OURTP behavior with g_{lum} values ranging from 0.013 to 0.098. The cross-linked structures are crucial in the fabrication of CP-OURTP materials. These findings indicate a bright outlook for the development of the innovative and high-performance CP-OURTP materials. Zhang, Yuan, and co-workers[335]

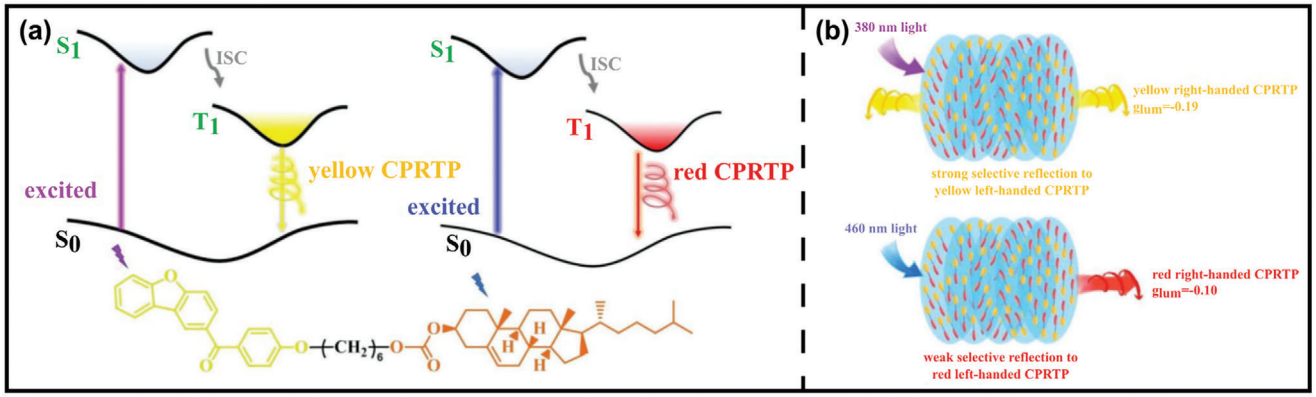

Figure 18. a) Schematic diagram of the CPRTP mechanism of Chol-C6-DF film. b) Mechanism diagram for producing CP-OURTP based on CLCs excited by different UV wavelength. Reproduced with permission.[66] Copyright 2023, John Wiley and Sons.

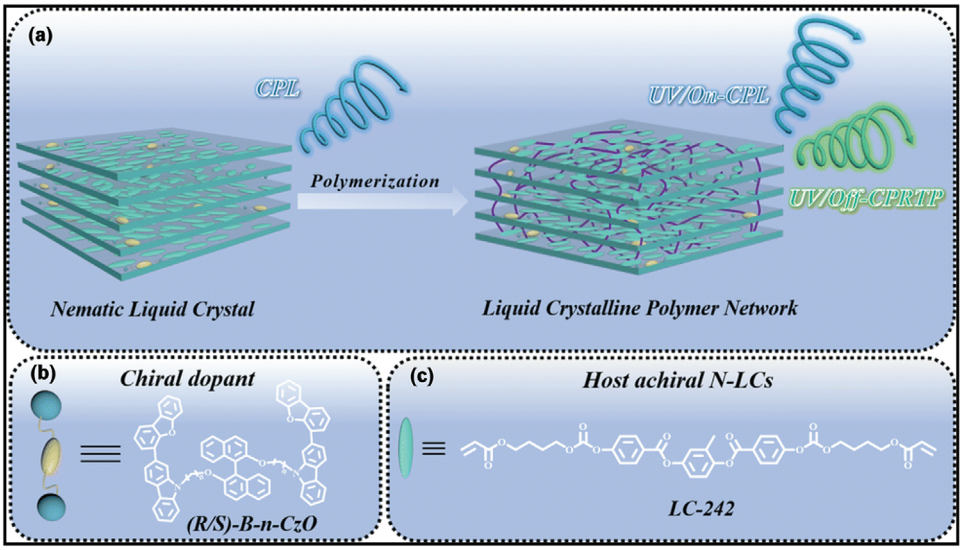

Figure 19. a) Schematic diagram of producing CP-OURTP based on LC polymer network. b) Molecular structures of the chiral dopant (*R*/*S*)-B-n-CzO) and c) host achiral nematic LC (LC-242). Reproduced with permission.[334] Copyright 2023, Royal Society of Chemistry.

developed an effective method to construct long-lived CPP materials by leveraging mesogen-jacketed LC polymers (MJLCPs). They used the phosphorescent monomer MJ0DFM and the chiral monomer MJ0Chol to create homopolymers PMJ0DFM and PMJ0Chol, and copolymers DFM(x)-Chol(y). While the homopolymers PMJ0Chol and PMJ0DFM did not exhibit CPL due to a lack of chiral phase structures, all copolymers DFM(x)-Chol(y) displayed significant CPL characteristics due to the existence of the chiral helical columnar phase by copolymerization. The CPL properties of these copolymers could be modulated by varying the cholesterol component. The g_{lum} values for CPF and CPP in copolymers initially increased and then decreased with higher cholesterol content. DFM(0.6)-Chol(0.4) showed both CPF with g_{lum} of -4.4×10^{-3} and CPP with g_{lum} of -7.1×10^{-3}. The phosphorescence lifetime was effectively enhanced up to 252 ms due to the "jacketing" effect. This study offers a straightforward and practical approach for preparing CPRTP materials.

Chen et al.[336] reported the axially chiral materials (*R*/*S*-chiral guest) exhibiting blue organic phosphorescence, exceptionally long phosphorescent lifetime, and strong CPL (**Figure 20**). Due to their rigid axially chiral skeleton, these ultralong organic phosphorescent materials demonstrated intense CPL, achieving a g_{lum} value of up to 0.34 when utilized as chiral inducers for LC materials. It is worth noting that hundredfold magnification can be readily achieved by doping the axially chiral materials into the achiral nematic LC (SLC1717) at extremely low concentration. In particular, the nematic LC doped with 1–2 wt% of *R*/*S*-1 (X = H) and *R*/*S*-2 (X = Ph) chiral guests exhibited g_{lum} values of +0.21/−0.26 and ±0.34, respectively, owing to the organized arrangement of the nematic LC induced by the chiral dopant (Figure 20b,c). This study offers a roadmap for developing novel pure organic materials that feature both ultralong organic phosphorescence and intense CPL.

The manipulation of organized helical superstructure blocks within LC media through chiral self-assembly has proven to be

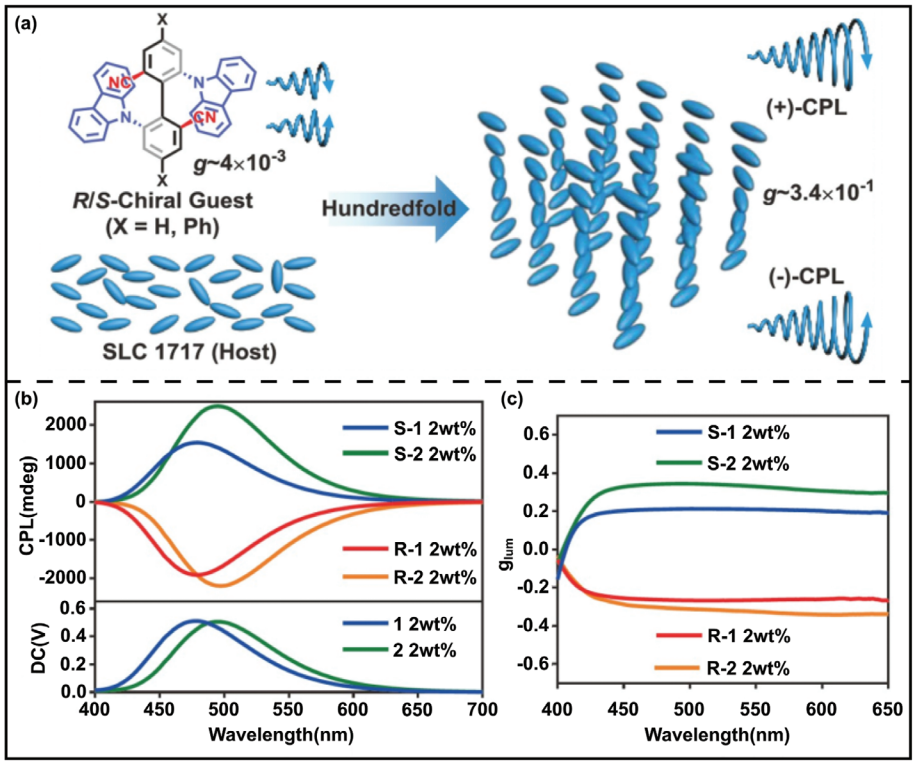

Figure 20. a) Diagram of 1 (X = H), 2 (X = Ph)-nematic LCs assembly for amplification. b) CPL spectra and c) g_{lum} curves of 1, 2-nematic LCs with 2 wt% doping after annealing. Reproduced with permission.[336] Copyright 2023, Springer Nature.

an effective approach for fabricating high-performance CPL materials. Zheng et al.[337] developed a new RTP system utilizing an LC polymer, which was achieved by designing two axially chiral emitters (BBXT-3-Br and BOHXT-3-Br) based on XT-3-Br and axially chiral 1, 1'-binaphthol (BINOL) backbones (**Figure 21**). XT-3-Br was identified as an RTP-active component owing to its π-conjugated planar structure, which could constrain the internal molecular motions, thereby reducing the non-radiative transitions. BINOL, as an essential chiral compound, was selected as a chiral dopant for CPL materials due to its good miscibility with LC molecules. The twisted configuration of its two naphthyl units in binaphthol hindered the formation of a densely packed arrangement, rendering it an appropriate choice as the emitting layer material in OLEDs. After the photo-initiated polymerization of an LC monomer and two axially chiral emitters, the chiral self-assembled LC polymers (BBXT-3-Br@PRM257 and BOHXT-3-Br@PRM257) were obtained, featuring the distinct RTP characteristics. It is worth noting that BBXT-3-Br@PRM257 enantiomers displayed a blue CPL emission ($|g_{FL}| = 0.071$) with an afterglow lifetime of 162.41 ms. While BOHXT-3-Br@PRM257 emitted the red RTP ($|g_{RTP}| = 0.057$) with a lifetime of 98.83 ms. This research presents a novel method for designing CPRTP materials utilizing the chiral self-assembled LCP framework.

3.3. Others

Endowing inorganic nanomaterials with CPL has facilitated the development of CPL-active materials due to the benefits of stability, high quantum efficiency, and adjustable emission wavelengths. Luminophores such as quantum dots (QDs)[257,338–340] and CDs[86,133,139,264–265,341–343] with CPF have attracted significant attention in detecting circularly polarized light and chiral optoelectronics. Deng, Zhao, Tian, and co-workers[44] introduced a convenient and effective approach to achieve the efficient CPF and CP-OURTP emissions in a bilayer composite film, consisting of CDs and a chiral helical polymer (CHP), by utilizing the chiral filter effect of the helical polymer (**Figure 22**). CDs with RTP property were synthesized using a microwave method; The RTP CDs/polyacetylene bilayer composite films were obtained by spin-coating chiral helical polyacetylene onto the CDs/poly(vinyl alcohol) (PVA) layer. Despite the straightforward interface contact between the layer of CDs and the chiral helical polymer layer, significant CPF and CP-OURTP were achieved, yielding g_{lum} values of 1.4×10^{-1} and 1.2×10^{-2}, respectively. These chiral luminescent films have potential applications in information displays.

Xiao, Suan, and co-workers[344] developed a convenient method for synthesizing intrinsically CPRTP carbonized polymer dots (using the sodium alginate and L-/D-arginine as precursors (**Figure 23**). Notably, the color-adjustable CPRTP was obtained by designing the chiral light-harvesting systems through circularly polarized phosphorescence resonance energy transfer (C-PRET). In such system, CPDs exhibiting green RTP, acted as both the initiators of chirality and light absorption, while the fluorescent dyes, served as the acceptors with the emission colors from yellow to red (Figure 23b). By employing either one-step or sequential C-PRET processes, the light-harvesting systems can achieve both energy transfer and chirality

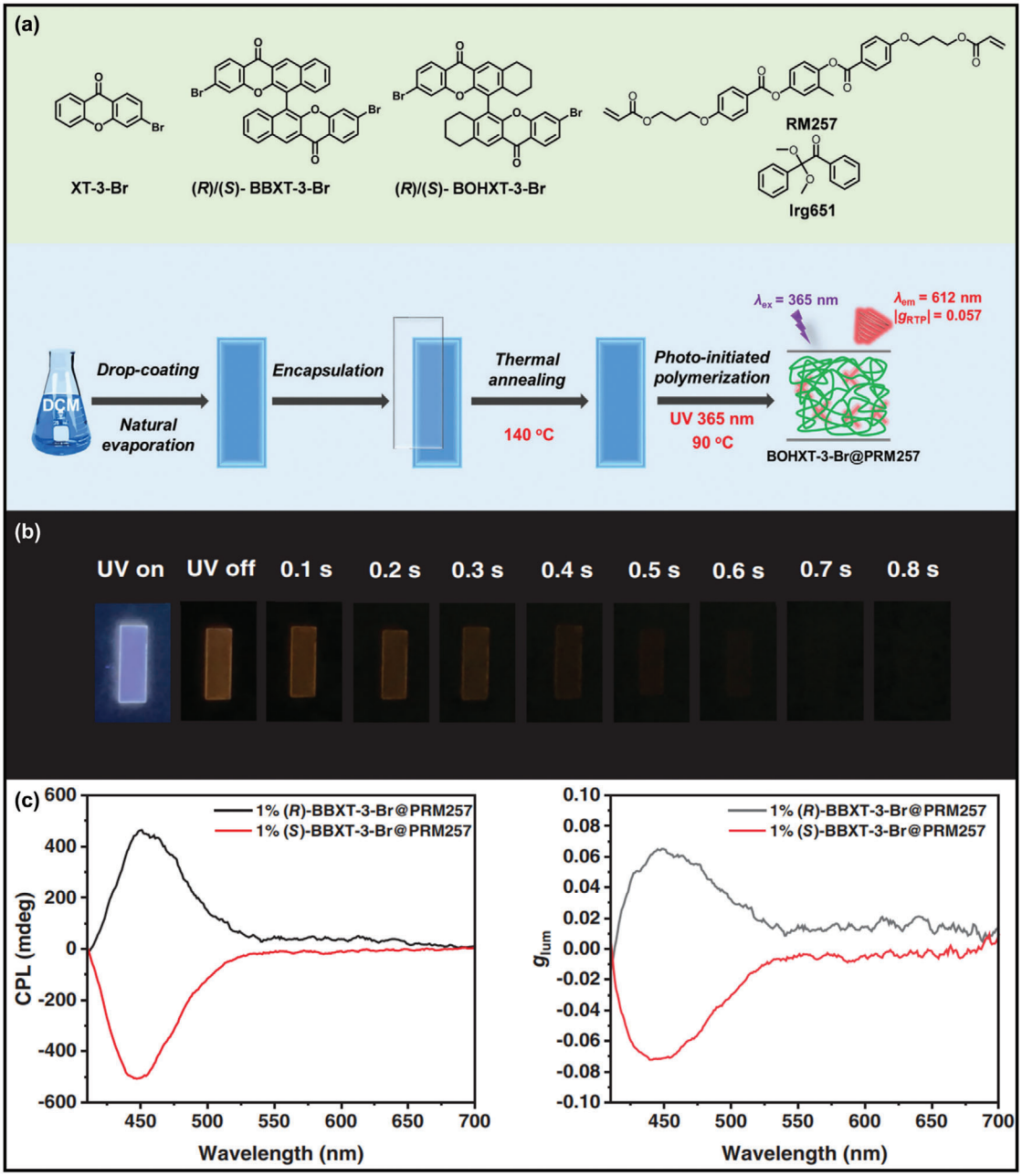

Figure 21. a) Chemical structures of compounds XT-3-Br, BBXT-3-Br, BOHXT-3-Br, RM257 and Irg651, and the preparation of BOHXT-3-Br@PRM257. b) Photographs taken of the BBXT-3-Br@PRM257 after ceasing UV light exposure. c) CPL spectra and g_{lum} of BBXT-3-Br@PRM257 were recorded when excited by 320 nm UV light. Reproduced with permission.[337] Copyright 2024, John Wiley and Sons.

transmission/amplification. The exhibited characteristics of multicolor long afterglow, and tunable lifetime, enables their potential applications in diverse information encryption scenarios. The relevant studies of CP-OURTP materials with luminescent characteristics are summarized in **Table 1**.

4. Applications

The research on CPP has attracted sustained and increasing interest in recent years. CPP materials with high quantum efficiency are crucial for applications in the fields of data encryption, advanced data anti-counterfeiting, optoelectronic devices, and bioimaging. Currently, significant efforts have been dedicated to developing novel CP-OURTP materials with high g_{lum} values. Due to their high luminescence quantum yields, exceptional processability, and unique chiroptical properties, CP-OURTP materials have gained more and more interest in the applications of circularly polarized organic light-emitting diodes (CP-OLEDs) and encryption displays.

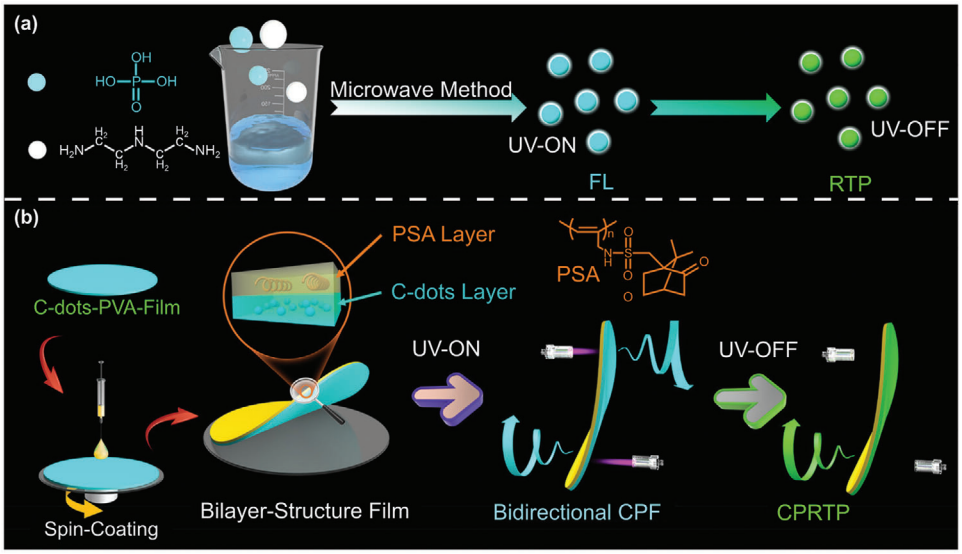

Figure 22. Illustration of a) preparation of RTP carbon dots (CDs) and b) fabrication of CDs/chiral helical polymer composite films with circularly polarized fluorescence (CPF) and CP-OURTP properties. Reproduced with permission.[44] Copyright 2023, American Chemical Society.

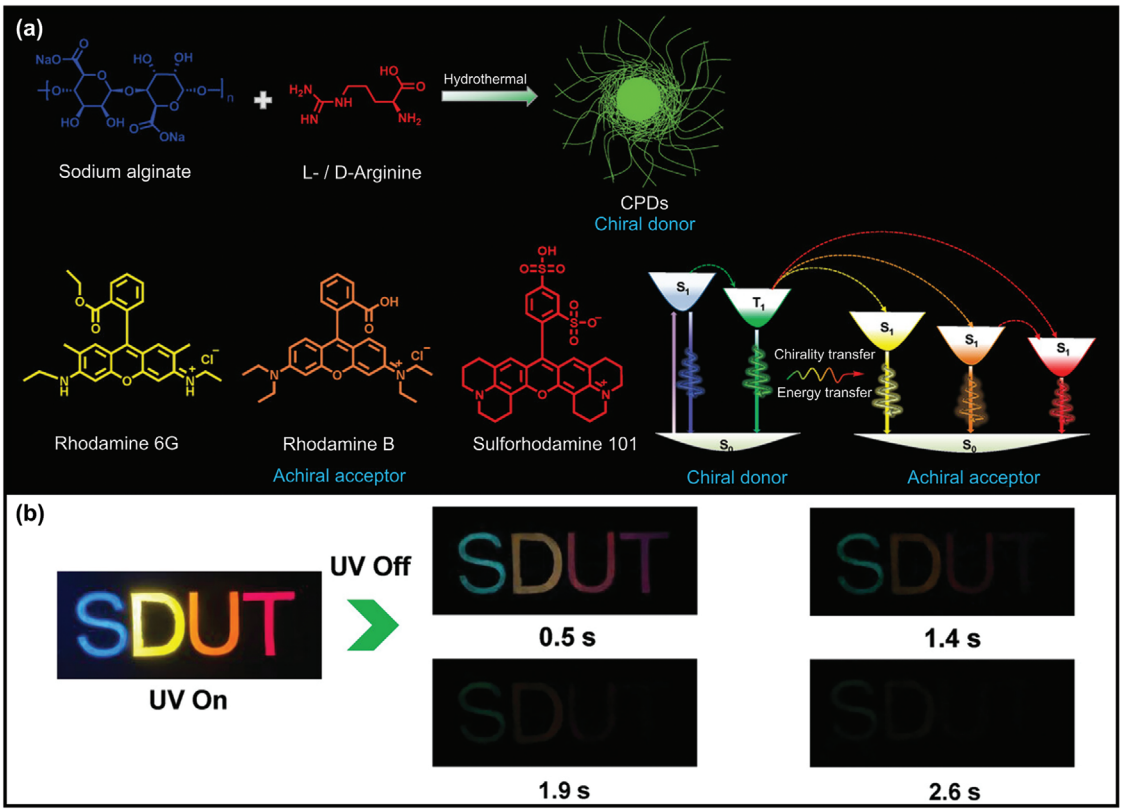

Figure 23. a) Schematic diagram for RTP carbonized polymer dots (CPDs) as chiral energy donors, molecular structures of achiral fluorescent dyes as energy acceptors, and simplified Jablonski diagram depicting the mechanism of circularly polarized phosphorescence resonance energy transfer (C-PRET). b) The letters "SDUT" written with PVA solution under the UV lamp on and off. Reproduced with permission.[344] Copyright 2023, John Wiley and Sons.

Table 1. Overview of CP-OURTP materials.

Compound	Strategy	Lifetime	$\|g_{lum}\|$	Refs.
TPA-(*R*/*S*)-PEA	Organic crystal	862 ms	2×10^{-2}	[79]
S/*R*-COOCz		0.6 s	2.2×10^{-3}	[156]
(*R*, *R*)-DAACH		587 ms	2.3×10^{-3}	[166]
(*R*/*S*)-PBNA	Copolymerization	0.68 s	9.4×10^{-3}	[167]
R/*S*-BPNaP		109.1 ms	0.84×10^{-3}	[169]
p(phNA-co-BrNpA)-PMMA	Host–guest systems	4.53 ms	0.019	[170]
(*R*/*S*)-DMBDA-doped *β*-estradiol		0.67 s	2.3×10^{-3}	[171]
bidibenzo[*b*, *d*]furan		0.56 s	0.12	[172]
MB-Br/TCNB		5.38 ms	5×10^{-3}	[174]
Na-R/PVP		601 ms	0.001–0.002	[176]
Heterohelicenes		0.16 s	5×10^{-3}	[185]
PAMCOOCzX/Fluc	Copolymerization and host–guest doping	3.0 s	10^{-2}	[186]
Q-NH_2@PVA fiber	Spinning and twisting	1.08 s	10^{-2}	[187]
(*R*/*S*)-AHBP/CB[8]	Supramolecular systems	0.49 ms	2.2×10^{-3}	[190]
LGluP/DGluP		180 ms	10^{-3}	[192]
PS-b-(M-1@PLLA) film		\	0.8×10^{-2}	[205]
CNS	CNC templates	1.082 s	0.13	[262]
CNCs/CDs		103 ms	0.47	[164]
CPLA films		40 min	0.67	[267]
CNCs/lignosulfonate		103 ms	0.21	[268]
NP-CNC		8 s	0.49	[269]
CPFP LCs	Thermotropic chiral LC templates	\	1.57	[273]
RTP-CHS		735 ms	1.49	[274]
TPB doped CLCE		367 ms	0.93	[298]
P1-SHS-M1		805 ms	1.38	[314]
NP-CPDs/PVA		8.0 s	1.09	[333]
Chol-C6-DF		567.7 ms	0.19	[66]
(*R*/*S*)-B-n-CzO doped LCs		0.83–1.03 s	0.013–0.098	[334]
R/*S*-2-nematic LCs		\	0.34	[336]
BBXT-3-Br@PRM257	LC polymer	162.41 ms	0.071	[337]
CDs/CHP film	Other	1.23 s	1.2×10^{-2}	[44]

4.1. Applications Based on Traditional Strategies

Developing functional materials that can encrypt and decrypt information more effectively is highly desirable. By leveraging the excellent color-adjustable CPOA emission, Chen et al.[166] created a multicolor CP-OURTP display and a visual UV color chart by using (*R*, *R*)-DAACH and (*S*, *S*)-DAACH (**Figure 24a**). Specifically, the letters "C" and "OO" in "COO" were packed with (*S*, *S*)-DAACH and (*R*, *R*)-DAACH, respectively. As the excitation wavelengths changed from 254 to 365 nm, "COO" turned from blue to yellowish green, indicting the successful fabrication of the multicolor CPOA displays. Zhao, Huang, An, and co-workers[167] successfully generated CP-OURTP materials from amorphous polymers via radical polymerization. These materials applications can be applied in security information encryption and flexible displays due to the straightforward processability and long-lived emission of CP-OURTP (Figure 24b). Under UV light exposure, the flexible films emitted blue light. Upon switching off UV light, a yellow afterglow emission was observed for ≈6 s by the naked eye at room temperature. Meanwhile, these polymers exhibit advantages such as flexibility, large-scale preparation, and high transparency, enabling them to be manufactured into flexible and large-area films. Ma, Tian, and co-workers[170] developed photoinduced CP-OURTP materials with controllable luminescent properties, flexibility, and plasticity, promoting the development of advanced photonic technologies (Figure 24c). When exposed to UV light, the polymethyl methacrylate (PMMA) films exhibited light-printing functionalities and the facile stencil printing was employed to construct informational patterns, enabling the self-erasing transient information storage and anti-counterfeiting. Under natural light, the numerical patterns remained invisible on wood, paper, glass, and polyester surface. However, the pattern gradually became visible, emitting orange under the continuous irradiation of 365 nm UV. It is noteworthy that although the number "0/5/0/9" displayed the similar emission color when excited by 365 nm UV, only the number "0/0" exhibited a discernible positive CPP signal. These CP-OURTP materials are competitive candidates that can be effectively utilized

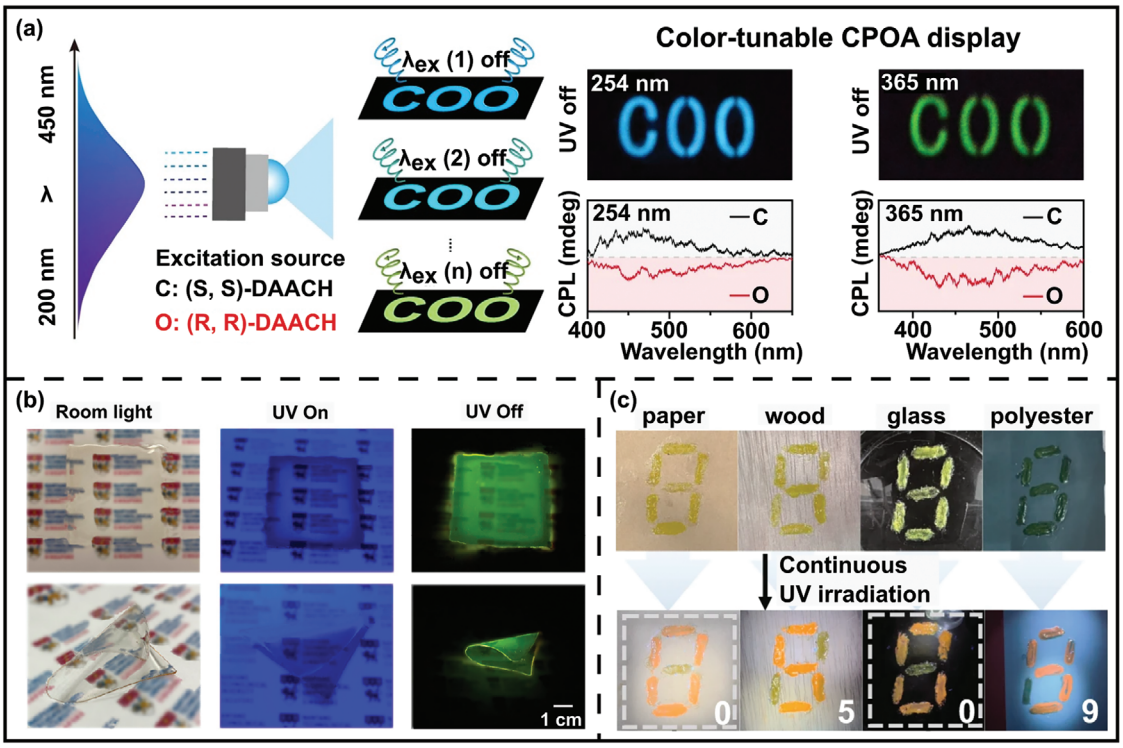

Figure 24. a) Schematic illustration of multicolor displays under the irradiation of UV with different excitation wavelengths. Reproduced with permission.[166] Copyright 2022, Springer Nature. b) Applications in information encryption. Reproduced with permission.[167] Copyright 2021, American Chemical Society. c) Applications of the photoprogrammable CP-OURTP materials. Reproduced with permission.[170] Copyright 2022, Springer Nature.

for the chiro-optical applications with outstanding processability and dynamic properties.

4.2. Applications Based on Lyotropic LC Systems

Screen-printing technology was utilized to create patterns on phosphor films for application in security label (**Figure 25a**).[267] While the phosphor patterns were not visible under white light, they displayed different structural colors due to the CNCs in the labels. However, the patterns became clearly visible under UV light. After turning off UV light, the afterglow was observed, which gradually diminished when the R- and L-CPFs were placed on the label surface. Organic afterglow materials with both high efficiencies and extended lifetime were desirable yet difficult due to the competition between the lifetime and the luminescence efficiencies. A multicolor CPLA integrated information encryption system was designed by using materials with different afterglows.[267] Benefiting from the features of time- and intensity-dependent light emission, the increasing complexity of information encryption facilitates the development for security demands. The remarkable capability of chiral nematic nanoporous silica (CNS) films exhibiting CP-OURTP with controlled handedness, presents the tremendous opportunities in the application of anti-counterfeiting optical labels (Figure 25b).[262] In detail, the optical label was made of CNS-455 (blue), CNS-600 (orange), and CNS-900 (colorless). When put in a black background under white light, the optical label exhibited a blue-orange-colorless pattern; the color was visible under L-CPF but vanished under R-CPF. The remarkable chiroptical characteristics exhibited by transparent CNS films enable the potential applications in optical encryption or other chiral optical devices. A white paper exhibited 16 letters emitting cyan light when exposed to 365 nm UV, as depicted in Figure 25c.[268] Upon the removal of 365 nm light, only three letters (C, P, and L) were visible in green, indicating the potential for data encryption. A display featuring an anti-counterfeiting pattern "888" by using different phosphors under the irradiation of 365 nm UV was demonstrated. The luminescent design depicted the digits "969" in green phosphorescence upon the removal of UV light. Upon placing a circular polarizer over the pattern, the digital numbers showed the digits "354." These findings showcase a novel approach to multilevel data encryption and decryption. The CNC films, exhibiting structural color, RTP, and CP-OURTP have been regarded as competitive candidates for multi-channel information encryption applications. Ye et al.[269] constructed an information pad using nine hybrid films, consisting of PP-CNC-396, NP-CNC-640, NP-CNC-409, and CNC-400 (Figure 25d). PP-CNC-396, NP-CNC-409, and CNC-400 all exhibited blue structural color, whereas NP-CNC-640 showed the red. The letter "H" could be observed under sunlight, while under UV light irradiation, the information disappeared as there was no visible fluorescence in the hybrid films. After switching off UV light, the films of PP-CNC-396, NP-CNC-640, and NP-CNC-409 exhibited afterglow emission due to the presence of phosphors within the films. Clearly, the letter "σ" appeared with pixels emitting red phosphorescence from pyrene within PP-CNC-396 films, while the array displayed a letter "T" due to the afterglow effect of

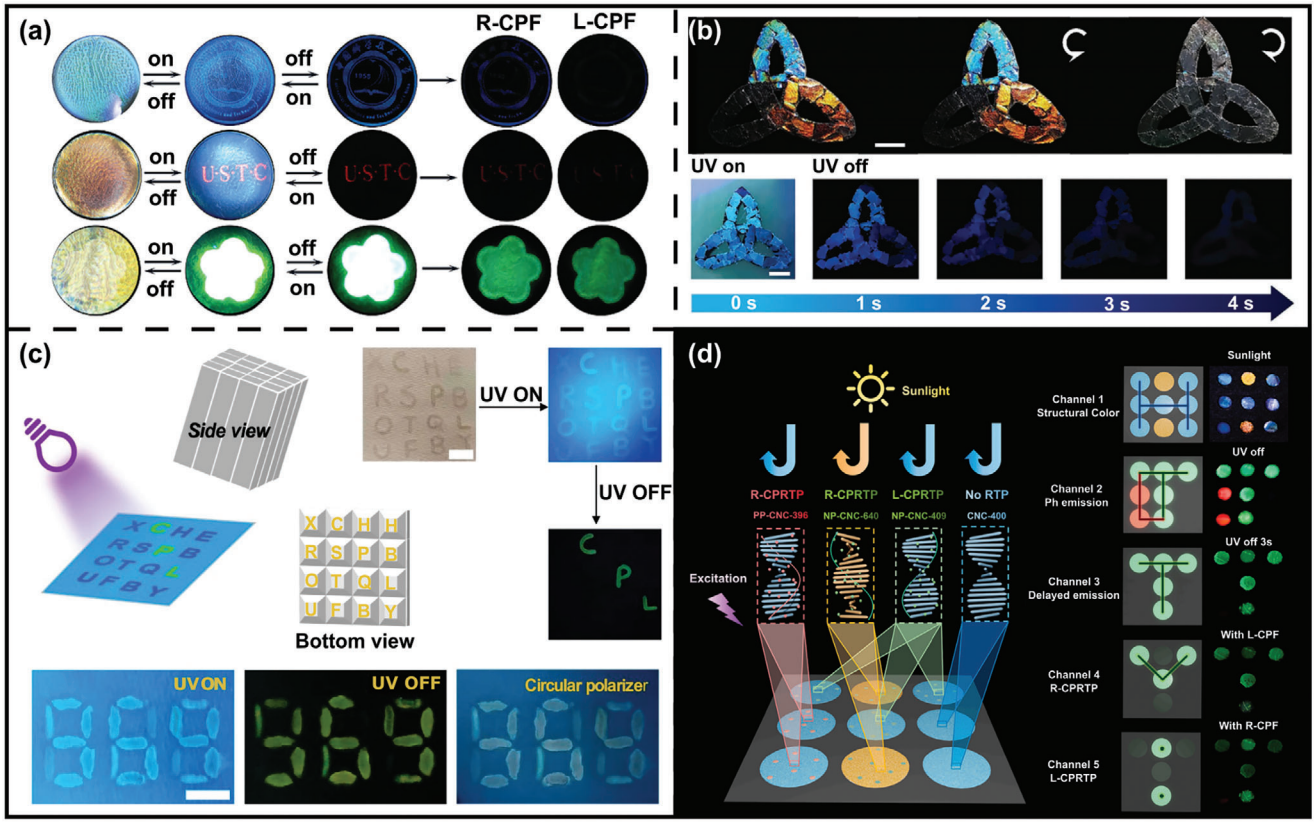

Figure 25. a) Circularly polarized long afterglow (CPLA) composite films under white light, under 365 nm UV light, and long afterglow under R-CPF or L-CPF. Reproduced with permission.[267] Copyright 2023, John Wiley and Sons. b) Applications of chiral nematic nanoporous silica (CNS) films in anticounterfeiting. Reproduced with permission.[262] Copyright 2022, John Wiley and Sons. c) Experiment with an anticounterfeiting device. Reproduced with permission.[268] Copyright 2024, Springer Nature. d) Applications of programmed CPRTP materials. Reproduced with permission.[269] Copyright 2024, Elsevier.

NP-CNC-640 and NP-CNC-409 films. Remarkably, NP-CNC-640 exhibited R-CPRTP with a negative g_{lum} value, while L-CPRTP displayed a positive g_{lum} in the visible region. Consequently, a letter "V" and a punctuation ":" can be decoded under L-CPF and R-CPF, respectively. As a result, encryption of data storage using 5-channel information was achieved with a 3 × 3 pixel's array. Leveraging the versatility of the pixel array, any letter or image could be stored across multiple channels, which shows significant applications for information storage and encryption.

4.3. Applications Based on Thermotropic Chiral LC Systems

Based on the composite photonic film with the bilayer structure, Guo et al.[333] developed various graphical patterns with CPRTP visualization (**Figure 26**). The NP-CPD/PVA solution, containing nitrogen (N) and phosphorus (P) co-doped carbonized polymer dots, was applied to the CLC polymer film through drop-coating using the hollow templates printed with a Chinese knot design (Figure 26a). After evaporating water from the NP-CPDs/PVA solution, a photonic film featuring a Chinese knot design was generated. Upon the irradiation of UV light, the blue Chinese knot pattern was observed. After switching off UV light, a vibrant green Chinese knot became visible either to the naked eye or through a L-CPF, appearing dark under a R-CPF. More intriguing designs were accomplished by manipulating CLC phase state. The composite photonic film displayed visible CP-OURTP when the top layer was in CLC phase within a suitable helical pitch. Nevertheless, when the top layer was in isotropic state, the photonic film exclusively emitted RTP but without any circularly polarized property. The CLC polymer film with tunable phase state was constructed by two-step photopolymerization. When observing the phosphorescent state with an L-CPF, only the panda's outline was discernible; the complete panda became visible when viewing through an R-CPF (Figure 26b). Different graphical patterns distinguished by CP-OURTP visualization were successfully fabricated through using the bilayer photonic film by controlling either CLC phase state or the shape of NP-CPDs/PVA layer.

5. Summary and Perspectives

In this review, we present the recent advancement in CP-OURTP materials, emphasizing their critical significance in technological applications, such as in data encryption, advanced data anticounterfeiting, and optoelectronic devices. This review provides a comprehensive overview of the up-to-date development in the construction of the CP-OURTP materials, which mainly includes

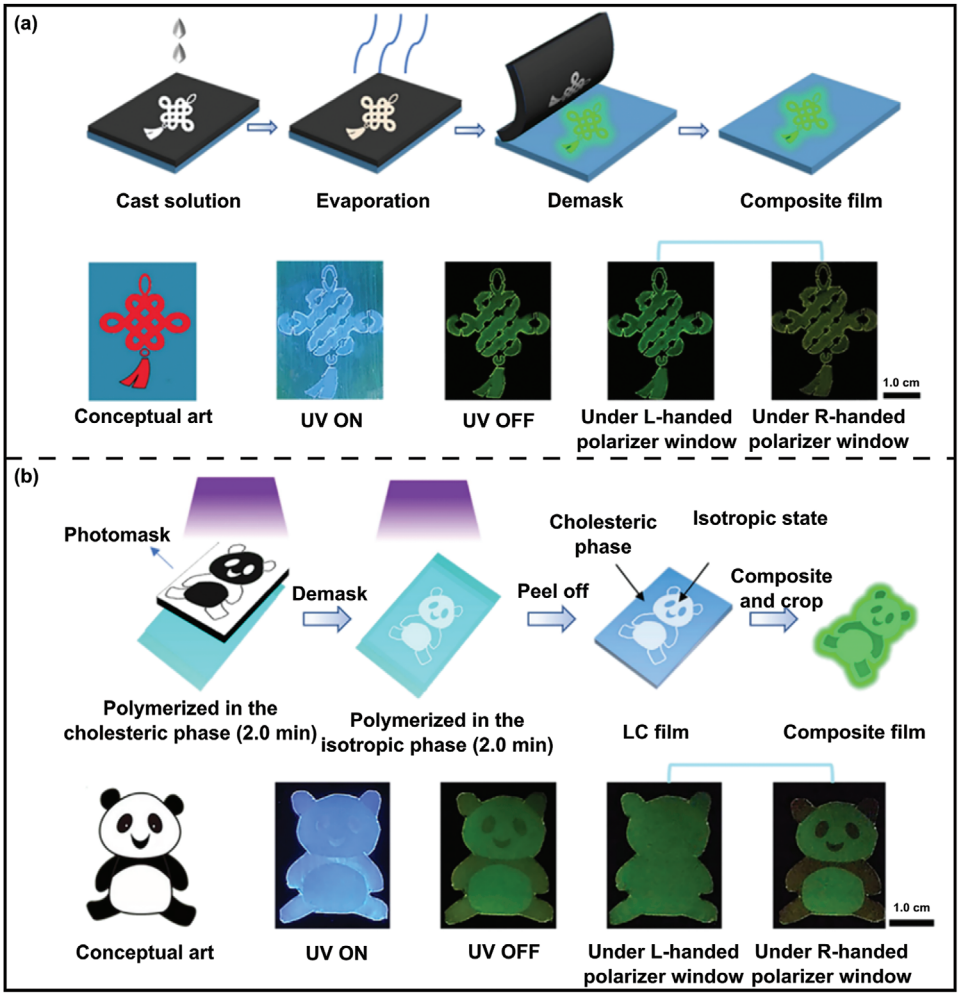

Figure 26. a) Schematic diagram and the corresponding photographs of the preparation process for the photonic film with designed patterns. b) Schematic diagram and corresponding photographs of the photonic film with shape design in different polarization states. Reproduced with permission.[333] Copyright 2023, American Chemical Society.

the fundamental design and synthesis of CP-OURTP materials with high luminous efficiencies and long lifetime through the strategies of organic crystals, copolymerization, host–guest doping, a combination of the copolymerization and host–guest doping, spinning and twisting technology, and supramolecular polymer assembly. Inspired by the chirality amplification of chiral LCs that can selectively reflect one polarized light but transmit the other due to the periodic helical superstructures, the CP-OURTP with high g_{lum} based on chiral soft matter systems, involving LLCs and chiral thermotropic LCs are systematically discussed. We then summarize the current challenges for CP-OURTP materials and put forward corresponding perspectives to circumvent the dilemmas. This overview of CP-OURT materials is anticipated to provide a promising platform and guidance for the fundamental understanding of CP-OURTP materials and provoke the cutting-edge development of CP-OURTP materials toward the next generation applications in anti-counterfeiting technologies. Despite great efforts obtained in the realm of RTP materials, many novel approaches have been developed to accelerate the maturation of this exciting field. CP-OURTP materials are still in their infant stages of development and current research still encounters several challenges.

1) Most reported CPP systems exhibit low g_{lum} ranging from 10^{-4} to 10^{-2} by utilizing chiral small molecules as the chiral source for the fabrication of CP-OURTP materials, which are still far from satisfying the requirements of applications. The inherent single molecular chirality in these molecules can induce low degrees of polarization, thereby leading to low g_{lum}. Currently, only a few cases such as RTP-chiral LC systems, have achieved high g_{lum} values exceeding 10^{-1}. While chiral LC hosts can significantly enhance the g_{lum} due to the intrinsic chirality amplification, the compatibility issue between LCs and RTP polymers remains unsolved, which obviously hinders the advancement of CP-OURTP materials. Therefore, substantial efforts are urgently needed to develop novel RTP materials that have better compatibility with chiral LCs to guarantee high g_{lum} values, long lifetime, and high quantum yields by strengthening the spin–orbit coupling (SOC)[94] with

the ISC process and restricting the molecular motions to suppress non-radiative decays of triplet excitons.

2) Given that CLCs selectively reflect circularly polarized light with the same handedness as their helix, the dynamic manipulation of CLC handedness upon external stimuli holds great promise for developing stimuli-responsive CP-OURTP materials for diverse technological applications. Chiral molecular photoswitches or molecular motors with high helical twisting power, which confer the handedness inversion capability to CLCs upon light irradiation, require to be strategically and judiciously designed to have a good compatibility with LCs. Dynamically controlling the handedness in stimuli-responsive CPL materials has been investigated extensively but remains challenging in CP-OURTP materials, particularly in the successful manipulation of g_{lum} in a wide spectra range. The current focus of research revolves on the combination of light-driven handedness inversion of CLCs with RTP materials due to the benefits of the remote and spatiotemporal control over CLCs.
3) A range of structural-colored materials have been developed by utilizing cholesteric cellulose LCs to achieve dynamic photonic adaptability and intricate patterns with high resolution. It is imperative to develop the structurally colored chiroptical CP-OURTP materials with tunable handedness and excellent processability in cholesteric cellulose LCs systems, using the developed chemical 2D and 3D printing,[345] and soft lithography patterning techniques toward the tunable and sustainable photonic structures. Recently, expediting CPL-active for security ink applications or printing CPL-active materials based on hydroxypropyl cellulose (HPC)[346,347] enables the construction of the desired flexible stereoscopic displays due to their distinct optical rotation features. However, the absence of printable CP-OURTP materials hampers the realization of flexible 3D devices. The development of the controllable and macroscopic production methods for printable CP-OURTP-active photonic paints, will undoubtedly enrich the printing of customized graphics. Therefore, it is necessary to advance the controllable and large-scale manufacturing technique for printable CP-OURTP-active materials for the printing of customized graphics.
4) The predominant CPP-OLEDs utilize the precious metal complexes with high cost and complicated preparation conditions,[145] whereas there are almost no reports on the utilization of emerging pure RTP materials with the distinct advantages of nontoxicity, long lifetime, and large Stoke shift. The novel CP-OURTP systems require the sophisticated molecular designs that meet the requirement of both chiral induction and stable triplet excitons, to achieve the long-lasting emission and high g_{lum}. Effective chirality transfer from chiral to phosphorescent constituents can be achieved via either covalent bonding or non-covalent interactions like hydrogen bonding, π–π stacking interactions, electrostatic interactions, and others. In addition, constructing a rigid environment to suppress the non-radiative decay of triplet state excitons is crucial for the long-lasting emission, which can be achieved by constraining molecular motion through the crystallization, or host–guest doping systems, supramolecular polymers, CNC templates, and LC polymer doping. Supramolecular polymers are typically created from supramonomers through highly directional noncovalent interactions, including hydrogen bonding, van der Waals, and π–π interactions. Molecules need to be specially engineered to exhibit these strong interactions and include a chiral center that facilitates chiral self-assembly into supramolecular nanostructures. The supramolecular nanostructures with dense packing can effectively suppress molecular motion, decrease non-radiative decay, and enhance long-lasting emissions at room temperature. For CNCs, they can be assembled with water-soluble polymers such as PVA, polyethylene glycol, or RTP polymers to create responsive photonic films via hydrogen-bonding interactions. The PVA or polyethylene glycol network can build a rigid polymer microenvironment that restricts molecular motion and prevents oxygen quenching, playing a crucial role in suppressing the non-radiative decay of RTP polymers and enabling the long-lasting emission. For LC polymers, effectively controlling the degree of polymerization allows for the considerable CPRTP in LC polymer systems while preserving self-organized helical superstructures. On the one hand, incorporating RTP polymers into LC polymers can effectively produce long-lasting CPRTP, as the extensive interactions among polymer chains can significantly restrict molecular motion of RTP molecules, thereby reducing the non-radiative relaxation pathways. Additionally, introducing organic phosphorescent luminogens into LC polymers that contain dynamic covalent bonds enables the phosphorescent guest molecules to effectively compensate for the rigidity limitations of LC polymers. Therefore, long-afterglow CPRTP can be obtained from the rigid LC polymers, which can suppress the non-radiative triplet states.

Undoubtedly, CP-OURTP materials have attracted considerable attention for the scientific investigations and practical applications, significantly contributing to the progress of the functional and smart materials with various possibilities. The significant advancement of luminescent materials achieved in recent decades has laid a sturdy foundation for potential applications for CP-OURTP materials. The progress of advanced CP-OURTP materials is anticipated to offer unlimited opportunities, ensuring that it remains a thriving research field with the collaboration from multidisciplinary fields such as chemistry, biology, materials science, physics, nanoscience, and beyond. This review could offer crucial insights into the design of CP-OURTP materials, shedding important light on the development of multifunctional and high-performance novel organic molecules for advanced optoelectronic applications.

Acknowledgements

J.L. and X.Z. contributed equally to this work. The work was supported by the National Key R&D Program of China (Nos. 2022YFA1405000 and 2022YFA1204404), the National Natural Science Foundation of China (No. 62375141), the Natural Science Foundation of Jiangsu Province, Major Project (No. BK20212004), the Natural Science Foundation of Jiangsu Province (BK20240656), the National Natural Science Foundation of China (No. 62405142), Nanjing University of Posts and Telecommunications Talent Introduction Research Fund Project (Natural Science, No. NY222105), Natural Science Research Start-up Foundation of Recruiting Talents of Nanjing University of Posts and Telecommunications (No. NY222053), Jiangsu Innovation Team Program, and National Natural Science Foundation of China (No. 22302036).

Conflict of Interest

The authors declare no conflict of interest.

Keywords

circularly polarized phosphorescence, information encryption, luminescent dissymmetry factor, organic room-temperature phosphorescence material

Received: August 3, 2024
Revised: September 11, 2024
Published online: October 16, 2024

[1] C. Zhu, C. Wang, A. Young, F. Liu, I. Gunkel, D. Chen, D. Walba, J. Maclennan, N. Clark, A. Hexemer, *Nano Lett.* **2015**, *15*, 3420.
[2] K. Kim, H. Kim, S.-Y. Jo, F. Araoka, D. K. Yoon, S.-W. Choi, *ACS Appl. Mater. Interfaces* **2015**, *7*, 22686.
[3] D. Chen, J. E. Maclennan, R. Shao, D. K. Yoon, H. Wang, E. Korblova, D. M. Walba, M. A. Glaser, N. A. Clark, *J. Am. Chem. Soc.* **2011**, *133*, 12656.
[4] J.-J. Lee, B.-C. Kim, H.-J. Choi, S. Bae, F. Araoka, S.-W. Choi, *ACS Nano* **2020**, *14*, 5243.
[5] X. Zhang, Y. Xu, C. Valenzuela, X. Zhang, L. Wang, W. Feng, Q. Li, *Light: Sci. Appl.* **2022**, *11*, 223.
[6] M. Liu, L. Zhang, T. Wang, *Chem. Rev.* **2015**, *115*, 7304.
[7] N. A. Kotov, L. M. Liz-Marzán, P. S. Weiss, *ACS Nano* **2021**, *15*, 12457.
[8] Y. Ru, L. Ai, T. Jia, X. Liu, S. Lu, Z. Tang, B. Yang, *Nano Today* **2020**, *34*, 100953.
[9] M. S. P. Wenge Jiang, H. Vali, J. J. Gray, M. D. McKee, *Sci. Adv.* **2018**, *4*, 9819.
[10] E. S. A. Goerlitzer, A. S. Puri, J. J. Moses, L. V. Poulikakos, N. Vogel, *Adv. Opt. Mater.* **2021**, *9*, 2100378.
[11] Y. Wu, M. Li, Z.-g. Zheng, Z.-Q. Yu, W.-H. Zhu, *J. Am. Chem. Soc.* **2023**, *145*, 12951.
[12] J. Song, M. Wang, X. Xu, L. Qu, X. Zhou, H. Xiang, *Dalton Trans.* **2019**, *48*, 4420.
[13] Y. He, S. Lin, J. Guo, Q. Li, *Aggregate* **2021**, *2*, e141.
[14] G. Zheng, J. He, V. Kumar, S. Wang, I. Pastoriza-Santos, J. Pérez-Juste, L. M. Liz-Marzán, K.-Y. Wong, *Chem. Soc. Rev.* **2021**, *50*, 3738.
[15] W. Jiang, D. Athanasiadou, S. Zhang, R. Demichelis, K. B. Koziara, P. Raiteri, V. Nelea, W. Mi, J.-A. Ma, J. D. Gale, M. D. McKee, *Nat. Commun.* **2019**, *10*, 2318.
[16] H. Zhang, S. Li, A. Qu, C. Hao, M. Sun, L. Xu, C. Xu, H. Kuang, *Chem. Sci.* **2020**, *11*, 12937.
[17] Y.-J. Kong, J.-H. Hu, X.-Y. Dong, Y. Si, Z.-Y. Wang, X.-M. Luo, H.-R. Li, Z. Chen, S.-Q. Zang, T. C. W. Mak, *J. Am. Chem. Soc.* **2022**, *144*, 19739.
[18] M. Wang, Y. Han, L.-X. Guo, B.-P. Lin, H. Yang, *Liq. Cryst.* **2018**, *46*, 1231.
[19] I. Dierking, *Symmetry* **2014**, *6*, 444.
[20] D. Vila-Liarte, N. A. Kotov, L. M. Liz-Marzán, *Chem. Sci.* **2022**, *13*, 595.
[21] Y. Dai, J. Chen, C. Zhao, L. Feng, X. Qu, *Angew. Chem., Int. Ed.* **2022**, *61*, 202211822.
[22] J. Fan, N. A. Kotov, *Adv. Mater.* **2020**, *32*, 1906738.
[23] G. Albano, G. Pescitelli, L. Di Bari, *Chem. Rev.* **2020**, *120*, 10145.
[24] Y. Luo, C. Chi, M. Jiang, R. Li, S. Zu, Y. Li, Z. Fang, *Adv. Opt. Mater.* **2017**, *5*, 1700040.
[25] X. Lan, X. Lu, C. Shen, Y. Ke, W. Ni, Q. Wang, *J. Am. Chem. Soc.* **2014**, *137*, 457.
[26] D. G. G. Catherine, D. Edgar, *Cellulose* **2001**, *8*, 5.
[27] L. Xiao, T. An, L. Wang, X. Xu, H. Sun, *Nano Today* **2020**, *30*, 100824.
[28] H.-E. Lee, H.-Y. Ahn, J. Mun, Y. Y. Lee, M. Kim, N. H. Cho, K. Chang, W. S. Kim, J. Rho, K. T. Nam, *Nature* **2018**, *556*, 360.
[29] A. Kuzyk, R. Schreiber, H. Zhang, A. O. Govorov, T. Liedl, N. Liu, *Nat. Mater.* **2014**, *13*, 862.
[30] Y. Li, X. Wang, J. Miao, J. Li, X. Zhu, R. Chen, Z. Tang, R. Pan, T. He, J. Cheng, *Adv. Mater.* **2020**, *32*, 1905585.
[31] M. S. Mario Hentschel, X. Duan, H. Giessen, N.a Liu, *Sci. Adv.* **2017**, *3*, 1602735.
[32] Y. Zhao, A. N. Askarpour, L. Sun, J. Shi, X. Li, A. Alù, *Nat. Commun.* **2017**, *8*, 14180.
[33] Z. Geng, Y. Zhang, Y. Zhang, Y. Quan, Y. Cheng, *Angew. Chem., Int. Ed.* **2022**, *61*, 202202718.
[34] J. Han, S. Guo, J. Wang, L. Wei, Y. Zhuang, S. Liu, Q. Zhao, X. Zhang, W. Huang, *Adv. Opt. Mater.* **2017**, *5*, 1700359.
[35] C. Dee, F. Zinna, W. R. Kitzmann, G. Pescitelli, K. Heinze, L. Di Bari, M. Seitz, *Chem. Commun.* **2019**, *55*, 13078.
[36] G. Park, H. Kim, H. Yang, K. R. Park, I. Song, J. H. Oh, C. Kim, Y. You, *Chem. Sci.* **2019**, *10*, 1294.
[37] S. Jiang, N. A. Kotov, *Adv. Mater.* **2022**, *35*, 2108431.
[38] X. Zhang, L. Li, Y. Chen, C. Valenzuela, Y. Liu, Y. Yang, Y. Feng, L. Wang, W. Feng, *Angew. Chem., Int. Ed.* **2024**, *63*, 202404202.
[39] Y. Guan, Z. Wang, B. Ai, C. Chen, W. Zhang, Y. Wang, G. Zhang, *ACS Appl. Mater. Interfaces* **2020**, *12*, 50192.
[40] Y. He, S. Zhang, H. K. Bisoyi, J. Qiao, H. Chen, J. Gao, J. Guo, Q. Li, *Angew. Chem., Int. Ed.* **2021**, *60*, 27158.
[41] M. Zhang, Q. Guo, Z. Li, Y. Zhou, S. Zhao, Z. Tong, Y. Wang, G. Li, S. Jin, M. Zhu, T. Zhuang, S.-H. Yu, *Sci. Adv.* **2023**, *9*, 9944.
[42] F. Nie, K.-Z. Wang, D. Yan, *Nat. Commun.* **2023**, *14*, 1654.
[43] W. Hao, Y. Li, M. Liu, *Adv. Opt. Mater.* **2021**, *9*, 2100452.
[44] S. Ma, H. Ma, K. Yang, Z. Tan, B. Zhao, J. Deng, *ACS Nano* **2023**, *17*, 6912.
[45] Z. Geng, Y. Zhang, Y. Zhang, Y. Li, Y. Quan, Y. Cheng, *J. Mater. Chem. C* **2021**, *9*, 12141.
[46] B. Yang, H. Ni, H. Wang, Y. Hu, K. Luo, W. Yu, *J. Phys. Chem. C* **2020**, *124*, 23879.
[47] T. Usuki, H. Uchida, K. Omoto, Y. Yamanoi, A. Yamada, M. Iwamura, K. Nozaki, H. Nishihara, *J. Org. Chem.* **2019**, *84*, 10749.
[48] Y. P. Zhang, M. X. Mao, S. Q. Song, Y. Wang, Y. X. Zheng, J. L. Zuo, Y. Pan, *Angew. Chem., Int. Ed.* **2022**, *61*, 202200290.
[49] Z. Jiang, J. Wang, T. Gao, J. Ma, Z. Liu, R. Chen, *ACS Appl. Mater. Interfaces* **2020**, *12*, 9520.
[50] J. R. Brandt, X. Wang, Y. Yang, A. J. Campbell, M. J. Fuchter, *J. Am. Chem. Soc.* **2016**, *138*, 9743.
[51] X. Jin, Y. Sang, Y. Shi, Y. Li, X. Zhu, P. Duan, M. Liu, *ACS Nano* **2019**, *13*, 2804.
[52] J. Song, M. Wang, X. Zhou, H. Xiang, *Chem. Eur. J.* **2018**, *24*, 7128.
[53] Z. P. Yan, X. F. Luo, W. Q. Liu, Z. G. Wu, X. Liang, K. Liao, Y. Wang, Y. X. Zheng, L. Zhou, J. L. Zuo, Y. Pan, H. Zhang, *Chem. Eur. J.* **2019**, *25*, 5672.
[54] J. Yan, F. Ota, B. A. San Jose, K. Akagi, *Adv. Funct. Mater.* **2016**, *27*, 1604529.
[55] Z. L. Tu, Z. P. Yan, X. Liang, L. Chen, Z. G. Wu, Y. Wang, Y. X. Zheng, J. L. Zuo, Y. Pan, *Adv. Sci.* **2020**, *7*, 2000804.
[56] Y. H. Zhou, Q. L. Xu, H. B. Han, Y. Zhao, Y. X. Zheng, L. Zhou, J. L. Zuo, H. Zhang, *Adv. Opt. Mater.* **2016**, *4*, 1726.
[57] R. Inoue, R. Kondo, Y. Morisaki, *Chem. Commun.* **2020**, *56*, 15438.
[58] G. Park, D. Y. Jeong, S. Y. Yu, J. J. Park, J. H. Kim, H. Yang, Y. You, *Angew. Chem., Int. Ed.* **2023**, *62*, 202309762.
[59] B. C. Kim, H. J. Choi, J. J. Lee, F. Araoka, S. W. Choi, *Adv. Funct. Mater.* **2019**, *29*, 1903246.
[60] S. Liu, X. Liu, Y. Wu, D. Zhang, Y. Wu, H. Tian, Z. Zheng, W.-H. Zhu, *Matter* **2022**, *5*, 2319.

[61] L. E. MacKenzie, R. Pal, *Nat. Rev. Chem.* **2020**, *5*, 109.
[62] E. M. Sánchez-Carnerero, A. R. Agarrabeitia, F. Moreno, B. L. Maroto, G. Muller, M. J. Ortiz, S. de la Moya, *Chem. Eur. J.* **2015**, *21*, 13488.
[63] D. Yang, P. Duan, L. Zhang, M. Liu, *Nat. Commun.* **2017**, *8*, 15727.
[64] F. Wang, W. Ji, P. Yang, C.-L. Feng, *ACS Nano* **2019**, *13*, 7281.
[65] L. Ji, Y. Zhao, M. Tao, H. Wang, D. Niu, G. Ouyang, A. Xia, M. Liu, *ACS Nano* **2020**, *14*, 2373.
[66] W. Gong, G. Huang, Y. Yuan, H. Zhang, *Adv. Opt. Mater.* **2023**, *11*, 2300745.
[67] Y. Shi, J. Han, C. Li, T. Zhao, X. Jin, P. Duan, *Nat. Commun.* **2023**, *14*, 6123.
[68] Y. Chen, Y. Zhang, H. Li, Y. Li, W. Zheng, Y. Quan, Y. Cheng, *Adv. Mater.* **2022**, *34*, 2202309.
[69] T. Ikai, S. Shimizu, S. Awata, K.-i. Shinohara, *Macromolecules* **2018**, *51*, 2328.
[70] H. Maeda, Y. Bando, K. Shimomura, I. Yamada, M. Naito, K. Nobusawa, H. Tsumatori, T. Kawai, *J. Am. Chem. Soc.* **2011**, *133*, 9266.
[71] X.-X. Yang, N. Li, C. Li, Z.-B. Jin, Z.-Z. Ma, Z.-G. Gu, J. Zhang, *J. Am. Chem. Soc.* **2024**, *146*, 16213.
[72] Y. Sang, J. Han, T. Zhao, P. Duan, M. Liu, *Adv. Mater.* **2019**, *32*, 1900110.
[73] H. Zheng, W. Li, W. Li, X. Wang, Z. Tang, S. X. A. Zhang, Y. Xu, *Adv. Mater.* **2018**, *30*, 1705948.
[74] C. Duan, B. Wang, J. Li, J. Xu, J. Zeng, J. Li, Z. Zhao, W. Gao, G. Ying, K. Chen, *Small* **2022**, *18*, 2204199.
[75] J. Han, P. Duan, X. Li, M. Liu, *J. Am. Chem. Soc.* **2017**, *139*, 9783.
[76] T. Zhao, J. Han, X. Qin, M. Zhou, P. Duan, *J. Phys. Chem. Lett.* **2019**, *11*, 311.
[77] C. Li, P. Duan, *Chem. Lett.* **2021**, *50*, 546.
[78] Y. Shi, J. Han, X. Jin, W. Miao, Y. Zhang, P. Duan, *Adv. Sci.* **2022**, *9*, 2201565.
[79] H. Li, H. Li, W. Wang, Y. Tao, S. Wang, Q. Yang, Y. Jiang, C. Zheng, W. Huang, R. Chen, *Angew. Chem., Int. Ed.* **2020**, *59*, 4756.
[80] Y. Zhou, Y. Wang, Y. Song, S. Zhao, M. Zhang, G. Li, Q. Guo, Z. Tong, Z. Li, S. Jin, H.-B. Yao, M. Zhu, T. Zhuang, *Nat. Commun.* **2024**, *15*, 251.
[81] Y. Chen, Y. Li, H. Li, L. Li, Y. Quan, Y. Cheng, *Sci. China: Chem.* **2023**, *67*, 1250.
[82] C. Zhang, S. Li, X. Y. Dong, S. Q. Zang, *Aggregate* **2021**, *2*, e48.
[83] R. Inoue, R. Kondo, Y. Morisaki, *Chem. Mater.* **2022**, *34*, 7959.
[84] T. R. Schulte, J. J. Holstein, L. Krause, R. Michel, D. Stalke, E. Sakuda, K. Umakoshi, G. Longhi, S. Abbate, G. H. Clever, *J. Am. Chem. Soc.* **2017**, *139*, 6863.
[85] J. Liu, Z. P. Song, L. Y. Sun, B. X. Li, Y. Q. Lu, Q. Li, *Responsive Mater.* **2023**, *1*, 20230005.
[86] H. Zheng, B. Ju, X. Wang, W. Wang, M. Li, Z. Tang, S. X. A. Zhang, Y. Xu, *Adv. Opt. Mater.* **2018**, *6*, 1801246.
[87] C. Zhang, Z. S. Li, X. Y. Dong, Y. Y. Niu, S. Q. Zang, *Adv. Mater.* **2022**, *34*, 2109496.
[88] S. Lin, Y. Tang, W. Kang, H. K. Bisoyi, J. Guo, Q. Li, *Nat. Commun.* **2023**, *14*, 3005.
[89] T. Zhang, X. Ma, H. Wu, L. Zhu, Y. Zhao, H. Tian, *Angew. Chem., Int. Ed.* **2020**, *59*, 11206.
[90] Y. Seino, S. Inomata, H. Sasabe, Y. J. Pu, J. Kido, *Adv. Mater.* **2016**, *28*, 2638.
[91] H. Uoyama, K. Goushi, K. Shizu, H. Nomura, C. Adachi, *Nature* **2012**, *492*, 234.
[92] L. Gu, H. Wu, H. Ma, W. Ye, W. Jia, H. Wang, H. Chen, N. Zhang, D. Wang, C. Qian, Z. An, W. Huang, Y. Zhao, *Nat. Commun.* **2020**, *11*, 944.
[93] X. Wu, W. Li, P. Wu, C. Ma, Y. Liu, M. Xu, S. Liu, *Eng. Sci.* **2018**, *4*, 111.
[94] H. Wang, Y. Zhang, C. Zhou, X. Wang, H. Ma, J. Yin, H. Shi, Z. An, W. Huang, *Light: Sci. Appl.* **2023**, *12*, 90.
[95] Z. Lin, R. Kabe, N. Nishimura, K. Jinnai, C. Adachi, *Adv. Mater.* **2018**, *30*, 1803713.
[96] Z. Pan, Y.-Y. Lu, F. Liu, *Nat. Mater.* **2011**, *11*, 58.
[97] X. Ma, C. Xu, J. Wang, H. Tian, *Angew. Chem., Int. Ed.* **2018**, *57*, 10854.
[98] Z. Yang, Z. Mao, X. Zhang, D. Ou, Y. Mu, Y. Zhang, C. Zhao, S. Liu, Z. Chi, J. Xu, Y. C. Wu, P. Y. Lu, A. Lien, M. R. Bryce, *Angew. Chem., Int. Ed.* **2016**, *55*, 2181.
[99] Z. An, C. Zheng, Y. Tao, R. Chen, H. Shi, T. Chen, Z. Wang, H. Li, R. Deng, X. Liu, W. Huang, *Nat. Mater.* **2015**, *14*, 685.
[100] J. Du, D. Poelman, *Adv. Opt. Mater.* **2019**, *8*, 1901848.
[101] H. Li, H. Li, J. Gu, F. He, H. Peng, Y. Tao, D. Tian, Q. Yang, P. Li, C. Zheng, W. Huang, R. Chen, *Chem. Sci.* **2021**, *12*, 3580.
[102] L. Huang, B. Chen, X. Zhang, C. O. Trindle, F. Liao, Y. Wang, H. Miao, Y. Luo, G. Zhang, *Angew. Chem., Int. Ed.* **2018**, *57*, 16046.
[103] Z. Li, Y. Han, F. Nie, M. Liu, H. Zhong, F. Wang, *Angew. Chem., Int. Ed.* **2021**, *60*, 8212.
[104] X. Ma, J. Wang, H. Tian, *Acc. Chem. Res.* **2019**, *52*, 738.
[105] Y. Zhou, W. Qin, C. Du, H. Gao, F. Zhu, G. Liang, *Angew. Chem., Int. Ed.* **2019**, *58*, 12102.
[106] H. Chen, X. Yao, X. Ma, H. Tian, *Adv. Opt. Mater.* **2016**, *4*, 1397.
[107] X. Zhang, L. Du, W. Zhao, Z. Zhao, Y. Xiong, X. He, P. F. Gao, P. Alam, C. Wang, Z. Li, J. Leng, J. Liu, C. Zhou, J. W. Y. Lam, D. L. Phillips, G. Zhang, B. Z. Tang, *Nat. Commun.* **2019**, *10*, 5161.
[108] R. Kabe, N. Notsuka, K. Yoshida, C. Adachi, *Adv. Mater.* **2015**, *28*, 655.
[109] G. Zhang, G. M. Palmer, M. W. Dewhirst, C. L. Fraser, *Nat. Mater.* **2009**, *8*, 747.
[110] K. Wan, B. Tian, Y. Zhai, Y. Liu, H. Wang, S. Liu, S. Li, W. Ye, Z. An, C. Li, J. Li, T. D. James, Z. Chen, *Nat. Commun.* **2022**, *13*, 5508.
[111] B. Chen, W. Huang, G. Zhang, *Nat. Commun.* **2023**, *14*, 1514.
[112] X. Yang, D. Yan, *Adv. Opt. Mater.* **2016**, *4*, 897.
[113] S. Hirata, K. Totani, J. Zhang, T. Yamashita, H. Kaji, S. R. Marder, T. Watanabe, C. Adachi, *Adv. Funct. Mater.* **2013**, *23*, 3386.
[114] Y. Gong, L. Zhao, Q. Peng, D. Fan, W. Z. Yuan, Y. Zhang, B. Z. Tang, *Chem. Sci.* **2015**, *6*, 4438.
[115] H. Li, J. Jin, Y. Xiang, Y. Zhang, Y. Tao, M. Li, Q. Xue, G. Xie, W. Huang, R. Chen, *Sci. China: Chem.* **2020**, *63*, 1645.
[116] S. Shen, Q. Xie, S. R. Sahoo, J. Jin, G. V. Baryshnikov, H. Sun, H. Wu, H. Ågren, Q. Liu, L. Zhu, *Adv. Mater.* **2024**, 2404888.
[117] J. Wei, C. Liu, J. Duan, A. Shao, J. Li, J. Li, W. Gu, Z. Li, S. Liu, Y. Ma, W. Huang, Q. Zhao, *Nat. Commun.* **2023**, *14*, 627.
[118] L. Gu, X. Wang, M. Singh, H. Shi, H. Ma, Z. An, W. Huang, *J. Phys. Chem. Lett.* **2020**, *11*, 6191.
[119] X. Chen, C. Xu, T. Wang, C. Zhou, J. Du, Z. Wang, H. Xu, T. Xie, G. Bi, J. Jiang, X. Zhang, J. N. Demas, C. O. Trindle, Y. Luo, G. Zhang, *Angew. Chem., Int. Ed.* **2016**, *55*, 9872.
[120] Z. He, H. Gao, S. Zhang, S. Zheng, Y. Wang, Z. Zhao, D. Ding, B. Yang, Y. Zhang, W. Z. Yuan, *Adv. Mater.* **2019**, *31*, 1807222.
[121] M. He, C. Ding, H. Guo, Q. Li, *Responsive Mater.* **2024**, *2*, 20240014.
[122] J. Yang, X. Zhen, B. Wang, X. Gao, Z. Ren, J. Wang, Y. Xie, J. Li, Q. Peng, K. Pu, Z. Li, *Nat. Commun.* **2018**, *9*, 840.
[123] T. Ogoshi, H. Tsuchida, T. Kakuta, T.-a. Yamagishi, A. Taema, T. Ono, M. Sugimoto, M. Mizuno, *Adv. Funct. Mater.* **2018**, *28*, 1707369.
[124] D. W. Zhang, M. Li, C. F. Chen, *Angew. Chem., Int. Ed.* **2022**, *61*, 202213130.
[125] M. Hayduk, S. Riebe, J. Voskuhl, *Chem. - Eur. J.* **2018**, *24*, 12221.
[126] Z. Y. Zhang, Y. Chen, Y. Liu, *Angew. Chem., Int. Ed.* **2019**, *58*, 6028.
[127] W. Zhao, Z. He, B. Z. Tang, *Nat. Rev. Mater.* **2020**, *5*, 869.
[128] H. R. Fu, N. Wang, X. X. Wu, F. F. Li, Y. Zhao, L. F. Ma, M. Du, *Adv. Opt. Mater.* **2020**, *8*, 2000330.

[129] Z. He, W. Zhao, J. W. Y. Lam, Q. Peng, H. Ma, G. Liang, Z. Shuai, B. Z. Tang, *Nat. Commun.* **2017**, *8*, 416.
[130] Y. Lei, W. Dai, J. Guan, S. Guo, F. Ren, Y. Zhou, J. Shi, B. Tong, Z. Cai, J. Zheng, Y. Dong, *Angew. Chem., Int. Ed.* **2020**, *59*, 16054.
[131] Y. Su, Y. Zhang, Z. Wang, W. Gao, P. Jia, D. Zhang, C. Yang, Y. Li, Y. Zhao, *Angew. Chem., Int. Ed.* **2019**, *59*, 9967.
[132] L. Gu, H. Shi, L. Bian, M. Gu, K. Ling, X. Wang, H. Ma, S. Cai, W. Ning, L. Fu, H. Wang, S. Wang, Y. Gao, W. Yao, F. Huo, Y. Tao, Z. An, X. Liu, W. Huang, *Nat. Photonics* **2019**, *13*, 406.
[133] J. Liu, H. Zhang, N. Wang, Y. Yu, Y. Cui, J. Li, J. Yu, *ACS Mater. Lett.* **2019**, *1*, 58.
[134] X. Yan, H. Peng, Y. Xiang, J. Wang, L. Yu, Y. Tao, H. Li, W. Huang, R. Chen, *Small* **2021**, *18*, 2104073.
[135] X. Wang, S. Ma, B. Zhao, J. Deng, *Adv. Funct. Mater.* **2023**, *33*, 2214364.
[136] Z. Y. Zhang, W. W. Xu, W. S. Xu, J. Niu, X. H. Sun, Y. Liu, *Angew. Chem., Int. Ed.* **2020**, *59*, 18748.
[137] W. Zhao, Z. He, J. W. Y. Lam, Q. Peng, H. Ma, Z. Shuai, G. Bai, J. Hao, B. Z. Tang, *Chem* **2016**, *1*, 592.
[138] E. Lucenti, A. Forni, C. Botta, L. Carlucci, C. Giannini, D. Marinotto, A. Pavanello, A. Previtali, S. Righetto, E. Cariati, *Angew. Chem., Int. Ed.* **2017**, *56*, 16302.
[139] S. Tao, S. Lu, Y. Geng, S. Zhu, S. A. T. Redfern, Y. Song, T. Feng, W. Xu, B. Yang, *Angew. Chem., Int. Ed.* **2018**, *57*, 2393.
[140] N. Gan, H. Shi, Z. An, W. Huang, *Adv. Funct. Mater.* **2018**, *28*, 1802657.
[141] H. Liu, D.-D. Ren, P.-F. Gao, K. Zhang, Y.-P. Wu, H.-R. Fu, L.-F. Ma, *Chem. Sci.* **2022**, *13*, 13922.
[142] N. Feng, Z. Wang, D. Sun, P. Sun, X. Xin, X. Cheng, H. Li, *Adv. Opt. Mater.* **2022**, *10*, 2102319.
[143] L. Wang, H. Xiao, L. Qu, J. Song, W. Zhou, X. Zhou, H. Xiang, Z.-X. Xu, *Inorg. Chem.* **2021**, *60*, 13557.
[144] N. Hellou, M. Srebro-Hooper, L. Favereau, F. Zinna, E. Caytan, L. Toupet, V. Dorcet, M. Jean, N. Vanthuyne, J. A. G. Williams, L. Di Bari, J. Autschbach, J. Crassous, *Angew. Chem., Int. Ed.* **2017**, *56*, 8236.
[145] G. Lu, Z. G. Wu, R. Wu, X. Cao, L. Zhou, Y. X. Zheng, C. Yang, *Adv. Funct. Mater.* **2021**, *31*, 2102898.
[146] S. Garain, S. Sarkar, B. Chandra Garain, S. K. Pati, S. J. George, *Angew. Chem., Int. Ed.* **2022**, *61*, 202115773.
[147] Z.-L. Gong, X. Zhu, Z. Zhou, S.-W. Zhang, D. Yang, B. Zhao, Y.-P. Zhang, J. Deng, Y. Cheng, Y.-X. Zheng, S.-Q. Zang, H. Kuang, P. Duan, M. Yuan, C.-F. Chen, Y. S. Zhao, Y.-W. Zhong, B. Z. Tang, M. Liu, *Sci. China: Chem.* **2021**, *64*, 2060.
[148] A. Nitti, D. Pasini, *Adv. Mater.* **2020**, *32*, 1908021.
[149] J. Gong, X. Zhang, *Coord. Chem. Rev.* **2022**, *453*, 214329.
[150] Q. Jiang, X. Xu, P.-A. Yin, K. Ma, Y. Zhen, P. Duan, Q. Peng, W.-Q. Chen, B. Ding, *J. Am. Chem. Soc.* **2019**, *141*, 9490.
[151] Y. Deng, M. Wang, Y. Zhuang, S. Liu, W. Huang, Q. Zhao, *Light: Sci. Appl.* **2021**, *10*, 76.
[152] Z. Yang, C. Xu, W. Li, Z. Mao, X. Ge, Q. Huang, H. Deng, J. Zhao, F. L. Gu, Y. Zhang, Z. Chi, *Angew. Chem., Int. Ed.* **2020**, *59*, 17451.
[153] Y. Tao, R. Chen, H. Li, J. Yuan, Y. Wan, H. Jiang, C. Chen, Y. Si, C. Zheng, B. Yang, G. Xing, W. Huang, *Adv. Mater.* **2018**, *30*, 1803856.
[154] G. X. Hao Peng, Y. Cao, L. Zhang, X.i Yan, X. Zhang, S. Miao, Y.e Tao, H. Li, C. Zheng, W. Huang, R. Chen, *Sci. Adv.* **2022**, *8*, 2925.
[155] Y. Tao, C. Liu, Y. Xiang, Z. Wang, X. Xue, P. Li, H. Li, G. Xie, W. Huang, R. Chen, *J. Am. Chem. Soc.* **2022**, *144*, 6946.
[156] W. Chen, Z. Tian, Y. Li, Y. Jiang, M. Liu, P. Duan, *Chem. - Eur. J.* **2018**, *24*, 17444.
[157] M. Hu, H.-T. Feng, Y.-X. Yuan, Y.-S. Zheng, B. Z. Tang, *Coord. Chem. Rev.* **2020**, *416*, 213329.
[158] J. Li, H. K. Bisoyi, J. Tian, J. Guo, Q. Li, *Adv. Mater.* **2019**, *31*, 1807751.
[159] B. Zhao, K. Pan, J. Deng, *Macromolecules* **2018**, *52*, 376.
[160] T. Zhao, J. Han, X. Jin, M. Zhou, Y. Liu, P. Duan, M. Liu, *Research* **2020**, *2020*, 6452123.
[161] J. Han, J. You, X. Li, P. Duan, M. Liu, *Adv. Mater.* **2017**, *29*, 1606503.
[162] T. Nishikawa, Y. Nagata, M. Suginome, *ACS Macro Lett.* **2017**, *6*, 431.
[163] J.-A. Li, Z. Song, Y. Chen, C. Xu, S. Li, Q. Peng, G. Shi, C. Liu, S. Luo, F. Sun, Z. Zhao, Z. Chi, Y. Zhang, B. Xu, *Chem. Eng. J.* **2021**, *418*, 129167.
[164] M. Xu, X. Wu, Y. Yang, C. Ma, W. Li, H. Yu, Z. Chen, J. Li, K. Zhang, S. Liu, *ACS Nano* **2020**, *14*, 11130.
[165] X. Liang, T. T. Liu, Z. P. Yan, Y. Zhou, J. Su, X. F. Luo, Z. G. Wu, Y. Wang, Y. X. Zheng, J. L. Zuo, *Angew. Chem.* **2019**, *131*, 17380.
[166] H. Li, J. Gu, Z. Wang, J. Wang, F. He, P. Li, Y. Tao, H. Li, G. Xie, W. Huang, C. Zheng, R. Chen, *Nat. Commun.* **2022**, *13*, 429.
[167] L. Gu, W. Ye, X. Liang, A. Lv, H. Ma, M. Singh, W. Jia, Z. Shen, Y. Guo, Y. Gao, H. Chen, D. Wang, Y. Wu, J. Liu, H. Wang, Y.-X. Zheng, Z. An, W. Huang, Y. Zhao, *J. Am. Chem. Soc.* **2021**, *143*, 18527.
[168] K. Takaishi, Y. Nakatsuka, H. Asano, Y. Yamada, T. Ema, *Chem. - Eur. J.* **2021**, *28*, 202104212.
[169] R. Liu, B. Ding, D. Liu, X. Ma, *Chem. Eng. J.* **2021**, *421*, 129732.
[170] Z. Huang, Z. He, B. Ding, H. Tian, X. Ma, *Nat. Commun.* **2022**, *13*, 7841.
[171] S. Hirata, M. Vacha, *J. Phys. Chem. Lett.* **2016**, *7*, 1539.
[172] W. Huang, C. Fu, Z. Liang, K. Zhou, Z. He, *Angew. Chem., Int. Ed.* **2022**, *61*, 202202977.
[173] A. W. Baochun Wang, *ACS Nano* **2015**, *9*, 10637.
[174] S. An, L. Gao, A. Hao, P. Xing, *ACS Nano* **2021**, *15*, 20192.
[175] S. Fu, Y. Chen, Y. Xie, Z. Li, *Chin. J. Chem.* **2024**, *42*, 2499.
[176] Y. Jiang, C. Zhang, R. Wang, Y. Lei, W. Dai, M. Liu, H. Wu, Y. Tao, X. Huang, *Adv. Opt. Mater.* **2023**, *12*, 2302482.
[177] Y. Chen, S. Huang, T. Wang, Z. Dong, H. Yu, *Macromolecules* **2019**, *52*, 1892.
[178] L. Wang, A. Hao, P. Xing, *ACS Appl. Mater. Interfaces* **2022**, *14*, 44902.
[179] Z. Luo, T. Friščić, R. Z. Khaliullin, *Phys. Chem. Chem. Phys.* **2018**, *20*, 898.
[180] T. Friščić, R. W. Lancaster, L. Fábián, P. G. Karamertzanis, *Proc. Natl. Acad. Sci. U. S. A.* **2010**, *107*, 13216.
[181] T. Friščić, *Chem. Soc. Rev.* **2012**, *41*, 3493.
[182] C. Guo, Q. Zhang, B. Zhu, Z. Zhang, X. Ma, W. Dai, X. Gong, G. Ren, X. Mei, *Cryst. Growth Des.* **2020**, *20*, 3053.
[183] C. Shen, E. Anger, M. Srebro, N. Vanthuyne, K. K. Deol, T. D. Jefferson, G. Muller, J. A. G. Williams, L. Toupet, C. Roussel, J. Autschbach, R. Réau, J. Crassous, *Chem. Sci.* **2014**, *5*, 1915.
[184] Z.-H. Zhao, M.-Y. Zhang, D.-H. Liu, C.-H. Zhao, *Org. Lett.* **2018**, *20*, 7590.
[185] S. Tanaka, D. Sakamaki, N. Haruta, T. Sato, M. Gon, K. Tanaka, H. Fujiwara, *J. Mater. Chem. C* **2023**, *11*, 4846.
[186] M. Zeng, W. Wang, S. Zhang, Z. Gao, Y. Yan, Y. Liu, Y. Qi, X. Yan, W. Zhao, X. Zhang, N. Guo, H. Li, H. Li, G. Xie, Y. Tao, R. Chen, W. Huang, *Nat. Commun.* **2024**, *15*, 3053.
[187] Q. Liu, X. Liu, X. Yu, X. Zhang, M. Zhu, Y. Cheng, *Angew. Chem., Int. Ed.* **2024**, *63*, 202403391.
[188] Y. Yang, H. Hu, L. Chen, H. Bai, S. Wang, J.-F. Xu, X. Zhang, *Mater. Chem. Front.* **2019**, *3*, 806.
[189] S. Dong, Y. Luo, X. Yan, B. Zheng, X. Ding, Y. Yu, Z. Ma, Q. Zhao, F. Huang, *Angew. Chem., Int. Ed.* **2011**, *50*, 1905.
[190] C. Xu, C. Yin, W. Wu, X. Ma, *Sci. China: Chem.* **2021**, *65*, 75.
[191] Y. Yu, Y. Li, X. Wang, H. Nian, L. Wang, J. Li, Y. Zhao, X. Yang, S. Liu, L. Cao, *J. Org. Chem.* **2017**, *82*, 5590.
[192] J. M. Heo, J. Kim, M. I. Hasan, H. Woo, J. Lahann, J. Kim, *Adv. Opt. Mater.* **2024**, *12*, 2400572.
[193] O. Bolton, K. Lee, H.-J. Kim, K. Y. Lin, J. Kim, *Nat. Chem.* **2011**, *3*, 205.
[194] W. Zhao, T. S. Cheung, N. Jiang, W. Huang, J. W. Y. Lam, X. Zhang, Z. He, B. Z. Tang, *Nat. Commun.* **2019**, *10*, 1595.

[195] Kenry, C. C., B. Liu, *Nat. Commun.* **2019**, *10*, 2111.
[196] W. Shao, H. Jiang, R. Ansari, P. M. Zimmerman, J. Kim, *Chem. Sci.* **2022**, *13*, 789.
[197] H. Shi, L. Song, H. Ma, C. Sun, K. Huang, A. Lv, W. Ye, H. Wang, S. Cai, W. Yao, Y. Zhang, R. Zheng, Z. An, W. Huang, *J. Phys. Chem. Lett.* **2019**, *10*, 595.
[198] W. Shao, J. Kim, *Acc. Chem. Res.* **2022**, *55*, 1573.
[199] M. S. Kwon, Y. Yu, C. Coburn, A. W. Phillips, K. Chung, A. Shanker, J. Jung, G. Kim, K. Pipe, S. R. Forrest, J. H. Youk, J. Gierschner, J. Kim, *Nat. Commun.* **2015**, *6*, 8947.
[200] S. Wang, D. Hu, X. Guan, S. Cai, G. Shi, Z. Shuai, J. Zhang, Q. Peng, X. Wan, *Angew. Chem., Int. Ed.* **2021**, *60*, 21918.
[201] M. Li, L.-J. Chen, Y. Cai, Q. Luo, W. Li, H.-B. Yang, H. Tian, W.-H. Zhu, *Chem* **2019**, *5*, 634.
[202] S. M. C. Schoenmakers, A. J. H. Spiering, S. Herziger, C. Böttcher, R. Haag, A. R. A. Palmans, E. W. Meijer, *ACS Macro Lett.* **2022**, *11*, 711.
[203] Y. Hashimoto, T. Nakashima, M. Yamada, J. Yuasa, G. Rapenne, T. Kawai, *J. Phys. Chem. Lett.* **2018**, *9*, 2151.
[204] S. Du, X. Zhu, L. Zhang, M. Liu, *ACS Appl. Mater. Interfaces* **2021**, *13*, 15501.
[205] B. Yue, X. Feng, C. Wang, M. Zhang, H. Lin, X. Jia, L. Zhu, *ACS Nano* **2022**, *16*, 16201.
[206] T. Kato, J. Uchida, T. Ichikawa, T. Sakamoto, *Angew. Chem., Int. Ed.* **2018**, *57*, 4355.
[207] H. K. Bisoyi, Q. Li, *Chem. Rev.* **2016**, *116*, 15089.
[208] C. Cuerva, M. Cano, C. Lodeiro, *Chem. Rev.* **2021**, *121*, 12966.
[209] Q. Li, Hari Krishna Bisoyi, *Prog. Mater. Sci.* **2019**, *104*, 1.
[210] Q. Li, *Nanoscience with Liquid Crystals: From Self-Organized Nanostructures to Applications*, Springer, Heidelberg, Germany **2014**.
[211] L. Wang, D. Huang, L. Lam, Z. Cheng, *Liq. Cryst. Today* **2017**, *26*, 85.
[212] H. K. Bisoyi, Q. Li, *Chem. Rev.* **2021**, *122*, 4887.
[213] A. Shinde, D. Huang, M. Saldivar, H. Xu, M. Zeng, U. Okeibunor, L. Wang, C. Mejia, P. Tin, S. George, L. Zhang, Z. Cheng, *ACS Nano* **2019**, *13*, 12461.
[214] M. Zeng, D. King, D. Huang, C. Do, L. Wang, M. Chen, S. Lei, P. Lin, Y. Chen, Z. Cheng, *Proc. Natl. Acad. Sci. U. S. A.* **2019**, *116*, 18322.
[215] P. Lv, X. Lu, L. Wang, W. Feng, *Adv. Funct. Mater.* **2021**, *31*, 2104991.
[216] R. Mezzenga, J. M. Seddon, C. J. Drummond, B. J. Boyd, G. E. Schröder-Turk, L. Sagalowicz, *Adv. Mater.* **2019**, *31*, 1900818.
[217] L. Wang, A. M. Urbas, Q. Li, *Adv. Mater.* **2018**, *32*, 1801335.
[218] I. Dierking, A. Martins Figueiredo Neto, *Crystals* **2020**, *10*, 604.
[219] M. Chen, A. Shinde, L. Wang, C. Ye, M. Zeng, Q. Yan, P. Lin, Y. Chen, Z. Cheng, *2D Mater.* **2019**, *6*, 025031.
[220] C. Tschierske, D. J. Photinos, *J. Mater. Chem.* **2010**, *20*, 4263.
[221] H. K. Bisoyi, S. Kumar, *Liq. Cryst.* **2011**, *38*, 1427.
[222] Y. Liu, Z. Xu, W. Gao, Z. Cheng, C. Gao, *Adv. Mater.* **2017**, *29*, 1606794.
[223] H. Zhou, J. Xu, X. Liu, H. Zhang, D. Wang, Z. Chen, D. Zhang, T. Fan, *Adv. Funct. Mater.* **2017**, *28*, 1705309.
[224] B. D. Wilts, H. M. Whitney, B. J. Glover, U. Steiner, S. Vignolini, *Mater. Today: Proc.* **2014**, *1*, 177.
[225] S. Vignolini, P. J. Rudall, A. V. Rowland, A. Reed, E. Moyroud, R. B. Faden, J. J. Baumberg, B. J. Glover, U. Steiner, *Proc. Natl. Acad. Sci. U. S. A.* **2012**, *109*, 15712.
[226] Y. Cao, P. X. Wang, F. D'Acierno, W. Y. Hamad, C. A. Michal, M. J. MacLachlan, *Adv. Mater.* **2020**, *32*, 1907376.
[227] K. E. Shopsowitz, H. Qi, W. Y. Hamad, M. J. MacLachlan, *Nature* **2010**, *468*, 422.
[228] F. Reinitzer, *Monatsh. Chem.* **1888**, *9*, 421.
[229] J. Bao, R. Lan, C. Shen, R. Huang, Z. Wang, W. Hu, L. Zhang, H. Yang, *Adv. Opt. Mater.* **2021**, *10*, 2101910.
[230] S. Tokunaga, Y. Itoh, Y. Yaguchi, H. Tanaka, F. Araoka, H. Takezoe, T. Aida, *Adv. Mater.* **2016**, *28*, 4077.
[231] Y. Li, A. Urbas, Q. Li, *J. Am. Chem. Soc.* **2012**, *134*, 9573.
[232] M. G. M. J. Alessandro Bosco, R. Eelkema, N. Katsonis, E. Lacaze, A. Ferrarini, B. L. Feringa, *J. Am. Chem. Soc.* **2008**, *130*, 14615.
[233] M. Giese, M. K. Khan, W. Y. Hamad, M. J. MacLachlan, *ACS Macro Lett.* **2013**, *2*, 818.
[234] Z.-g. Zheng, Y. Li, H. K. Bisoyi, L. Wang, T. J. Bunning, Q. Li, *Nature* **2016**, *531*, 352.
[235] A. Chanishvili, G. Chilaya, G. Petriashvili, R. Barberi, R. Bartolino, G. Cipparrone, A. Mazzulla, L. Oriol, *Adv. Mater.* **2004**, *16*, 791.
[236] B. Liu, C.-L. Yuan, H.-L. Hu, H. Wang, Y.-W. Zhu, P.-Z. Sun, Z.-Y. Li, Z.-G. Zheng, Q. Li, *Nat. Commun.* **2022**, *13*, 2712.
[237] C. E. Boott, A. Tran, W. Y. Hamad, M. J. MacLachlan, *Angew. Chem., Int. Ed.* **2019**, *59*, 226.
[238] K. Chung, S. Yu, C. J. Heo, J. W. Shim, S. M. Yang, M. G. Han, H. S. Lee, Y. Jin, S. Y. Lee, N. Park, J. H. Shin, *Adv. Mater.* **2012**, *24*, 2375.
[239] H. Kim, H. Lee, I. Ha, J. Jung, P. Won, H. Cho, J. Yeo, S. Hong, S. Han, J. Kwon, K. J. Cho, S. H. Ko, *Adv. Funct. Mater.* **2018**, *28*, 1801847.
[240] W. Zhang, A. A. F. Froyen, A. P. H. J. Schenning, G. Zhou, M. G. Debije, L. T. de Haan, *Adv. Photonics Res.* **2021**, *2*, 2100016.
[241] M. Mitov, *Adv. Mater.* **2012**, *24*, 6260.
[242] M. E. Kyle Georgea, J. Wangb, N. Taheri-Qazvini, A. Abbaspourradb, M. Sadati, *Proc. Natl. Acad. Sci. U. S. A.* **2023**, *120*, 2220032120.
[243] S. H. A. Josh Vura-Weis, R. Shukla, R. Rathore, M. A. Ratner, M. R. Wasielewski, *Science* **2010**, *328*, 1547.
[244] F. Zinna, U. Giovanella, L. D. Bari, *Adv. Mater.* **2015**, *27*, 1791.
[245] C. W. Lee, J. Y. Lee, *Adv. Mater.* **2013**, *25*, 5450.
[246] K. Yao, Q. Meng, V. Bulone, Q. Zhou, *Adv. Mater.* **2017**, *29*, 1701323.
[247] P. R. Anusuyadevi, R. Shanker, Y. Cui, A. V. Riazanova, M. Järn, M. P. Jonsson, A. J. Svagan, *Adv. Mater.* **2021**, *33*, 2101519.
[248] B. E. Droguet, H.-L. Liang, B. Frka-Petesic, R. M. Parker, M. F. L. De Volder, J. J. Baumberg, S. Vignolini, *Nat. Mater.* **2021**, *21*, 352.
[249] J. Zhu, F. Wu, Z. Han, Y. Shang, F. Liu, H. Yu, L. Yu, N. Li, B. Ding, *Nano Lett.* **2021**, *21*, 3573.
[250] G. Cheng, D. Xu, Z. Lu, K. Liu, *ACS Nano* **2019**, *13*, 1479.
[251] I. A. Sacui, R. C. Nieuwendaal, D. J. Burnett, S. J. Stranick, M. Jorfi, C. Weder, E. J. Foster, R. T. Olsson, J. W. Gilman, *ACS Appl. Mater. Interfaces* **2014**, *6*, 6127.
[252] D. Klemm, F. Kramer, S. Moritz, T. Lindström, M. Ankerfors, D. Gray, A. Dorris, *Angew. Chem., Int. Ed.* **2011**, *50*, 5438.
[253] R. J. Moon, A. Martini, J. Nairn, J. Simonsen, J. Youngblood, *Chem. Soc. Rev.* **2011**, *40*, 3941.
[254] I. I. Smalyukh, *Adv. Mater.* **2020**, *33*, 2001228.
[255] S. Shi, P. Lv, C. Valenzuela, B. Li, Y. Liu, L. Wang, W. Feng, *Small* **2023**, *19*, 2301957.
[256] G. Chu, X. Wang, H. Yin, Y. Shi, H. Jiang, T. Chen, J. Gao, D. Qu, Y. Xu, D. Ding, *ACS Appl. Mater. Interfaces* **2015**, *7*, 21797.
[257] R. Xiong, S. Yu, M. J. Smith, J. Zhou, M. Krecker, L. Zhang, D. Nepal, T. J. Bunning, V. V. Tsukruk, *ACS Nano* **2019**, *13*, 9074.
[258] M. Xu, G. Li, W. Li, B. An, J. Sun, Z. Chen, H. Yu, J. Li, G. Yang, S. Liu, *Angew. Chem., Int. Ed.* **2022**, *61*, 202117042.
[259] D. Qu, M. Archimi, A. Camposeo, D. Pisignano, E. Zussman, *ACS Nano* **2021**, *15*, 8753.
[260] O. Kose, A. Tran, L. Lewis, W. Y. Hamad, M. J. MacLachlan, *Nat. Commun.* **2019**, *10*, 510.
[261] T. Hiratani, W. Y. Hamad, M. J. MacLachlan, *Adv. Mater.* **2017**, *29*, 1606083.
[262] D. Zhang, H. Zheng, X. Ma, L. Su, X. Gao, Z. Tang, Y. Xu, *Adv. Opt. Mater.* **2022**, *10*, 2102015.
[263] A. Ivanova, M. C. Fravventura, D. Fattakhova-Rohlfing, J. Rathouský, L. Movsesyan, P. Ganter, T. J. Savenije, T. Bein, *Chem. Mater.* **2015**, *27*, 6205.
[264] Y. Deng, P. Li, H. Jiang, X. Ji, H. Li, *J. Mater. Chem. C* **2019**, *7*, 13640.

[265] X. Li, M. Rui, J. Song, Z. Shen, H. Zeng, *Adv. Funct. Mater.* **2015**, *25*, 4929.
[266] J. Liu, D. Li, K. Zhang, M. Yang, H. Sun, B. Yang, *Small* **2018**, *14*, 1703919.
[267] S. Zhao, G. Li, Q. Guo, Y. Wang, M. Zhang, Y. Zhou, S. Jin, M. Zhu, T. Zhuang, *Adv. Opt. Mater.* **2023**, *11*, 2202933.
[268] M. Cao, Y. Ren, Y. Wu, J. Shen, S. Li, Z.-Q. Yu, S. Liu, J. Li, O. J. Rojas, Z. Chen, *Nat. Commun.* **2024**, *15*, 2375.
[269] X. Wang, Q. Miao, W. Zhang, Y. Zhou, R. Xiong, Y. Duan, X. Meng, C. Ye, *Chem. Eng. J.* **2024**, *481*, 148463.
[270] J. You, C. Yin, S. Wang, X. Wang, K. Jin, Y. Wang, J. Wang, L. Liu, J. Zhang, J. Zhang, *Nat. Commun.* **2024**, *15*, 7149.
[271] R. Chen, R. Feng, Z. Huang, D. Feng, Y. Long, J. Zhang, Y. Yang, Z. Ma, Z. Yuan, S. Lu, Z. Zhao, X. Chen, *Adv. Funct. Mater.* **2024**, 2404602, https://doi.org/10.1002/adfm.202404602299.
[272] J. W. Goodby, *Proc. R. Soc. A* **2012**, *468*, 1521.
[273] X. Wang, B. Zhao, J. Deng, *Adv. Mater.* **2023**, *35*, 2304405.
[274] J. Liu, Z. P. Song, J. Wei, J. J. Wu, M. Z. Wang, J. G. Li, Y. Ma, B. X. Li, Y. Q. Lu, Q. Zhao, *Adv. Mater.* **2023**, *36*, 2306834.
[275] Y. Wang, A. Dang, Z. Zhang, R. Yin, Y. Gao, L. Feng, S. Yang, *Adv. Mater.* **2020**, *32*, 2004270.
[276] R. Liang, H. Yu, L. Wang, D. Shen, *Adv. Funct. Mater.* **2022**, *33*, 2211914.
[277] L. Chen, D. Chu, Z.-A. Cheng, M. Wang, S. Huang, *Polymer* **2020**, *208*, 122962.
[278] W. Liu, L.-X. Guo, B.-P. Lin, X.-Q. Zhang, Y. Sun, H. Yang, *Macromolecules* **2016**, *49*, 4023.
[279] Z. Liu, H. K. Bisoyi, Y. Huang, M. Wang, H. Yang, Q. Li, *Angew. Chem., Int. Ed.* **2021**, *61*, 202115755.
[280] Y. Wang, H. Cui, Q. Zhao, X. Du, *Matter* **2019**, *1*, 626.
[281] M. Wang, S. M. Sayed, L.-X. Guo, B.-P. Lin, X.-Q. Zhang, Y. Sun, H. Yang, *Macromolecules* **2016**, *49*, 663.
[282] M. H. Saeed, M.-Y. Choi, K. Kim, J.-H. Lee, K. Kim, D. Kim, S.-U. Kim, H. Kim, S.-k. Ahn, R. Lan, J.-H. Na, *ACS Appl. Mater. Interfaces* **2023**, *15*, 56285.
[283] Q. Fan, Y. Tang, H. Sun, D. Guo, J. Ma, J. Guo, *Adv. Mater.* **2024**, 2401315.
[284] J. Ma, Y. Yang, C. Valenzuela, X. Zhang, L. Wang, W. Feng, *Angew. Chem., Int. Ed.* **2022**, *61*, 202116219.
[285] M. Yang, Y. Xu, X. Zhang, H. K. Bisoyi, P. Xue, Y. Yang, X. Yang, C. Valenzuela, Y. Chen, L. Wang, W. Feng, Q. Li, *Adv. Funct. Mater.* **2022**, *32*, 2201884.
[286] H. Yang, F. Zhang, B.-P. Lin, P. Keller, X.-Q. Zhang, Y. Sun, L.-X. Guo, *J. Mater. Chem. C* **2013**, *1*, 1482.
[287] L. Wang, W. Liu, L.-X. Guo, B.-P. Lin, X.-Q. Zhang, Y. Sun, H. Yang, *Polym. Chem.* **2017**, *8*, 1364.
[288] L. Chen, H. K. Bisoyi, Y. Huang, S. Huang, M. Wang, H. Yang, Q. Li, *Angew. Chem., Int. Ed.* **2021**, *60*, 16394.
[289] S. k. Ahn, T. H. Ware, K. M. Lee, V. P. Tondiglia, T. J. White, *Adv. Funct. Mater.* **2016**, *26*, 5819.
[290] L.-X. Guo, M.-H. Liu, S. M. Sayed, B.-P. Lin, P. Keller, X.-Q. Zhang, Y. Sun, H. Yang, *Chem. Sci.* **2016**, *7*, 4400.
[291] Y. Ni, X. Li, J. Hu, S. Huang, H. Yu, *Chem. Mater.* **2019**, *31*, 3388.
[292] S. Huang, Y. Shen, H. K. Bisoyi, Y. Tao, Z. Liu, M. Wang, H. Yang, Q. Li, *J. Am. Chem. Soc.* **2021**, *143*, 12543.
[293] M. Wang, Y. Song, H. K. Bisoyi, J. F. Yang, L. Liu, H. Yang, Q. Li, *Adv. Sci.* **2021**, *8*, 2102674.
[294] S. Nam, W. Jung, J. H. Shin, S. S. Choi, *Light: Sci. Appl.* **2024**, *13*, 114.
[295] S. T. Kim, H. Finkelmann, *Macromol. Rapid. Commun.* **2001**, *22*, 429.
[296] J. Ma, Y. Yang, X. Zhang, P. Xue, C. Valenzuela, Y. Liu, L. Wang, W. Feng, *Mater. Horiz.* **2024**, *11*, 217.
[297] S.-U. Kim, Y.-J. Lee, J. Liu, D. S. Kim, H. Wang, S. Yang, *Nat. Mater.* **2021**, *21*, 41.
[298] Q. Fan, Z. Li, K. Jiang, J. Gao, S. Lin, J. Guo, *Cell Rep. Phys. Sci.* **2023**, *4*, 101583.
[299] X. Wang, K. Yang, B. Zhao, J. Deng, *Small* **2024**, 2404576, https://doi.org/10.1002/sml.202404576.
[300] C. Liu, H. Li, Y. Chen, D. Xu, Y. Cheng, *Chem. Eng. J.* **2024**, *486*, 150442.
[301] Y. Wang, Q. Li, *Adv. Mater.* **2012**, *24*, 1926.
[302] N. T. M. Mathews, *J. Am. Chem. Soc.* **2008**, *130*, 11409.
[303] U. A. Hrozhyk, S. V. Serak, N. V. Tabiryan, T. J. Bunning, *Adv. Funct. Mater.* **2007**, *17*, 1735.
[304] T. Yoshioka, T. Ogata, T. Nonaka, M. Moritsugu, S. N. Kim, S. Kurihara, *Adv. Mater.* **2005**, *17*, 1226.
[305] H. Akiyama, V. A. Mallia, N. Tamaoki, *Adv. Funct. Mater.* **2006**, *16*, 477.
[306] Y. Ji, T. Song, H. Yu, *Angew. Chem., Int. Ed.* **2024**, *63*, 202401208.
[307] H. C. J. T. H. Lin, C. H. Chen, Y. J. Chen, T. H. Wei, C. W. Chen, A. Y. G. Fuh, *Appl. Phys. Lett.* **2006**, *88*, 061122.
[308] M. E. McConney, V. P. Tondiglia, L. V. Natarajan, K. M. Lee, T. J. White, T. J. Bunning, *Adv. Opt. Mater.* **2013**, *1*, 417.
[309] J. Xiang, Y. Li, Q. Li, D. A. Paterson, J. M. D. Storey, C. T. Imrie, O. D. Lavrentovich, *Adv. Mater.* **2015**, *27*, 3014.
[310] J. Xiang, S. V. Shiyanovskii, C. Imrie, O. D. Lavrentovich, *Phys. Rev. Lett.* **2014**, *112*, 217801.
[311] M. J. Escuti, C. C. Bowley, G. P. Crawford, S. Žumer, *Appl. Phys. Lett.* **1999**, *75*, 3264.
[312] B. Y. T. H. Yu, J. Li, L. Li, *Opt. Express* **2005**, *13*, 7243.
[313] Y. C. Hsiao, Z. H. Yang, D. Shen, W. Lee, *Adv. Opt. Mater.* **2018**, *6*, 1701128.
[314] J. Liu, J. J. Wu, J. Wei, Z. J. Huang, X. Y. Zhou, J. Y. Bao, R. C. Lan, Y. Ma, B. X. Li, H. Yang, Y. Q. Lu, Q. Zhao, *Angew. Chem., Int. Ed.* **2024**, *63*, 202319536.
[315] H. Khandelwal, M. G. Debije, T. J. White, A. P. H. J. Schenning, *J. Mater. Chem. A* **2016**, *4*, 6064.
[316] K. G. Gutierrez-Cuevas, L. Wang, Z. g. Zheng, H. K. Bisoyi, G. Li, L. S. Tan, R. A. Vaia, Q. Li, *Angew. Chem., Int. Ed.* **2016**, *55*, 13090.
[317] Q. Li,*Intelligent Stimuli-Responsive Materials: From Well-Defined Nanostructures to Applications*, John Wiley & Sons, Hoboken, NJ, USA **2013**.
[318] S. Pieraccini, S. Masiero, A. Ferrarini, G. P. Spada, *Chem. Soc. Rev.* **2011**, *40*, 258.
[319] Q. Li, Y. Li, J. Ma, D. K. Yang, T. J. White, T. J. Bunning, *Adv. Mater.* **2011**, *23*, 5069.
[320] H. K. Bisoyi, Q. Li, *Acc. Chem. Res.* **2014**, *47*, 3184.
[321] H. K. Bisoyi, Q. Li, *Angew. Chem., Int. Ed.* **2016**, *55*, 2994.
[322] L. Wang, H. Dong, Y. Li, R. Liu, Y. F. Wang, H. K. Bisoyi, L. D. Sun, C. H. Yan, Q. Li, *Adv. Mater.* **2015**, *27*, 2065.
[323] Z. g. Zheng, R. S. Zola, H. K. Bisoyi, L. Wang, Y. Li, T. J. Bunning, Q. Li, *Adv. Mater.* **2017**, *29*, 1701903.
[324] L. Zhang, L. Wang, U. S. Hiremath, H. K. Bisoyi, G. G. Nair, C. V. Yelamaggad, A. M. Urbas, T. J. Bunning, Q. Li, *Adv. Mater.* **2017**, *29*, 1700676.
[325] L. Wang, Q. Li, *Chem. Soc. Rev.* **2018**, *47*, 1044.
[326] A. C. Arsenault, D. P. Puzzo, I. Manners, G. A. Ozin, *Nat. Photonics* **2007**, *1*, 468.
[327] Q. Zhang, D.-H. Qu, H. Tian, B. L. Feringa, *Matter* **2020**, *3*, 355.
[328] S. Lin, K. G. Gutierrez-Cuevas, X. Zhang, J. Guo, Q. Li, *Adv. Funct. Mater.* **2020**, *31*, 2007957.
[329] W. Kang, Y. Tang, X. Meng, S. Lin, X. Zhang, J. Guo, Q. Li, *Angew. Chem., Int. Ed.* **2023**, *62*, 202311486.
[330] H. Wang, Y. Tang, H. K. Bisoyi, Q. Li, *Angew. Chem., Int. Ed.* **2023**, *138*, 202216600.
[331] R. S. Z. Manoj Mathews, S. Hurley, D.-K. Yang, T. J. White, T. J. Bunning, Q. Li, *J. Am. Chem. Soc.* **2010**, *132*, 18361.

[332] Y. Li, C. Xue, M. Wang, A. Urbas, Q. Li, *Angew. Chem.* **2013**, *125*, 13948.
[333] K. Jiang, Q. Fan, D. Guo, C. Song, J. Guo, *ACS Appl. Mater. Interfaces* **2023**, *15*, 26037.
[334] A. Huang, J. Huang, H.-Y. Luo, Z.-W. Luo, P. Wang, P. Wang, Y. Guan, H.-L. Xie, *J. Mater. Chem. C* **2023**, *11*, 4104.
[335] Z. Liu, F. Deng, S. Huang, C. Fan, Y. Yuan, H. Zhang, *ACS Appl. Polym. Mater.* **2024**, *6*, 9582.
[336] D.-W. Zhang, M. Li, C.-F. Chen, *Sci. China Mater.* **2023**, *66*, 4030.
[337] D. Xu, C. Liu, H. Li, Y. Cheng, W. H. Zheng, *Adv. Opt. Mater.* **2024**, *12*, 2303019.
[338] M. Xu, C. Ma, J. Zhou, Y. Liu, X. Wu, S. Luo, W. Li, H. Yu, Y. Wang, Z. Chen, J. Li, S. Liu, *J. Mater. Chem. C* **2019**, *7*, 13794.
[339] S. Kang, G. M. Biesold, H. Lee, D. Bukharina, Z. Lin, V. V. Tsukruk, *Adv. Funct. Mater.* **2021**, *31*, 2104596.
[340] X. Yang, C. Valenzuela, X. Zhang, Y. Chen, Y. Yang, L. Wang, W. Feng, *Matter* **2023**, *6*, 1278.
[341] X. Wu, C. Ma, J. Liu, Y. Liu, S. Luo, M. Xu, P. Wu, W. Li, S. Liu, *ACS Sustainable Chem. Eng.* **2019**, *7*, 18801.
[342] M. Tuerhong, Y. Xu, X.-B. Yin, *Chin. J. Anal. Chem.* **2017**, *45*, 139.
[343] C. Xia, S. Zhu, T. Feng, M. Yang, B. Yang, *Adv. Sci.* **2019**, *6*, 1901316.
[344] F. Wang, S. Zhou, Y. Zhang, Y. Wang, R. Guo, H. Xiao, X. Sun, *Small* **2023**, *20*, 2306969.
[345] C. Zhang, H. Zheng, J. Sun, Y. Zhou, W. Xu, Y. Dai, J. Mo, Z. Wang, *Adv. Mater.* **2021**, *34*, 2105996.
[346] C. L. C. Chan, I. M. Lei, G. T. van de Kerkhof, R. M. Parker, K. D. Richards, R. C. Evans, Y. Y. S. Huang, S. Vignolini, *Adv. Funct. Mater.* **2022**, *32*, 2108566.
[347] Z. Zhang, Z. Chen, Y. Wang, Y. Zhao, L. Shang, *Adv. Funct. Mater.* **2021**, *32*, 2107242.

Jiao Liu received her Ph.D. degree in Advanced Material and Liquid Crystal Institute (AMLCI) at Kent State University in 2022. She is currently an assistant professor at Nanjing University of Posts and Telecommunications. Her research focuses on circularly polarized luminescent liquid crystal materials, liquid crystal elastomer, lyotropic liquid crystals, and stimuli-responsive soft matter.

Xin-Yu Zhou is currently a graduate student in Nanjing University of Posts and Telecommunications. His research mainly focuses on circularly polarized luminescent liquid crystal materials, chiral liquid crystal elastomers, and stimuli-responsive soft matter.

Bing-Xiang Li received his Ph.D. degree in Chemical Physics from Advanced Material and Liquid Crystal Institute at Kent State University in 2019. He is currently a professor in Nanjing University of Posts and Telecommunications. His current research spans from liquid crystals, stimuli-responsive soft matter, active matter, to biological physics.

Yan-Qing Lu received both his B.S. and Ph.D. degrees from Nanjing University, China, in 1991 and 1996, respectively. He has 5 years of experience in telecom industries in the United States and China. He is currently a Changjiang Distinguished Professor at Nanjing University and a Fellow of the Optical Society of America and Chinese Optical Society. His research interests include liquid crystal photonics, fiber optics, and nonlinear optics.

Quan Li is Distinguished Chair Professor and Director of Institute of Advanced Materials at Southeast University. He held appointments in USA, Germany, and France. Li received his Ph.D. from Chinese Academy of Sciences in Shanghai, where he was promoted to a youngest Full Professor in February 1998. He has been elected as a member of the European Academy of Sciences and the European Academy of Sciences and Arts. His current research interest spans from stimuli-responsive smart soft matter, advanced photonics, and optoelectronic materials to functional biocompatible materials, biomedicial materials, and nanoparticles to nanoengineering and device fabrication.